



UNIVERSITY OF BERGEN

**Peroxisome Proliferator-Activated Receptors
(PPARs) As Tools For Studying Effects Of
Contaminants On The Lipid Metabolism In
Atlantic Cod (*Gadus morhua*)**

Sofie Söderström

Master Thesis in Environmental Toxicology

University of Bergen, Norway

Department of Biology

Thesis submitted in partial fulfillment of the requirements for the degree of Master of Science

Table of Contents

I.	List of Abbreviations	I
II.	Acknowledgments	IV
III.	Abstract	V
1	INTRODUCTION	1
1.1	The Big Picture	1
1.2	Contaminants in the Marine Environment	2
1.2.1	Legacy Environmental Contaminants.....	2
1.2.2	Emerging Environmental Contaminants	5
1.3	Atlantic Cod as a Model Species	5
1.4	Peroxisome Proliferator-Activated Receptors Role in Lipid Metabolism	7
1.4.1	Peroxisome Proliferator-Activated Receptors	7
1.5	Gene Reporter Assays to Study Ligand Binding and Transcriptional Activation	14
1.5.1	Luciferase Reporter Assay (LRA).....	14
1.6	Objectives.....	16
2	MATERIALS	17
2.1.1	List of Chemicals	17
2.1.2	List of Equipment	19
2.1.3	List of Enzymes.....	19
2.1.4	List of Kits	19
2.1.5	List of Primers.....	20
2.1.6	List of Software and Online Tools	21
2.1.7	List of Cell Lines.....	21
2.1.8	List of Vectors and Plasmids.....	21
2.1.9	Growth Media	22
2.1.10	Buffers.....	23
2.1.11	SDS-PAGE.....	24

2.1.12	Coomassie Brilliant Blue & WB	25
2.1.13	List of Ligands	27
3	METHODS.....	30
3.1	Atlantic Cod	30
3.2	RNA Extraction from Atlantic Cod Tissue	30
3.3	Spectrophotometric Measurements - NanoDrop	31
3.4	Agarose Gel Electrophoresis.....	31
3.4.1	Denaturing RNA Electrophoresis in TBE Agarose Gels	32
3.5	Synthesis of Complementary DNA from Total RNA - Reverse Transcription.....	32
3.6	Isolation and Amplification of the Atlantic Cod PPARs.....	33
3.6.1	Primer Design.....	35
3.6.2	Purification of PCR Products Through Gel Extraction.....	36
3.7	Molecular Cloning	36
3.7.1	Ligation.....	36
3.7.2	Transformation.....	37
3.7.3	Plating of Transformed E. coli	38
3.8	Identifying Positive Transformants By PCR Colony Screening.....	38
3.9	Plasmid Purification	39
3.9.1	Mini-Prep	40
3.9.2	Midi-Prep.....	41
3.10	DNA Sequencing	41
3.11	Effector Plasmids Construction	42
3.11.1	Restriction Digestion	43
3.11.2	Dephosphorylation.....	43
3.11.3	Ligation	44
3.12	Ligand activation Analysis	45
3.12.1	Luciferase Reporter Gene Assay (LRA).....	45
3.12.2	Reporter and Control Plasmids.....	45

3.12.3	Control of LRA Plasmids Integrity	46
3.12.4	COS-7 Cell Culturing	46
3.12.5	Seeding of COS-7 for LRA.....	47
3.12.6	Transient Transfection of COS-7 Cells	47
3.12.7	Exposure to Ligands.....	47
3.12.8	Cell Lysis and Measurement of Luciferase- and β -galactosidase Activity.....	48
3.13	Cell Viability Assays	49
3.14	Testing for Presence of Expressed Fusion Proteins in COS-7 Cells	51
3.14.1	Protein Sample Preparation	51
3.14.2	Sodium Dodecyl Sulphate Polyacrylamide Gel Electrophoresis (SDS-PAGE) and Sample Preparation.....	53
3.14.3	Coomassie Brilliant Blue Staining.....	54
3.14.4	Western Blotting.....	55
3.15	Data Treatment and Statistics	56
3.16	<i>In Silico</i> Sequence Analyses	57
4	RESULTS	58
4.1	Molecular Cloning of the Ligand Binding Domains of the Atlantic Cod PPAR Subtypes	59
4.1.1	RNA Extraction from Atlantic Cod Tissue.....	59
4.1.2	cDNA Synthesis, PCR Amplification and Cloning.....	60
4.1.3	Colony Screening for Transformants.....	61
4.1.4	Sequencing and Examination.....	62
4.1.5	Phylogenetic Analysis	65
4.1.6	Amino Acids Important for Ligand Binding	66
4.2	Effector Plasmid Construction.....	68
4.2.1	Restriction Digestion and Ligation.....	68
4.2.2	Colony Screening for Positive Transformants.....	69
4.2.3	LRA Plasmids and Integrity Control.....	70

4.3	Luciferase Reporter Gene Assay	71
4.3.1	Establishing Positive Controls for Ligand Activation of Atlantic Cod PPAR Constructs	71
4.3.2	Optimization of Receptor- Reporter Plasmid Ratio in LRA.....	74
4.3.3	Ligand Activation Assay	76
4.4	Cell Viability Assays	82
4.5	Examining the Presence of Expressed Fusion Proteins in COS-7 Cells	85
4.5.1	Protein Concentration Measurements	85
4.5.2	Sodium Dodecyl Sulphate Polyacrylamide Gel Electrophoresis (SDS-PAGE).....	86
4.5.3	Western Blotting.....	87
5	Discussion	88
5.1	Sequence Analyses	88
5.2	Ligand Activation Analyses	90
5.3	Conclusion.....	100
5.4	Future work	100
6	Referenses	103
7	Appendix I.....	114
8	Appendix II	115
9	Appendix III	116
10	Appendix IV	117
11	Appendix V.....	118
12	Appendix VI	119
13	Appendix VII	120

I. List of Abbreviations

1-triple-TTA	2-(tridec-12-yn-1-ylthio) acetic acid
15-HETE	15-hydroxyeicosatetraenoic acid
15d-PGJ2	15-deoxy- Δ 12,14-prostaglandin J2
8(S)-HETE	8(S)-hydroxyeicosatetraenoic acid
AMP	Adenosine monophosphate
ATP	Adenosine triphosphate
A_x	Absorbance measurements at x nanometer (nm)
BSA	Bovine serum albumin
cDNA	Complementary DNA
CFDA-AM	5-carboxyfluorescein diacetate acetoxymethyl ester
D4	Octamethylcyclotetrasiloxane
D5	Decamethylcyclopentasiloxane
DBD	DNA binding domain
ddNTP	Dideoxynucleotides
DDT	Dichlorodiphenyltrichloroethane
DDT	DL-Dithiothreitol
DEHP	Di(2-ethylhexyl) phthalate
DiDP	Diisodecyl phthalate
DMSO	Dimethyl sulfoxide
DNA	Deoxyribonucleic acid
dNTPs	Deoxynucleotides
DPTE	2,3-dibromopropyl-2,4,6-tribromophenyl ether
EC₅₀	Effective concentration
EDTA	Ethylenediaminetetraacetic acid disodium salt dehydrate
EGTA	Ethylene glycol-bis(2-aminoethylether)-N,N,N',N'-tetraacetic acid
FBS	Fetal Bovine Serum
Fwd	Forward
GW501516	2-[2-Methyl-4-[[[4-methyl-2-[4-(trifluoromethyl)phenyl]-5-thiazolyl]methyl]thio]phenoxy]-acetic acid
LB	Lysogeny broth

LBD	Ligand binding domain
LRA	Luciferase reporter gene assay
MBP	mono-Butyl phthalate
MBzP	mono-Benzyl phthalate
MCS	Multiple cloning site
mRNA	Messenger RNA
MUFAs	Monounsaturated fatty acids
NRs	Nuclear receptors
ON	Over night
ONGP	Ortho Nitrophenyl- β -galactoside
ONP	o-nitrophenol
PBS	Phosphate-buffered saline
PCB 153	2,2',4,4',5,5'-Hexachlorobiphenyl
PCBs	Polychlorinated biphenyls
PFASs	Perfluorinated alkylated substances
PFCAs	Perfluorinated carboxylic acids
PFCs	Perfluorinated compounds
PFH_xS	Perfluorohexanesulfonic acid
PFNA	Perfluorononanoic acid
PFOA	Perfluorooctanoic acid
PFOS	Perfluorooctanesulfonic acid
PFSAs	Perfluorinated sulfonic acids
PFUnDA	Perfluoroundecanoic acid
PMSF	Phenylmethanesulfonyl fluoride
POPs	Persistent organic pollutants
PPARs	Peroxisome proliferator-activated receptors
PPCPs	Pharmaceuticals and personal care products
PPREs	Peroxisome proliferator response elements
PUFAs	Polyunsaturated fatty acids
rDNA	Recombinant DNA
Rev	Reverse
RNA	Ribonucleic acid
Rosi	Rosiglitazone

rRNA	Ribosomal RNA
RT	Room temperature
RXR	Retinoid X receptor
SAP	Shrimp Alkaline Phosphatase
SDS-PAGE	Sodium dodecyl sulfate polyacrylamide gel electrophoresis
SEM	Standard error of mean
SOC	Super Optimal broth with catabolite repression
TBBPA	Tetrabromobisphenol A
TBE	Tris-borate-EDTA
totRNA	Total Ribonucleic Acid
TTA	Tetradecylthioacetic acid
TZDs	Thiazolidinedione's
UAS	Upstream activation sequence
WY14643	4-chloro-6-[(2,3-dimethylphenyl)amino]-2-pyrimidinyl]thio]-acetic acid
β-gal	β-Galactosidase

II. Acknowledgments

The work comprised in this thesis was carried out at the Environmental Toxicology research group, at the Department of Biology, University of Bergen. The work is part of the project *iCod 2.0: Integrative environmental genomics of Atlantic cod (Gadus morhua)*, funded by the Research Council of Norway grant iCod 2.0 (project no. 244564/E40).

First, I would like to express my sincere gratitude to my main supervisor Dr. Odd André Karlsen and co-supervisor Prof. Anders Goksøyr. Thank you for providing instructive guidance and motivation throughout this thesis, for being understanding, and for giving me the privilege to attend inspiring conferences.

A special thanks to Odd André Karlsen, for your generosity with your time, frequent follow-ups, and resilience to stay supportive throughout the battles of lab work going sideways. Grateful thanks go to Roger Lille-Langøy, for sharing your knowledge regarding methods and your tricks to make things work.

Huge thanks to the entire tox-group, previous and current members, for providing a nice work atmosphere with support, laughter, and way too much cake and sweets. Extended thanks to the “tox-girls” for cultural breaks, and support both in and outside of work.

I would also like to thank my family and friends for their tireless support and encouragement. Finally, my greatest gratitude to my dearest M, whose believe in me and infinite support gave me the strength to see this through.

Bergen, October 2017

Sofie Söderström

III. Abstract

Due to its habitats near offshore oil platforms, petroleum recovery facilities, as well as coastal industries and municipal wastewater treatment plants, Atlantic cod (*Gadus morhua*) must cope with both legacy and emerging environmental contaminants. Peroxisome proliferator-activated receptors (PPARs) are ligand-activated transcription factors. Upon activation by either endogenous ligands (e.g., fatty acids and lipid derivatives) or contaminants of certain structures, PPARs control the expression of genes involved in lipid- and carbohydrate metabolism. By studying how the Atlantic cod PPARs can bind and become activated by contaminants, especially by the emerging and far less documented ones, the main objective of this thesis was to contribute with new baseline data that can give insight into how the regulation of the energy metabolism in Atlantic cod can be modulated by environmental pollutants. The Atlantic cod PPARx hinge+LBDs were cloned from cod tissue using standard molecular techniques, and further subcloned into eukaryotic expression vectors. *In silico* sequence and phylogenetic analyses confirmed the Atlantic cod PPAR identities. The ligand-binding characteristics of Atlantic cod PPARs were examined by establishing *in vitro* UAS/Gal4-DBD based luciferase reporter gene assays in a COS-7 cell line. WY14643 and GW501516 are well-established model compounds that act as strong agonists of mammalian PPAR α and PPAR β/δ , respectively. Similarly, WY14643 elicited a maximum activation of 126-fold on the Atlantic cod PPAR α construct at 125 μ M (EC_{50} = 41 μ M), and 128-fold on the PPAR α b construct at 41 μ M (EC_{50} = 26 μ M). GW501516 elicited a maximum activation of 126-fold on the Atlantic cod PPAR β/δ construct at 11.3 μ M (EC_{50} = 2 μ M). But then, none of the typical mammalian PPAR γ agonists activated the Atlantic cod PPAR γ construct. However, expression of the Gal4-PPAR γ construct in COS-7 cells was confirmed with Western Blotting using Gal-4 antibodies. Among fifteen pollutants tested, representing a structurally diverse group of ligands, perfluorooctanoic acid (PFOA) and perfluorononanoic acid (PFNA) were able to activate of the PPAR α b construct with a maximum activation of 8-fold at 150 μ M and 3-fold at 154 μ M, respectively. The other ligands tested did not activate any of the Atlantic cod PPAR constructs. Thus, exposure of Atlantic cod to compounds with long carbon-backbones that harbors a carboxyl-group, could potentially modulate the lipid- and carbohydrate metabolism through directly interfering with at least one PPAR subtype.

1 INTRODUCTION

1.1 The Big Picture

Like many of the world's oceans the Northeast (NE) Atlantic suffers from increased pressure of pollutants originating from various human activities. This includes marine- and coastal industries, such as offshore oil platforms and petroleum recovery facilities, as well as municipal effluent discharges (Bakke et al., 2013). Furthermore, long-range transportation via air and ocean currents enable pollutants released by inland industries to be transported to the most remote parts of the oceans, leaving few if any pristine areas on the globe (Julshamn et al., 2013b; Julshamn et al., 2013c). Pollutants present in the environment are often persistent and highly lipid-soluble, and tend to accumulate in lipid-rich biota. When within an organism, some pollutants can function as endocrine disruptors by either mimicking naturally occurring hormones or blocking their actions. The result of such an event could lead to alternation of hormone production or hormone signaling. Long-term exposure to chemicals possessing metabolic and endocrine disrupting abilities can lead to negative biological effects, such as impaired growth, reduced reproductive success, and ultimately reduced survival of a species (Foekema et al., 2012; Rigaud et al., 2013; Westerlund et al., 2000). Atlantic cod (*Gadus morhua*) in the NE Atlantic is of both commercial and ecological importance, as Norwegian fisheries are dependent on cod, and the Northeast arctic cod population influences the structure and function of the arctic ecosystem (Link et al., 2009). Thus, Atlantic cod is a highly relevant species, and the sequencing of the Atlantic cod genome in 2011 has made it a promising model-species that is becoming more frequently used in toxicological contexts (Bizarro et al., 2016; De Laender et al., 2011; Eide et al., 2014; Enerstvedt et al., 2017; Goksøyr et al., 1987; Karlsen et al., 2011; Star et al., 2011; Yadetie et al., 2016; Yadetie et al., 2014; Yadetie et al., 2013; Yadetie et al., 2017; Yin et al., 2016). Considering the amount of anthropogenic chemicals present in the environment, our knowledge is still scarce regarding how contaminants, alone or in mixtures, affect the biology of the Atlantic cod. This thesis addresses potential effects on the lipid homeostasis in Atlantic cod by focusing on the peroxisome proliferator-activated receptors (PPARs), which are ligand-activated transcription factors that control the expression of genes involved in lipid- and carbohydrate metabolism. By studying how PPARs can bind and become

activated by contaminants, especially by the emerging and far less documented ones, we aim to provide new insight into how the lipid metabolism in Atlantic cod can be modulated by environmental pollutants.

1.2 Contaminants in the Marine Environment

1.2.1 Legacy Environmental Contaminants

Persistent organic pollutants (POPs) are environmental contaminants that exhibit resistance against physical, chemical, and biochemical degradation. These properties make them reside in the environment for long periods of time. POPs are also prone to undertake long-range transportation via air mass movements (i.e., grasshopper effect), or through water and ocean currents, to areas far from the source of their release (Macdonald et al., 2000; Rigét et al., 2010; Shen and Wania, 2005). Most POPs are also highly lipophilic. This property makes these compounds accumulate in biota, and specifically in lipid-rich tissues. POPs may bioaccumulate over time if the organisms detoxification system is not able to metabolize and excrete the compound faster than they are absorbed from the environment (Bryan et al., 1979) (Fig 1). When accumulated inside an organism, the characteristics of the compound will also decide how much of the compound that will become bioavailable i.e., the amount able to reach its site of action (e.g., receptor activation) and potentially cause adverse toxic effects. In addition, if the organisms that bioaccumulate such compounds are at the lower trophic levels, the compound may biomagnify up through the food web causing predators at higher trophic levels to contain a high burden of pollutants (Suedel et al., 1994) (Fig 1).

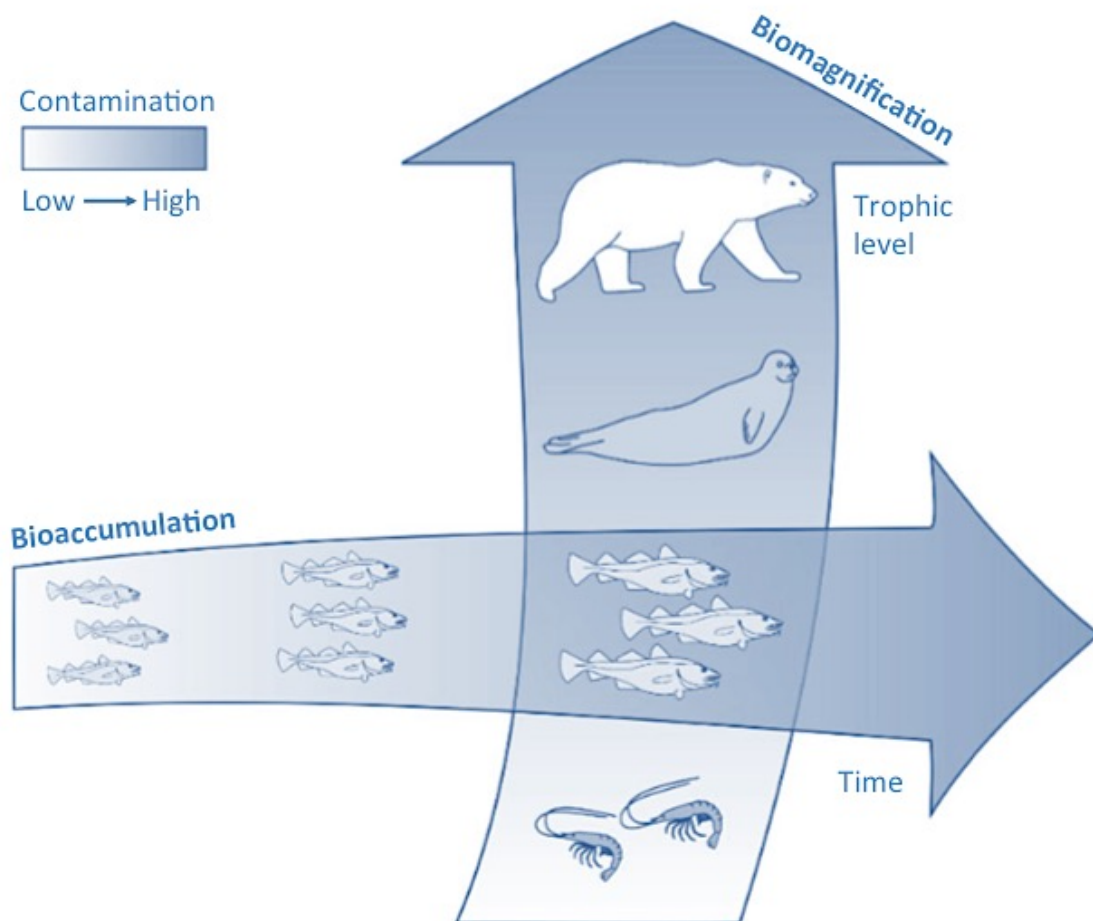


Figure 1. Schematic illustration of bioaccumulation and biomagnification of lipophilic environmental contaminants in organisms. Illustration source: modified version from Alexander Klevedal Madsen 2016.

There are many POPs (e.g., Aldrin, Mirex, DDT, Dioxins, and PCBs etc.) that after decades of commercial use were shown to cause adverse toxic effects to organisms (including humans) by being either carcinogenic, teratogenic, or exhibiting endocrine disrupting properties that cause damage to the immune-, nervous-, or reproduction systems (Bertazzi et al., 1998; Casals-Casas and Desvergne, 2011; Darnerud, 2003; Fisher, 1999; Fonnum et al., 2006; Fry, 1995; Organization, 2010; Tanabe, 2002; Tocher, 2003). Even though the production and use of several known toxic POPs have been banned or phased out, many of them can still be found in the environment today (Karl and Lahrssen-Wiederholt, 2009). Examples of such legacy POPs are “the dirty dozen” (Aldrin, Chlordane, DDT, Dieldrin, Endrin, Heptachlor, Hexachlorobenzene, Mirex, Toxaphene, PCB, Dioxin, and Furans) that were defined for global elimination or strict regulations by the Stockholm Convention on Persistent Organic Pollutants in 2004 (UNEP, 2001). In 2009, additional POPs were added to the Stockholm Convention’s list of elimination or strict regulation, “the nasty nine”

(Alpha-hexachlorocyclohexane, Beta-hexachlorocyclohexane, Lindane, Chlordecone, HEXAbromobiphenyl (HBB), Octabromodiphenyl ether (OBDE), Pentabromodiphenyl ether (PBDE), Pentachlorobenzene (PeCB), and perfluorooctanesulfonic acid (PFOS)), followed by the addition of “Evil endosulfan” to the list in 2011 (UNEP, 2011). Another agreement aiming to prevent dumping of pollution from offshore and land-based sources into the marine environment is the Convention for the Protection of the Marine Environment of the NE Atlantic (OSPAR Convention), which was ratified in 1998.

Perfluorinated compounds (PFCs) such as PFOS, as well as perfluorooctanoic acid (PFOA, currently under review by the Stockholm convention) are of high interest in this thesis due to their properties and characteristics. PFCs consist of hydrophobic fluorinated carbon backbones of different lengths and a hydrophilic functional group (Surma and Zieliński, 2015). The high-energy bonds between the carbons and fluorines make them resistant against abiotic and biotic degradation (Poothong et al., 2012). Martin et al. (2004) found that mammals and fish at higher trophic levels in the Canadian arctic food web contained higher concentrations of the fluorosurfactant PFOS than mammals feeding at lower trophic levels. Even though the PFOS concentrations of mammals living in the arctic were not as high as in the same species living at mid-latitude regions of USA, PFOS concentrations in arctic mammals were still measurable. Thus, showing that PFOS is a contaminant that both bioaccumulate and biomagnifies, and that somehow have ended up in remote arctic areas far from its source of release. It is difficult to assess how much PFOS that is directly released to the environment since PFOS can also result from degradation of several precursors and PFOS-related compounds (Lau et al., 2007; Moore et al., 2003). Due to the low volatility of PFOS and PFOAs, long-range transport in their gas phase via air is unlikely (Lau et al., 2007; Martin et al., 2002). It is hypothesized that precursors and perfluorinated-related compounds exhibiting higher volatility are undertaking long-range transport, and when deposited, they are broken down into PFOS and PFOA through abiotic (e.g., hydrolysis and photolysis) and biotic (e.g., microorganisms) degradation (Lau et al., 2007; Renner, 2001; Wallington et al., 2006). PFCs have been detected in the blood of Baltic cod, and liver of Atlantic cod along the Norwegian coast (Falandysz et al., 2006; Falandysz et al., 2007; Valdersnes et al., 2017).

1.2.2 Emerging Environmental Contaminants

International regulations and measures taken to lower the production and release of POPs have reduced their presence in biota in and around the NE Atlantic, especially in Polar and Arctic regions (Vorkamp and Rigét, 2014). However, it is continuously being produced new chemicals, where many are intended as substitutes for chemicals that have been banned after proven toxic to organisms. Unfortunately, many of these new chemicals exhibit similar characteristics as those found in other POPs. Currently, both new and previously undetected chemicals are emerging in environmental compartments in concerning concentrations (Bao et al., 2015; Vorkamp and Rigét, 2014), including in Atlantic cod (Herzke et al., 2013; Warner et al., 2014). Importantly, the toxicological data we possess of these emerging and far less characterized contaminants is still incomplete (e.g., transport potential, persistence, and toxicity) (Vorkamp and Rigét, 2014). Many of the emerging contaminants are still produced and utilized today and can be found in currently used pesticides (e.g., chlorpyrifos), flame retardants (e.g., 2,3-bibromopropyl-2,4,6-tribromophenyl ether (DPTE)), and “down the drain chemicals” such as pharmaceuticals and compounds found in personal care products (e.g., siloxanes and phthalates). Many anthropogenic chemical ends up in aquatic environments (Clark et al., 1989), so to assume that species living in, or close to, marine and limnic habitats are suffering increased risk of exposure is not farfetched. This demands for research to bridge the gap in knowledge needed to guide regulatory authorities to where action is needed, and where strict regulation of certain chemicals are required in order to protect marine nature and wildlife. Choosing Atlantic cod as a model species is a strategic choice. Its position in the trophic levels makes it highly ecologically relevant; both as a marine top predator, and at the same time a prey in the marine/terrestrial food web where it's preyed upon by marine mammals and birds (Fig 1).

1.3 Atlantic Cod as a Model Species

Atlantic cod is a common teleost in the North Atlantic Ocean with several populations distributed from east to west (Fig 2). The Norwegian fisheries are dependent on the cod stocks inhabiting the NE Atlantic. These stocks are separated according to their geographic distribution with 1) the Northeast arctic cod residing within the Barents Sea, 2) the North Sea cod residing in the North Sea, Skagerrak, and the eastern part of the English channel, and 3) the coastal cod inhabiting coastal areas of the Norwegian

Sea and along Norwegian fjords, where the environmental heterogeneity has given rise to several local subpopulations along the coastline. The Northeast arctic cod is the worlds largest cod population and influences the structure and function of the arctic ecosystem. In the Barents Sea it is one of the main piscivores predating on both capelin and herring, in addition it is also preyed upon by harp seals (*Pagophilus groenlandicus*) and minke whales (*Balaenoptera acutorostrata*) (Link et al., 2009).



Figure 2. Geographic distribution of Atlantic cod throughout the Atlantic Ocean. Map source: modified version from Aquamaps (2015).

Atlantic cod is used as a bioindicator species to monitor the presence of pollutants in the environment (OSPAR). In addition to legacy contaminants such as arsenic (As), mercury (Hg), cadmium (Cd), lead (Pb), dioxins, PCBs, alkylphenols (AP) and polyaromatic hydrocarbons (PAH) (Bakke et al., 2013; Julshamn et al., 2013a; Julshamn et al., 2013b; Julshamn et al., 2013c), there is found an increasing number of structurally diverse emerging environmental contaminants in the liver tissue of Atlantic cod, including polybrominated diphenyl ethers (PBDEs) (Julshamn et al., 2013a), perfluorinated alkylated substances (PFASs), brominated flame retardants (BFRs), chlorinated paraffins (CPs) (Herzke et al., 2013), siloxanes (Schlabach et al., 2007; Warner et al., 2010), phthalates, and organophosphorus flame retardants (PFRs) (Evenset, 2009; Green et al., 2015), as well as ingestion of microplastics (Bråte et al., 2016).

As in other vertebrates, the detoxification of xenobiotics (such as pollutants) in Atlantic cod occurs mainly in the liver through three phases in the biotransformation pathway. Phase I contributes to make the xenobiotics more hydrophilic by introducing or revealing a hydrophilic group (-OH, -NH₂, -SH, or -COOH) through oxidation, hydrolysis, or reduction. If phase I modifications are not sufficient to allow elimination of the xenobiotic compound, phase II reactions further increases the polarity of the xenobiotic by adding a larger polar group through conjugation reactions with specific enzymes (e.g. attachment of glutathione by glutathione S-transferase). Phase III is the final step in the biotransformation pathway, where the metabolites of the xenobiotics are transported out of the cell by membrane bound efflux transporter proteins. Cytochrome P-450 mono-oxygenase enzymes are crucial in phase I reactions, and have to some extent been characterized in Atlantic cod (Goksøyr, 1985; Goksøyr, 1995; Goksøyr et al., 1987; Goksøyr and Husøy, 1998; Goksøyr et al., 1986; Karlsen et al., 2012). However, the knowledge of how each contaminant alone, and in mixtures, affects the biology of the Atlantic cod is far from completely understood. The publishing of the Atlantic cod genome in 2011 (Star et al., 2011) made it possible to conduct large-scale toxicogenomic studies. Genomic and proteomic studies have been initiated where the ultimate goal is to obtain comprehensive data on toxicological responses to toxic compounds in Atlantic cod. (Bizarro et al., 2016; Eide et al., 2014; Karlsen et al., 2011; Yadetie et al., 2016; Yadetie et al., 2014; Yadetie et al., 2013; Yadetie et al., 2017).

1.4 Peroxisome Proliferator-Activated Receptors Role in Lipid Metabolism

1.4.1 Peroxisome Proliferator-Activated Receptors

Peroxisome proliferator-activated receptors (PPARs) are ligand-activated transcription factors that are members of the superfamily of nuclear receptors (NRs). Their longwinded name originates from the first discovery of a PPAR in rodents, demonstrating its regulation of peroxisome proliferation when activated by industrial chemicals. However, this was later found not to be the case for PPARs present in humans and primates, but still the transcription factors have kept their name despite being somewhat misleading and outdated. In humans and primates, it was later found that one of the main functions of PPARs is to regulate lipid homeostasis by controlling the expression of genes involved in the fatty acid utilization and storage (Colliar et al.,

2011; Desvergne and Wahli, 1999; Georgiadi and Kersten, 2012; Kliewer et al., 1997). In addition, it has also been shown that PPARs are involved in other cellular processes as well, such as glucose utilization, cell proliferation and differentiation, inflammatory processes, adipogenesis etc (Ferré, 2004).

The varying functions of PPARs are associated to the presence of several subtypes, and in mammals three PPAR paralogs have been described; PPAR α , PPAR β/δ , and PPAR γ (Desvergne and Wahli, 1999). In teleosts, one ortholog of the human PPAR β/δ and PPAR γ subtypes has been identified. However, two orthologs of the human PPAR α subtype (i.e., PPAR αa and PPAR αb) appear to be present in some teleosts, e.g. in Japanese puffer (*Fugu rubripes*) (Maglich et al., 2003), green spotted puffer (*Tetraodon nigroviridis*) (Metpally et al., 2007), zebrafish (*Danio rerio*) (Bertrand et al., 2007; Tseng et al., 2011), turbot (*Scophthalmus maximus*) (Urbatzka et al., 2013), and Atlantic cod (Star et al., 2011) (Eide, 2016. The Atlantic cod (*Gadus morhua*) chemical defensome lacks a pregnane x receptor, and the phylogeny of pxxr loss in fishes. Manuscript in prep). Although encoded by different genes, the PPAR subtypes share a high degree of sequence similarity (Desvergne and Wahli, 1999). The PPAR subtypes differ by their tissue distribution, ligand specificity and target genes in a species-specific manner. The different PPAR subtypes seem to predominate in tissues that reflect their different physiological functions. In mammals, PPAR α is highly expressed in liver, heart, and muscle tissue (Ferré, 2004; Georgiadi and Kersten, 2012) where they are mainly, but not exclusively, involved in releasing stored energy through peroxisomal and mitochondrial FA catabolism (Hihi et al., 2002) (Fig 3). Although less studied, mammalian PPAR β/δ tissue expression appears to be ubiquitous (Ferré, 2004; Georgiadi and Kersten, 2012). PPAR β/δ is believed to be involved in balancing energy homeostasis and building muscles by e.g. releasing energy stored as fat in muscles while initiating fat synthesis in the liver (Wagner and Wagner, 2010) (Fig 3). Mammalian PPAR γ is highly expressed in adipose tissue (Ferré, 2004; Georgiadi and Kersten, 2012) where their main role are to promote energy storage by lipid accumulation and adipogenesis (Hihi et al., 2002) (Fig 3).

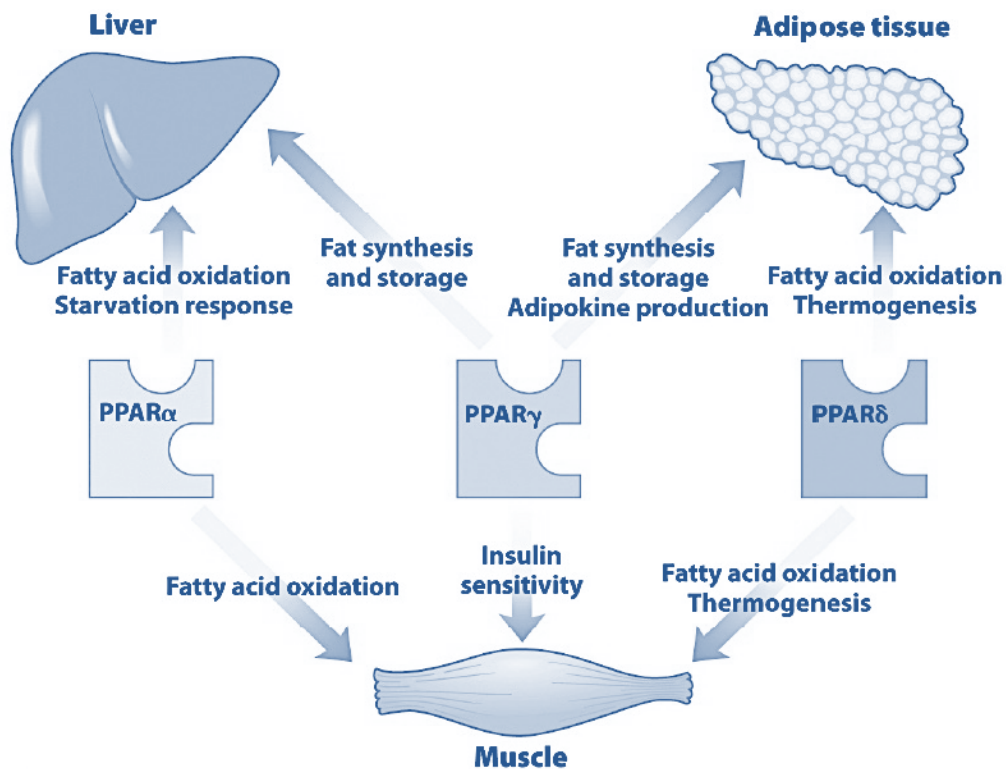


Figure 3. PPARs as metabolic regulators. Lipid and glucose homeostasis is maintained by the interacting roles of the three PPAR subtypes. The role of PPAR γ is to regulate lipid storage and insulin sensitivity, while PPAR α and PPAR δ/β counteract by regulating the lipid utilization and distribution. Picture source (Nelson et al., 2008)

Functional Domain Organization

PPARs exhibit four distinct functional domains that are shared by nearly all nuclear receptors. Starting at the N-terminal region, there is a ligand-independent domain with transcriptional activation function (AF-1), followed by a DNA binding domain (DBD), a hinge region providing flexibility between the functional parts of the protein, and finally a ligand binding domain (LBD) that includes a dimerization interface for retinoid X receptor (RXR) and a ligand-dependent activation function (AF-2) at its C-terminal region (Desvergne and Wahli, 1999; Ferré, 2004; Kota et al., 2005) (Fig 4).

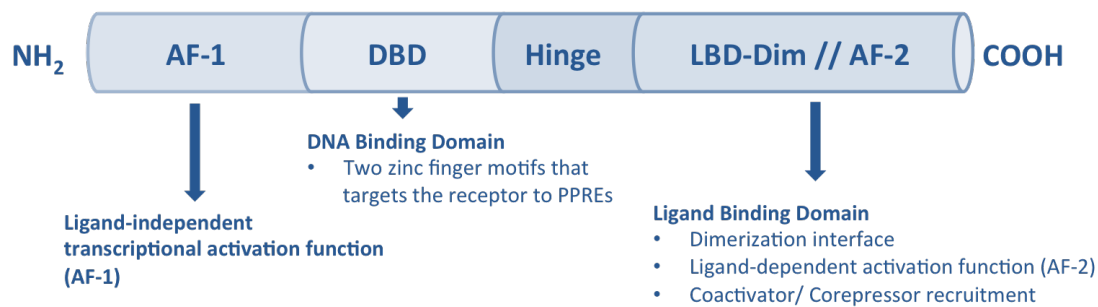


Figure 4. Schematic representation of a peroxisome proliferator-activated receptor (PPAR). General domain organization of a nuclear receptor is indicated. Illustration made by Sofie Söderström.

1.4.1.1 Ligand Binding and Activation of PPARs

PPARs bind to DNA as obligate heterodimers with the RXR (Desvergne and Wahli, 1999), and the heterodimerization is ligand-independent (Chandra et al., 2008) (Fig 5). The PPAR:RXR heterodimer is attached to specific DNA regulatory elements located in the promoter region of its target genes, denoted peroxisome proliferator response elements (PPREs). These response elements consist of two direct repeats of AGGTCA spaced with a single nucleotide (Ferré, 2004). While unbound to ligands, PPAR:RXR bound to PPREs will repress gene transcription because corepressors are associated to the heterodimer (Den Broeder et al., 2015). Upon binding of an endogenous or dietary PPAR agonist (e.g., fatty acids, fatty acid derivatives, phospholipids, eicosanoids, and prostaglandin) or RXR agonist (9-cis-retinoic acid) a conformational change occur in the PPAR:RXR heterodimer causing the corepressors to be released and coactivators to be recruited, further facilitating the docking of RNA polymerase and subsequent gene transcription of target genes (Fig 5) (Den Broeder et al., 2015; Ferré, 2004).

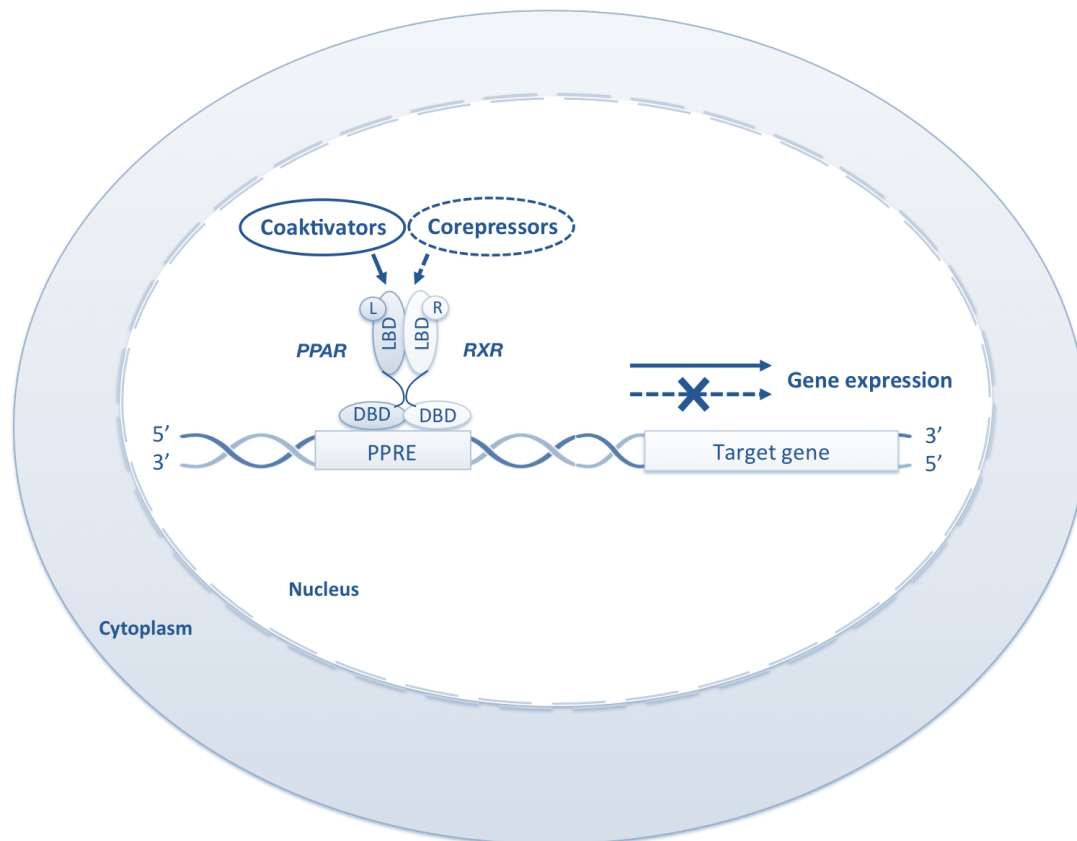


Figure 5. Peroxisome proliferator-activated receptors (PPARs) regulate transcriptional gene activation through heterodimerization with retinoid X receptor (RXR). The PPAR:RXR heterodimer binds at specific DNA regulatory elements called peroxisome proliferator response elements (PPREs) located in the promoter region of target genes. While unbound to ligands, PPAR:RXR heterodimers bound to PPREs will repress transcription due to the presence of corepressors. The PPAR:RXR heterodimer is permissive, i.e. either a PPAR agonists (L) or RXR agonist (R) can activate the PPAR:RXR complex, or by both ligands simultaneously. Ligand binding will cause corepressors to be released and coactivators to be recruited, allowing the transcription of the target genes. Illustration made by Sofie Söderström.

1.4.1.2 Endogenous and Dietary PPAR Ligands

Fatty acids are not only energy storing molecules but they also regulate metabolic processes through hormone-like signaling for transcription factors acting as lipid sensors, such as PPARs (Desvergne and Wahli, 1999; Kliewer et al., 1997; Varga et al., 2011). The shared structure for all fatty acids are the long carbon chains having a methyl group at one end and a carboxyl group at the other end of the molecule (one carboxyl group in monocarboxylic acids and two carboxyl groups in dicarboxylic acids). The most common saturated fatty acids have a chain length of 12-22 carbon atoms (often an even number), while monounsaturated fatty acids (MUFAs) have a chain length of 16-22 carbon atoms (Rustan and Drevon, 2005). Polyunsaturated fatty

acids (PUFAs) such as omega-3- and omega-6 fatty acids have a chain length of 18-22 carbon atoms (Holub, 2002) (Fig 6).

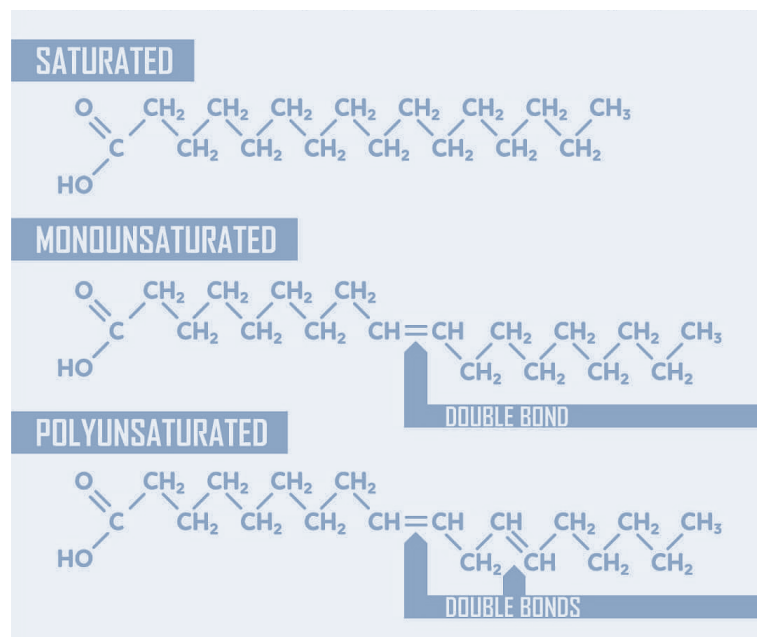


Figure 6. Fatty acids.

Schematic illustration of saturated-, monounsaturated-, and polyunsaturated fatty acids.

Picture originating from <http://ketogenic.com/wp-content/uploads/2017/01/Fat-Graphic.jpg>.

Due to their relatively large ligand binding pockets, PPARs are promiscuous compared to many other nuclear receptors as numerous ligands can bind with relatively low affinity (Kliwer et al., 2000; Varga et al., 2011). Endogenous and dietary fatty acids, fatty acid derivatives, phospholipids, eicosanoids (e.g. prostaglandin) are examples of endogenous ligands for PPARs (Chakravarthy et al., 2005; Delerive et al., 2000; Kliwer et al., 1997). MUFAs and PUFAs are more potent PPAR ligands than saturated FAs (Forman et al., 1997; Kliwer et al., 1997; Krey et al., 1997; Varga et al., 2011). Examples of eicosanoids, derived from 20 carbon long PUFA precursors, that are considered selective or potent agonists for human PPARs are 8(S)-hydroxyeicosatetraenoic acid (8(S)-HETE) for PPAR α (Choi and Bothwell, 2012; Ferré, 2004; Forman et al., 1997; Kliwer et al., 1997), 15-hydroxyeicosatetraenoic acid (15-HETE) for PPAR β/δ (Choi and Bothwell, 2012; Naruhn et al., 2010), and 15-deoxy- Δ 12,14-prostaglandin J₂ (15d-PGJ₂) for PPAR γ (Choi and Bothwell, 2012; Diab et al., 2002; Forman et al., 1995a; Kliwer et al., 1997; Sauer, 2015). Through *in vitro* transactivation assays with synthetic ligands, well-established agonists for the different mammalian PPAR subtypes have been identified, including WY14643 for PPAR α (Ip et al., 2004; Varga et al., 2011), GW501516 for PPAR β/δ (Barroso et al., 2011; Varga et al., 2011), and thiazolidinedione's (TZDs)

such as rosiglitazone (Rosi) for PPAR γ (Higgins and DePaoli, 2010; Lehmann et al., 1995; Sauer, 2015; Varga et al., 2011)

1.4.1.3 Exogenous PPAR Ligands

PPARs are normally activated by their natural ligands mentioned above. Although, *in vitro* transactivation assays have shown that several environmental contaminants are able to activate mammalian PPARs, such as phthalates and PFCs (Bility et al., 2004; Heuvel et al., 2006; Hurst and Waxman, 2003; Lapinskas et al., 2005; Shipley et al., 2004; Takacs and Abbott, 2007; Zhang et al., 2014). Mammalian PPARs have been studied quite extensively, however less information is currently available about teleost PPARs. This study will therefore test a set of structurally diverse contaminants comprised of both legacy- and emerging contaminants for agonistic effects on the Atlantic cod PPAR receptors. Contaminants have been selected according to relevance in regard to their presence in the marine environment and their structural characteristics. Environmental contaminants resembling fatty acids could be potential PPAR activators, for example both PFCs and phthalate molecules contain long carbon chains. One study has previously shown that human PPAR γ activation of perfluorinated carboxylic acids (PFCAs) increased with increasing carbon number up till C11 (Zhang et al., 2014). Another study showed mouse- and human PPAR α and PPAR γ activation of phthalates increased with increasing side-chain length of the molecules (Bility et al., 2004). Phthalates are not persistent in the environment and organisms rapidly metabolize them, however they are extensive and worldwide use in plastics and every day products (e.g., industrial paints, solvents, cosmetics, perfumes, medicines etc.), causing their continuous release and thus their prominent presence in the environment (Frederiksen et al., 2007). Acute or chronic exposure to exogenous ligands can cause an abnormal activation of the PPARs, where metabolic- or endocrine disruptions are possible consequences (Casals-Casas et al., 2008). For example, modulation of PPAR activation could disturb the regulation of their target genes and thus impact the lipid homeostasis.

1.5 Gene Reporter Assays to Study Ligand Binding and Transcriptional Activation

1.5.1 Luciferase Reporter Assay (LRA)

Luciferase reporter gene assays are established *in vitro* systems commonly used to study the function of different nuclear receptors (Bainy et al., 2013; Sotoca et al., 2010), including PPARs (Bility et al., 2004; Hurst and Waxman, 2003; Routti et al., 2016). These types of assays allow high-throughput ligand screening, and exhibit relatively low endogenous interference (Paguio et al., 2010). There are several types of reporter gene assays, and in this study a UAS/Gal4-DBD based luciferase reporter gene assay in a COS-7 simian kidney cell line has been established and utilized (Fig 7). In this system, COS-7 cells are co-transfected with a luciferase reporter gene plasmid harbouring a Gal4 upstream activation sequence (Gal4-UAS) that control the expression of a luciferase-encoding gene (Forman et al., 1995b), a β -galactosidase-encoding control plasmid (pCMV- β -Gal) that constitutively express β -galactosidase (through CMV promoter) (Blumberg et al., 1998), and an effector plasmid. The effector plasmid will constitutively express (through CMV promoter) the nuclear receptor-LBD of interest fused to the DBD acquired from Gal4; a transcription activator protein derived from yeast. When a ligand binds the LBD of the fusion protein, the protein will undergo a conformational change and become activated. This activation will make the fusion protein bind to the Gal4-UAS on the reporter plasmid via the Gal4-DBD. Thereby, the assembly of the transcription complex and docking of RNA polymerase will be facilitated, which in turn will initiate the transcription of the luciferase-encoding gene. After addition of luciferin, the translated luciferase protein will catalyse the oxidation of luciferin into the luminescent product, oxyluciferin. Ligand activation can thus be measured as luciferase activity, quantifiable as the amount of light (550-570 nm) emitted from the reaction it catalyzes (Fig 7).

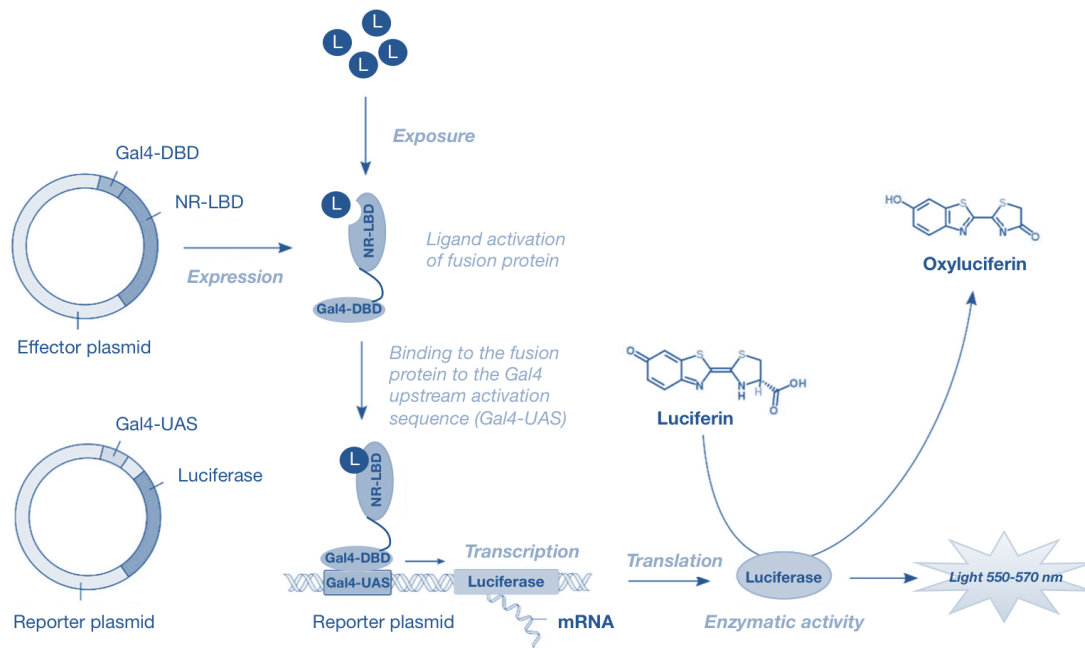
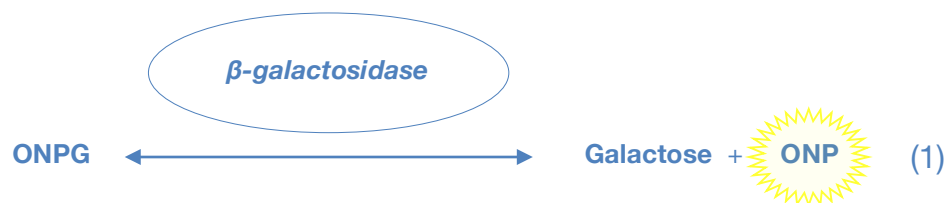


Figure 7. Luciferase reporter gene assay. The assay is performed by co-transfecting an effector plasmid containing the Nuclear Receptor (NR)-Ligand Binding Domain (LBD) fused to the Gal4-DNA binding domain (DBD) into COS-7 cells, together with a luciferase reporter gene plasmid. Luciferase will be expressed when the ligand-NR-LBD-Gal4-DBD fusion protein binds to the Gal4-Upstream activation sequence (UAS) in the reporter plasmid. Ligand activation of NR is measured as luciferase activity that can be quantified by the amount of light emitted during the conversion of luciferin into oxyluciferin (550-570 nm). Illustration source: modified version from Alexander Klevedal Madsen 2016.

The activity of β -galactosidase, measured at 420 nm, is used to normalize transfection efficiency between experimental replicates and experiments. By providing the β -galactosidase with the substrate ONGP (ortho Nitrophenyl- β -galactoside), it will catalyze the hydrolysis of ONGP into galactose and ONP (o-nitrophenol). ONP exhibits a yellow color and can be quantified by measuring the absorbance at 420 nm (Formula 1).



1.6 Objectives

Due to its habitats near offshore oil platforms, petroleum recovery facilities, as well as coastal industries and municipal wastewater treatment plants, Atlantic cod must cope with both legacy and emerging environmental contaminants. By studying how the Atlantic cod PPARs can bind and become activated by contaminants, especially by the emerging and far less documented ones, the main objective with this thesis is to contribute with new baseline data that can give insight into how the regulation of lipid- and carbohydrate metabolism in Atlantic cod can be modulated by environmental pollutants. This will be done by:

- Isolate and clone the hinge + ligand-binding domain (LBD) of the genes encoding PPAR α , PPAR β , PPAR δ , and PPAR γ from Atlantic cod.
- Phylogenetically examine and validate their identity as cod PPAR hinge+LBDs by comparison with PPAR-encoding genes from other relevant species.
- Examine Atlantic cod PPAR activation by using a luciferase gene reporter assays, i.e. to study their abilities to bind and become activated by a selected set of pollutants representing a structurally diverse group of compounds, including both legacy and emerging contaminants found in the NE Atlantic.

2 MATERIALS

2.1.1 List of Chemicals

Table 1. Chemicals and reagents utilized in the thesis.

Name	CAS #	Supplier
10x Loading buffer		TaKaRa
2-log DNA Ladder		New England Biolabs
5-CFDA-AM (5-Carboxyfluorescein Diacetate, Acetoxymethyl Ester)	124412-00-6	Thermo Fisher Scientific
Acetic acid	64-19-7	Sigma-Aldrich
Agar Agar	9002-18-0	Merck
Agarose	9012-36-6	Sigma-Aldrich
Ampicillin sodium salt	69-52-3	Sigma-Aldrich
ATP (Adenosine 5'-trifosfat dinatrium salthydrat)	34369-07-8	Sigma-Aldrich
Boric acid	10043-35-3	Sigma-Aldrich
Bovine Serum Albumin (BSA)	9048-46-8	Sigma-Aldrich
CHAPS hydrate	331717-45-4	Sigma-Aldrich
Chloroform	67-66-3	Sigma-Aldrich
Coenzyme A	18439-24-2	Fisher Scientific
Coomassie Brilliant Blue R250 staining solution		Bio-Rad
D-Luciferin Firefly	115144-35-9	Biosynth®
DDT (DL-Dithiothreitol)	3483-12-3	Sigma-Aldrich
DMSO (Dimethyl sulfoxide)	67-68-5	Sigma-Aldrich
Dulbecco's Modified Eagle's Medium (high glucose, with phenol red)		Sigma-Aldrich
Dulbecco's Modified Eagle's Medium (high glucose, without phenol red)		Sigma-Aldrich
EDTA (Ethylenediaminetetraacetic acid disodium salt dehydrate)	6381-92-6	Sigma-Aldrich
EGTA (Ethylene glycol-bis(2-aminoethylether)-N,N,N',N'-tetraacetic acid	67-42-5	Sigma-Aldrich
Ethanol	64-17-5	Sigma-Aldrich
Fetal Bovine Serum (FBS)		Sigma-Aldrich
GelRed		Botium
Glycerol	56-81-5	Sigma-Aldrich
Isooctane	540-84-1	Merck Millipore

Isopropanol	67-63-0	Sigma-Aldrich
L-Glutamine	56-85-9	Sigma-Aldrich
L- α -Phosphatidylcholine	8002-43-5	Sigma-Aldrich
Magnesium carbonate hydroxide pentahydrate	56378-72-4	Sigma-Aldrich
Magnesium chloride hexahydrate	7791-18-6	Sigma-Aldrich
Magnesium sulfate heptahydrate	10034-99-8	Sigma-Aldrich
Methanol	67-56-1	Sigma-Aldrich
ONPG (2-Nitrophenyl β -D-galactopyranoside)	369-07-3	Sigma-Aldrich
Opti-MEM. I Reduced Serum Medium		Gibco™
Penicillin-Streptomycin		Sigma-Aldrich
Phosphate-buffered saline (PBS) 10X		Sigma-Aldrich
Pierce™ 660nm Protein Assay Reagent		Thermo scientific
PMSF (Phenylmethanesulfonyl fluoride)	329-98-6	Sigma-Aldrich
Potassium chloride	7447-40-7	Sigma-Aldrich
Precision Plus Protein™ Kaleidoscope™		Bio-Rad
Prestained Protein Standards		
Resazurin sodium salt	62758-13-8	Sigma-Aldrich
SOC Outgrowth media		New England Biolabs
Sodium chloride	7647-14-5	Merck Millipore
Sodium hydroxide	1310-73-2	Merck Millipore
Sodium phosphate dibasic dihydrate	10028-24-7	Sigma-Aldrich
Sodium phosphate monobasic monohydrate	10049-21-5	Merck Millipore
Sodium pyruvate	113-24-6	Sigma-Aldrich
TransIT®-LT1		Mirus Bio LLC
TRI Reagent®		Sigma-Aldrich
Tricine	5704-04-1	Sigma-Aldrich
TriReagent	(T9424)	Sigma-Aldrich
Triton® X100	9002-93-1	Sigma-Aldrich
Trizma® base	77-86-1	Sigma-Aldrich
Trizma® phosphate dibasic	108321-11-5	Sigma-Aldrich
Trypan Blue solution 0.4%	72-57-1	Sigma-Aldrich
Trypsin-EDTA Solution 1X		Sigma-Aldrich
Trypton plus	91079-40-2	Sigma-Aldrich
Yeast extract		Fluka
β -Merkaptoethanol	60-24-2	Sigma-Aldrich

2.1.2 List of Equipment

Table 2. Listing of equipment and instruments utilized in the thesis.

Instrument	Application	Supplier
Bürker haemocytometer	Cell counting	Marienfeld
ChemiDoc™ XRS+ System	Gel scan	Bio-Rad
DOPPIO Thermal Cycler	PCR Thermo Cycler	VWR
EnSpire 2300 Multilabel Reader	Plate reader	PerkinElmer
G:BOX	Gel doc imaging system	Syngene
HS 501 Digital	Platform shaker	IKA-Werke
NanoDrop 1000	Spectrophotometer	Thermo Scientific
PowerPac™ HC	High-current power supply	Bio-Rad
Thermomixer compact	Heatblock	Eppendorf
Z 216 MK microliter centrifuge	Centrifuge	Hermle

2.1.3 List of Enzymes

Table 3. Listing of enzymes utilized in the thesis.

Enzymes	Application	Supplier
BamHI	Restriction endonuclease	TaKaRa
EcoRI	Restriction endonuclease	TaKaRa
PrimeSTAR® GXL DNA polymerase	PCR	TaKaRa
SuperScript® III RT	cDNA synthesis	Invitrogen
T4 DNA ligase	Ligation	TaKaRa

2.1.4 List of Kits

Table 4. SuperSignal West Pico Chemiluminescent Substrate

Kit	Supplier
NucleoBond® Xtra Midi plasmid purification kit	Macherey-Nagel
NucleoSpin® Gel and PCR Clean-up kit	Macherey-Nagel
NucleoSpin® Plasmid EasyPure ki	Macherey-Nagel
StrataClone Blunt PCR Cloning Kit	Agilent
SuperSignal West Pico Chemiluminescent Substrate	Thermo Scientific

2.1.5 List of Primers

Table 5. Primers designed to amplify and clone the hinge region and ligand binding domain (LBD) of Atlantic cod PPARs

ID	Primer name	Sequence (5' → 3')
MT993	PPARa-1 Fwd EcoRI	gaattcCAGTCGGAGAAACAGAGGTTGAAG
MT934	PPARa-1 Rev BamHI	ggatccTCAGTACATGTCCCTGTAAATCTCTTGC
MT935	PPARa-2 Fwd EcoRI	gaattcCAGTCGGAGAAGCTGAAGCTGA
MT936	PPARa-2 Rev BamHI	ggatccTCAGTACATGTCACGGTAGATCTCC
MT937	PPARdb COD Fwd EcoRI	gaattcTATGGACGCATGCCTGAAG
MT938	PPARdb COD Rev BamHI	ggatccCTAGTACATGTCTTTGTAGATCTCCTGC
MT1075	PPARg COD Fwd EcoRI	gaattcCTCCTCTACGACTCCTAC
MT1076	PPARg COD Rev BamHI	ggatccCTAATACAAGTCCTTCAGG

Lowercase indicate the restriction site for EcoRI in forward primer and for BamHI in reverse primer.

Table 6. Plasmid specific primers used for PCR colony screening and sequencing

ID	Primer name	Sequence (5' → 3')
	pSC-B Fwd (T3)	AATTAACCCTCACTAAAGGGA
	pSC-B Rev (T7)	GTAATACGACTCACTATAG
MT1077	pCMX Fwd	TGCCGTCACAGATAGATTGG
MT1078	pCMX Rev	ATTCTCTCTAGGTAGTTTGTCCA

2.1.6 List of Software and Online Tools

Table 7. Software and Online Tools utilized in this thesis

Software	Application	Provider
ApE- A plasmid Editor v 2.0.47	Primer evaluation	(Davis, 2012)
Chromato-vue TM-20 transilluminator	Agarose gel visualization	UVP, San Gabriel
Clustal Omega	Sequence alignments	EMBL-EBI
Ensembl	Genome database	(Cunningham et al., 2014)
Excel 2011	Data treatment and statistics	Microsoft
Jalview2.9.0b2	Visualization of alignments	(Waterhouse et al., 2009)
Mega 6.06	Phylogenetic analyzes	(Tamura et al., 2013)
Multiple Primer Analyzer	Primer evaluation	ThermoFisher
OligoEvaluator	Primer evaluation	Sigma-Aldrich
PowerPoint	Figures	Microsoft
Prism 6	Figures	GraphPad
UniProt	Protein database	(Consortium, 2014)
ExpASy Translate tool	Sequence translation	SIB Bioinformatics Resource Portal
ExpASy Compute pI/Mw tool	Comput. of theoretical Mw	SIB Bioinformatics Resource Portal

2.1.7 List of Cell Lines

Table 8. Cell lines utilized in this thesis

Cell line	Application
COS-7 cells	Eukaryote expression (African green monkey)
StrataClone Solo Pack competent cells	Prokaryote cloning (E. coli)

2.1.8 List of Vectors and Plasmids

Table 9. Vectors used for cloning and expression

Vector/ plasmid	Application
pSC-B-amp/kan	Prokaryote cloning vector
pCMX-Gal4-DBD	Eukaryote expression vector in LRA
Mh(100)x4tk luc-	Reporter plasmid in LRA
pCMV- β -Gal	Control plasmid in LRA

2.1.9 Growth Media

2.1.9.1 Bacterial Growth Media

Table 10. Bacterial growth media - Lysogeny broth (LB)

Component	LB-Agar (agar plates)	LB-Media
Tryptone	10 g/L	10 g/L
Yeast extract	5 g/L	5 g/L
Sodium chloride	10 g/L	10 g/L
Agar-agar	15 g/L	-
Ampicillin	ⁱ 100 mg/L	-

ⁱ Added after autoclaving at 121 °C for 30 minutes.

2.1.9.2 Cell Freezing Media

Table 11. Freezing media for storage of COS-7 cells

Component	Concentration
Dulbecco's modified Eagle medium (DMEM) with phenol red	1X
Fetal bovine serum (FBS)	10 %
L-glutamate	4 mM
Sodium-pyruvate	1 mM
Penicillin-Streptomycin	100 U/mL
Dimethyl sulfoxide (DMSO)	5 %

2.1.9.3 Cell Growth Media/ Cell Growth Media Used During Exposure

Table 12. Cell growth media/ cell growth media used during exposure of COS-7 cells

Component	Concentration
ⁱ Dulbecco's modified Eagle medium (DMEM)	1X
ⁱⁱ Fetal bovine serum (FBS)	10 %
L-glutamate	4 mM
Sodium-pyruvate	1 mM
Penicillin-Streptomycin	100 U/mL

ⁱ Cell growth media: DMEM with phenol red. Cell growth media used during exposure: DMEM without phenol red.

ⁱⁱ Super stripped FBS was used in the exposure media.

2.1.10 Buffers

2.1.10.1 LRA

Table 13. Cell lysis buffer (1X)

Component	Concentration
Tris-PO ₄ (pH 7.8)	25 mM
Glycerol	15 %
CHAPS	2 %
L- α -Phosphatidylcholine	1 %
BSA	1 %

Table 14. β -galaktosidase base buffer (1X)

Component	Concentration
Na ₂ HPO ₄	60 mM
NaH ₂ PO ₄	40 mM
KCl	10 mM
MgCl ₂	1 mM

Table 15. Luciferase base buffer (4X, pH 7.8)

Component	Concentration
Tricine	80 mM
(MgCO ₃) ₄ • Mg(OH) ₂ • 5H ₂ O	4.28 mM
EDTA	0.4 mM
MgSO ₄	10.68 mM

2.1.10.2 Cell Viability

Table 16. Triton lysis buffer

Component	Concentration
Tris-HCl (pH 7.4)	25 mM
NaCl	150 mM
EDTA	1 mM
Triton X-100	1 %
Glycerol	5 %

2.1.11 SDS-PAGE

2.1.11.1 12 % Resolving Gel

Table 17. Protocol for 10 mL 12 % resolving gel

Component	Concentration
Tris-HCl (pH 8.8)	375 mM
Acrylamide/bisacrylamide	12 %
SDS	0.1 %
Ammonium persulfate (APS)	0.1 %
N,N,N',N'-Tetramethylethane-1,2-diamine (TEMED)	0.1 %

2.1.11.2 4 % Stacking Gel

Table 18. Protocol for 5 mL 4 % stacking gel

Component	Concentration
Tris-HCl (pH 6.8)	125 mM
Acrylamide/bisacrylamide	4 %
SDS	0.1 %
Ammonium persulfate (APS)	0.1 %
N,N,N',N'-Tetramethylethane-1,2-diamine (TEMED)	0.2 %

2.1.11.3 1X SDS-PAGE-Running Buffer

Table 19. Protocol for 10X running buffer for SDS-PAGE

Component	Concentration
Tris	25 mM
Glycine	192 mM
SDS	0.1 %

2.1.12 Coomassie Brilliant Blue & WB

2.1.12.1 Staining/Destaining

Table 20. Coomassie Brilliant Blue R250 staining and destaining solutions

Component	Staining solution	Destaining solution
	Concentration	Concentration
Ethanol	40 %	40%
Acetic acid	10 %	10 %
Coomassie Brilliant Blue R250	0.1 %	-

2.1.12.2 1X Blotting Buffer

Table 21. Protocol for SDS-PAGE blotting buffer

Component	Concentration
Tris	25 Mm
Glycine	192 mM
Methanol	20 %
MilliQ	-

2.1.12.3 5X Tris Buffer Saline (TBS) (pH 7.5)

Table 22. Protocol for 5X TBS

Component	Concentration
Tris	24 g
NaCl	292.5 g
MilliQ	2000 mL

pH adjusted to 7.5 using 6 M HCl

2.1.12.4 0.05 % TBS-Tween

Table 23. Protocol for 0.05 % TBS-tween

Component	Concentration
5X TBS (Table 14)	1X
Tween 20	0.05 %
MilliQ	-

2.1.12.5 5 % Dry Milk**Table 24. Protocol for 5 % dry milk**

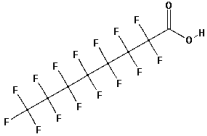
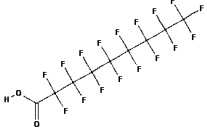
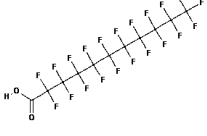
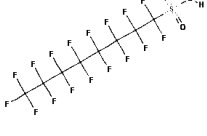
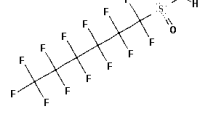
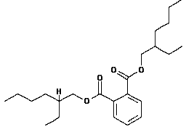
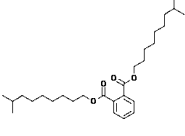
Component	Concentration
Dry milk	6.25 g
TBS-tween (Table 15)	125 mL

2.1.12.6 5X SDS-PAGE Sample Buffer (5XSB)**Table 25. Protocol for denaturing sample buffer used in SDS-PAGE**

Component	Concentration
TrisHCl (pH 6.8)	250 mM
SDS	10 %
Glycerol	30 %
β -Merkaptoethanol	5 %
Bromophenol blue	0.02 %

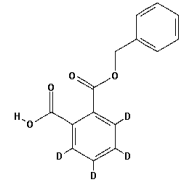
2.1.13 List of Ligands

Table 26. Ligands tested or used as agonists in this thesis

Ligand	Class	Structure
PFOA (Perfluorooctanoic acid)	Fluorosurfactant	
PFNA (Perfluorononanoic acid)	Fluorosurfactant	
PFUnDA (Perfluoroundecanoic acid)	Fluorosurfactant	
PFOS (Perfluorooctanesulfonic acid)	Fluorosurfactant	
PFHxS (Perfluorohexanesulfonic acid)	Fluorosurfactant	
DEHP (Di-2-ethylhexyl phthalate)	Phthalate	
DiDP (Di-isodecyl phthalate)	Phthalate	

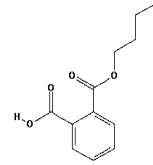
MBzP (mono-Benzyl phthalate)

Phthalate
(metabolite)



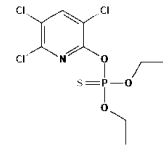
MBP (mono-Butyl phthalate)

Phthalate
(metabolite)



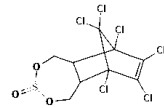
Chloropyrifos

Pesticide



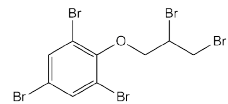
Endosulfan

Pesticide



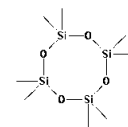
DPTE (2,3- dibromopropyl-2,4,6-tribromophenyl ether)

Brominated flame retardant



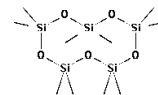
D4 (Octamethylcyclotetrasiloxane)

PPCPs



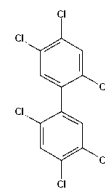
D5 (Decamethyl-cyclopentasiloxane)

PPCPs

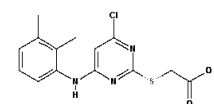


PCB 153 (2,2',4,4',5,5'-Hexachlorobiphenyl)

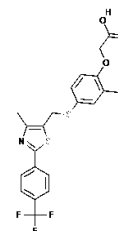
Organochlorine



WY14643

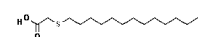
PPAR α agonist

GW501516

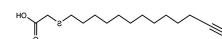
PPAR β/δ agonist

TTA (Tetradecylthioacetic acid)

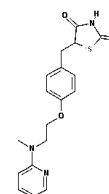
Synthetic fatty acid

1-triple-TTA
(2-(tridec-12-yn-1-ylthio) acetic acid)

Synthetic fatty acid

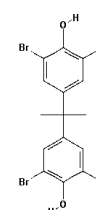


Rosi (Rosiglitazone)

PPAR γ agonist

TBBPA (Tetrabromobisphenol A)

Brominated flame retardant



All ligands were bought from Sigma-Aldrich, apart from TTA and its derivatives that were kindly provided by Haukeland University Hospital in Bergen, Norway.

3 METHODS

3.1 Atlantic Cod

Atlantic cod was acquired from the Institute of Marine Research (IMR)'s research station at Austevoll (Bergen, Norway). Cod were kept at ILAB (University of Bergen) in a 500 L reservoir with circulating seawater of 8 °C. The light/dark cycle was 12 hours dark and 12 hours light, and the cod were fed daily. The cod used in this study was a female that weighed 466 g.

3.2 RNA Extraction from Atlantic Cod Tissue

The cod was put to death by a blow to the head and subsequent severing of the spinal cord. Brain, heart, kidney, liver, muscle, and gill tissues were immediately harvested, and processed with TRI Reagent® (Sigma-Aldrich) according to the manufactures instruction; a liquid-liquid extraction technique revised from the work done by others (Aviv and Leder, 1972; Chomczynski, 1993; Chomczynski and Mackey, 1995; Louveau et al., 1991). The TRI Reagent contains phenol and guanidinium isothiocyanate, causing biological material to dissolve and protein to concurrently denaturate, while RNA remains intact through inhibition of RNase activity. Total RNA (totRNA) was extracted from the cod tissue by thoroughly homogenizing each tissue sample in 1 mL TRI Reagent per 100 mg tissue using a pellet pestle. The samples were then phase-separated by addition of chloroform and subsequent centrifugation using a Z 216 MK microliter centrifuge (HERMLE), leaving RNA in the upper aqueous phase, DNA in the interphase, and proteins in the lower organic phase. The aqueous phase containing the RNA could then carefully be recovered with a pipette, and further purified by precipitation by adding 0.5 mL 100 % isopropanol per 1 mL TRI Reagent used and subsequent centrifugation. The RNA pellet was washed with 75 % ethanol three times before air-dried for 10 minutes, and finally resuspended in 50 µL DEPC-treated water (0.1 %) and incubated at 60 °C using a Thermomixer compact (eppendorf) for 15 minutes. The concentration and purity of the extracted totRNA was measured spectrophotometrically (3.3), while the RNA integrity was assessed with denaturing RNA gel electrophoresis in TBE agarose gels (3.4).

3.3 Spectrophotometric Measurements - NanoDrop

The concentration (ng/ μ L) and purity ($A_{260/280}$, $A_{260/230}$) of RNA and DNA (including plasmids) prepared throughout this study were measured spectrophotometrically with a NanoDrop 1000 (Thermo Scientific). RNA and DNA have absorbance maximum at 260 nm, while proteins have an absorbance maximum at 280 nm. The ratio in absorbance between these wavelengths is commonly used to assess purity of the nucleic acid preparation; where RNA is considered pure at $A_{260/280} \sim 2.0$, and DNA at $A_{260/280} \sim 1.8$. $A_{260/230}$ is also calculated, since absorbance at 230 nm may indicate contamination of salts and certain solvents, e.g. phenol. The sample would be considered free from such contamination when $A_{260/230} \sim 2.0$ -2.2.

3.4 Agarose Gel Electrophoresis

Agarose gel electrophoresis (AGE) was used to separate and analyze nucleic acid molecules (i.e., RNA, amplicons and plasmids). The current used to create the electrical field in the electrophoresis is mainly carried by the ions in the running buffer. Since the agarose gel is prepared in the same buffer, current will also run through the gel and cause migration of the negatively charged nucleic acid towards the anode. The percentage of agarose in the gel will determine its density, and hence the surface resistance acting on the migrating nucleic acids. The separation of the nucleic acids will therefore depend on their shape and size. Nucleic acid samples that were separated and analyzed with AGE in this study were prepared with a 10X loading dye before loaded into the wells in the agarose gel. This loading dye contains two different dyes i.e., xylene cyanol FF and bromophenol blue. When run on a 0.5X TBE agarose gel, bromophenol blue migrates approximately equivalent to an 300 bp linear double stranded nucleic acid molecule, and xylene cyanol FF equivalent to an 4000 bp linear double stranded nucleic acid molecule (Kumar and Garg, 2005), thus allowing approximate visual tracking of the nucleic acid's migration and separation. In addition, the loading dye also contains glycerol that will increase the density of the nucleic acid samples and thereby reduce dispersion. In this study, all gels were made with 0.7 % agarose and 0.5X TBE, and nucleic acids were stained with GelRed (Biotium). A 2-log DNA Ladder was used as a molecular weight standard, and the running conditions were set to 110 V for 25 minutes using a PowerPac™ HC (Bio-Rad). The nucleic acids separated on the gels were visualized with UV-light and photographed using a G:BOX (Syngene).

3.4.1 Denaturing RNA Electrophoresis in TBE Agarose Gels

The highest percentage (>80 %) of purified totRNA is comprised of ribosomal RNA (rRNA), predominantly the 28S and 18S rRNA subunits (in a ~2:1 ratio). Messenger RNA (mRNA) species only makes out approx. 1-3 % of the totRNA and is thus difficult to visualize on agarose gels. Instead, distinct bands representing the 28S and 18S rRNA after separation of total RNA on agarose gels are conventionally considered to reflect the integrity of mRNA species as well. Thus, RNA quality of each sample were assessed by separating 200 ng of totRNA with 0.5X TBE agarose gel electrophoresis (3.4) under denaturing conditions, i.e. secondary structures (internal hairpin loops) were disrupted by chemical (formamide, 50 % v/v) and thermal (65 °C, 5 minutes) denaturation prior to the electrophoresis. RNA samples were thereafter stored at -80 °C until further use.

3.5 Synthesis of Complementary DNA from Total RNA - Reverse Transcription

Single stranded complementary DNA (cDNA) was synthesized from the previously extracted totRNA, using SuperScript® III RT (Invitrogen). This reverse transcriptase (RT) enzyme uses mRNA transcripts as templates, and together with suitable oligonucleotide primers, it synthesizes cDNA strands. The Oligo(dT) primers used were 12-18 deoxy-thymine nucleotides long; they hybridizes to the 3' poly(A) tail of the mRNA transcripts, and thereby facilitating full-length cDNA synthesis. Secondary structures on the mRNA template could potentially lead to interruption of the transcription. Therefore, random hexamer primers were used in addition to oligo(dT)'s. Random hexamers are shorter oligonucleotides (six nucleotids long with random base sequences), which will bind un-specifically to the mRNA transcripts giving a more even coverage of the entire mRNA template. RNA/primer mixtures were prepared according to Table 27:

Table 27. RNA/primer mixture for reverse transcription

Component	Concentration/amount
totRNA	2 µg
Oligo (dT) ₁₂₋₁₈	500 ng
Random hexamers	50 pmol
Deoxynucleosid triphosphates (dNTPs) mixture	0.5 mM
DEPC-treated MilliQ water	-

The RNA/primer mixture were denatured at 65 °C for 5 minutes using a Thermo Cycler (DOPPIO Thermal Cycler with dual 48 well blocks, VWR). The samples were subsequently placed on ice for 1 minute, allowing the primers to anneal to the RNA templates. The RNA/primer mixtures were then supplemented with a cDNA synthesis mix, which was prepared in the following order (Table 28):

Table 28. cDNA synthesis mix for reverse transcription

Component	Concentration/amount
First strand buffer (incl. MgCl ₂)	1X
DDT	5 mM
RNaseOUT™	2 U/µL
SuperScript III RT	10 U/µL

The RNA/primer/cDNA synthesis mixtures were then further incubated in the Thermo Cycler at 50 °C for 50 minutes. The reaction was then terminated at 80 °C for 5 minutes. The mixtures were cooled on ice, before Ribonuclease H (RNase H) (0.1 U/ µL) was added and further incubated an additional 20 minutes at 37 °C to remove any excess mRNA from the mixtures and avoid RNA:DNA hybridization. The cDNA was then stored at -25 °C until further downstream applications.

3.6 Isolation and Amplification of the Atlantic Cod PPARs

Polymerase chain reaction (PCR) is an *in vitro* method used to isolate and amplify specific DNA sequences (Mullis, 1990). In this case PCR was used to isolate and amplify fragments of the genes encoding the four different subtypes of Atlantic cod PPARs, specifically the hinge region and the ligand-binding domain. This was achieved by using the synthesized cDNA as template and the thermostable PrimeSTAR® GXL DNA polymerase (TaKaRa), which is a proofreading DNA

polymerase producing blunt-end PCR products. The amplification reaction was prepared according to the manufacturers instruction (Table 29):

Table 29. Reaction mixture for PCR using PrimeSTAR® GXL DNA polymerase

Component	Concentration/ amount
cDNA as template	2 µL
PrimeSTAR GXL buffer (with Mg ²⁺)	1X
dNTPs	200 µM of each
ⁱ Forward (fwd) primer	0.2 µM
ⁱ Reverse (rev) primer	0.2 µM
PrimeSTAR® GXL DNA polymerase	1.25 U
MilliQ water	(Up to 25 µL total volume)

ⁱ*Synthetic oligonucleotide primer sequences that had been designed to amplify the Atlantic cod PPAR_x hinge+LBD (see 3.6.1 below).*

The PCR was run in thermal cycles (Table 30) using a Thermo Cycler (DOPPIO Thermal Cycler with dual 48 well blocks, VWR). Each cycle included three temperature shifts allowing three events to occur: 1) Denaturation: the temperature was increased to 98 °C to disrupt any hydrogen bonds between base pairs. 2) Annealing: the temperature were lowered to allow the primers to anneal to the template strands by forming hydrogen bonds, and thus specifying the location of the segment of interest. 3) Extension: the temperature was raised to the temperature optimum of the DNA polymerase, where the primer sequences facilitated the starting point of where the dNTPs should be assembled by the DNA polymerase, i.e. the primers became part of the newly synthesized strands, also allowing restriction sites to be introduced to the amplified Atlantic cod PPAR_x-hinge+LBD.

Table 30. PCR thermal cycle program

Cycle		Temperature	Duration
2	Denaturation	98 °C	10 seconds
	Annealing	50 °C	15 seconds
	Extension	68 °C	1 minute/kb
28	Denaturation	98 °C	10 seconds
	Annealing	ⁱ 55 °C	15 seconds
	Extension	68 °C	1 minute/kb

ⁱ*Annealing temperature increased after 2 cycles to 55 °C, due to the introduction of the restriction sites in the primer ends increased their T_m after the 2 first cycles.*

3.6.1 Primer Design

The primers used to amplify the Atlantic cod PPAR_x-hinge+LBD was based on the predicted PPAR gene-encoding sequences available in the Ensembl cod genome database: PPAR_α ENSGMOG00000005934; PPAR_{αβ} ENSGMOG00000001060; PPAR_{β/δ} ENSGMOG00000008225; and PPAR_γ ENSGMOG00000001375. However, the PPAR_γ-encoding sequence deposited in the Ensembl database was lacking the 3'-end of the gene-encoding sequence, and therefore had to be supplemented with new sequencing data provided by collaborators at CEES – Centre for Ecological and Evolutionary Synthesis, University in Oslo. To achieve proper primer function, primers should be designed to meet a few favorable criteria. This includes: 1) Sufficient length to allow specificity to the DNA segment of interest, though still short enough to be able to anneal the DNA strand at annealing temperature. 2) In order for the temperature cycling program to work on both fwd and rev primer simultaneously, their guanine (G) and cytosine (C) content needs to be fairly similar and evenly distributed along the primers since it will affect their melting temperature (*T_m*). 3) To make the annealing of the primer to the cDNA template more robust, it is an advantage to give the 3'-end of the primer a GC clamp, as the bond between G-C is stronger than A-T. 4) To avoid formation of primer-dimers and hairpin structures, fwd and rev primers should exhibit low complimentary sequence to each other as well as not being self-complimentary. Primer-dimers and secondary structures may reduce the number of active primers in the amplification reaction. Thus, the primers designed to amplify the Atlantic cod PPAR_x-hinge+LBD were between 24-34 nucleotids long, exhibited a GC content between 47-52 %, had a *T_m* that did not differ more than 3 °C between primer-pairs, and contained one to two guanine or cytosine-nucleotides for clamping the 3'-ends. For constructing the Gal4-DBD-PPAR_x-hinge+LBD fusion proteins, the PPAR_x-hinge+LBD had to be restriction enzyme digested from a cloning vector, and ligated into an expression vector. Introducing an EcoRI-restriction site to the 5'-end of the fwd primers, and a BamHI-restriction site to the 5'-end of the rev primers facilitated the translocation of the PPAR_x-hinge+LBD into the eukaryotic expression vector, which contained the same restriction sites within its multiple cloning site (MCS). The primers tendency to form secondary structures was assessed *in silico*, using the online programs OligoEvaluator (Sigma-Aldrich), Multiple Primer Analyzer (ThermoFisher), and ApE (v.2.0.47). The designed primers were ordered from Sigma-Aldrich (Table 5)

3.6.2 Purification of PCR Products Through Gel Extraction

The PCR products were analyzed and separated with AGE (3.4). The DNA fragments were only briefly visualized with UV-light using a chromato-vue TM-20 transilluminator (UVP, San Gabriel) to reduce the risk of causing damage to the DNA. The DNA fragments that corresponded to the expected sizes of the PPAR_x-hinge+LBD were excised from the gel, and purified using NucleoSpin® Gel and PCR Clean-up kit (MACHEREY-NAGEL) according the manufacturers instructions. The excised gel slices were dissolved in a buffer with high ionic strength at 50 °C for 10 minutes before centrifuged through a silica-based column in a Z 216 MK microliter centrifuge (HERMLE). The DNA fragments bound to the column. The column-bound DNA was washed with an ethanolic buffer to remove impurities, and subsequently centrifuged dry from any residual ethanol. Purified DNA was then eluted in 25 µL of a slightly alkaline elution buffer with low ionic strength. The concentration of the gel extracted DNA was measured spectrophotometrically with a NanoDrop 1000 (3.3)

3.7 Molecular Cloning

A plasmids ability to replicate separately from bacterial chromosomal DNA was exploited by transforming recombinant DNA (rDNA) into a prokaryotic host cell and allowing it to be replicated in large amounts *in vivo*. rDNA was constructed *in vitro* by recombining the blunt PCR product with a blunt cloning vector, using the StrataClone Blunt PCR Cloning Kit (Agilent), according to a modified version of the manufacturers protocol.

3.7.1 Ligation

The PPAR_x-hinge+LBD was ligated into a linearized StrataClone Blunt PCR Cloning Vector (pSC-B-amp/kan) by forming phosphodiester bonds through Topoisomerase I ligase activity, creating a linear vector^{ori}-PPAR_x-hinge+LBD-vector^{amp/kan} (Fig 8).

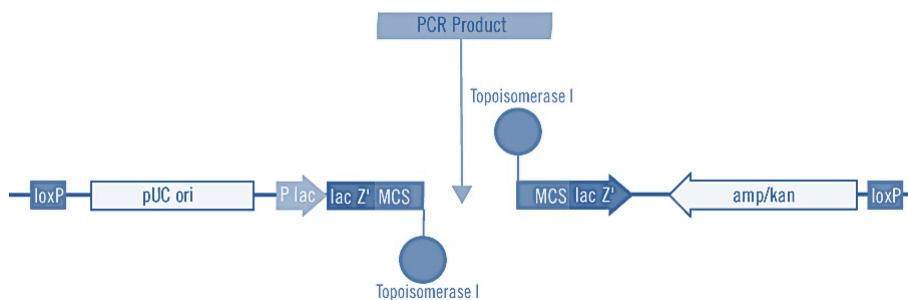


Figure 8. Linear StrataClone Blunt PCR Cloning Vector (pSC-B-amp/kan). The PCR products (amplicons of Atlantic cod PPAR α -hinge+LBD) are ligated into the multiple cloning site (MCS) of the cloning vector. Source: StrataClone Blunt PCR Cloning Kit (Agilent) (MANUAL)

Preparation of the ligation mixtures were made accordingly (Table 31):

Table 31. Ligation mixture - StrataClone Blunt PCR Cloning Kit

Component	Volume
StrataClone Blunt Cloning Buffer	1.5 μ L
Purified PCR product	2 μ L
StrataClone Blunt Vector Mix amp/kan	0.5 μ L

The components were added from top to bottom order, and incubated at room temperature (RT) for 5 minutes before put on ice.

3.7.2 Transformation

The ligation mixture containing the linear vector^{ori}-PPAR α -hinge+LBD-vector^{amp/kan} prepared in the previous step was transformed by the heat-shock procedure into StrataClone Solo Pack competent *E. coli* cells. These competent cells are transiently expressing Cre recombinase. The activity of this enzyme mediates the recombination of the linear vector^{ori}-PPAR α -hinge+LBD-vector^{amp/kan} into a circular plasmid (Fig 9), which can then be transcribed, translated, and expressed by *E. coli*. Transformation mixtures were prepared by adding 3 μ L ligation mixture to 25 μ L competent *E. coli* cells. To achieve an abrupt temperature change, the transfection mixtures were kept on ice for 20 minutes prior to the heat-shock. The heat-shock was carried out in a 42 °C warm water bath (GD100, Grant), and the transformation was allowed to occur for 45 seconds before putting the transfection mixtures back on ice for 5 minutes.

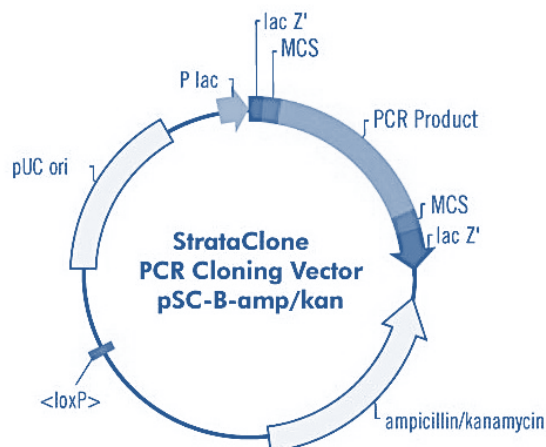


Figure 9. Circular StrataClone Blunt PCR Cloning Vector (pSC-B-amp/kan). Source: StrataClone Blunt PCR Cloning Kit (Agilent) (MANUAL)

3.7.3 Plating of Transformed *E. coli*

Positive transformants, i.e. *E. coli* that has acquired recombinant plasmid-DNA from the previous step, were selected for by their ampicillin (amp)-resistance provided by the “amp-gene” in the cloning vector. The heat-shocked cells were added 475 μ L SOC-media and allowed an outgrowth period of 1 hour, at 37 °C and 300 rpm, before plated onto petri dishes with lysogeny broth (LB)-agar containing amp (0.1 mg/mL) and incubated over night (ON) at 37 °C.

3.8 Identifying Positive Transformants By PCR Colony Screening

Selection of positive transformants only by ampicillin resistance does not guarantee that the plasmids taken up by the *E. coli* cells contain the insert of interest. For instance, the vector could have re-ligated without the insert, or have become contaminated with some other unwanted DNA. Single colonies of positive transformants were screened through colony PCR, using vector specific primers and a DreamTaq DNA polymerase (Thermo Scientific) to establish if the inserts are of the expected lengths corresponding to the PPARx-hinge+LBD. The colony PCR reaction mixtures were prepared according to Table 32:

Table 32. Reaction mixture for colony PCR using DreamTaq DNA polymerase

Component	Concentration/ amount
Positive transformants as template	2 μ L
Taq Green Buffer	1X
dNTPs	200 μ M
Vector specific fwd primer	0.5 μ M
Vector specific rev primer	0.5 μ M
DreamTaq DNA polymerase	0.0125 U/ μ L
MilliQ water	(Up to 10 μ L total volume)

The colony PCR was run in thermal cycles (Table 33) using a Thermo Cycler (DOPPIO Thermal Cycler with dual 48 well blocks, VWR).

Table 33. Colony PCR thermal cycle program

Cycle		Temperature	Duration
	Initial denaturation	95 °C	2 minutes
	Denaturation	95 °C	30 seconds
35	Annealing	55 °C	30 seconds
	Extension	72 °C	1 minute/kb

The colony PCR products were evaluated with AGE (3.4). Positive transformants of interest were then inoculated under selective conditions, and plasmids were purified (3.9.1). The inserts of the plasmids were verified through sequencing (3.10).

3.9 Plasmid Purification

Depending on the requirement of downstream applications, cloning vectors were purified with different yields and purity levels. Minipreparation (mini-prep) is a fast way to purify a small amount of cloning vectors, and was used when the purpose was to determine if the vectors contained the PPARx-hinge+LBD insert of interest. When the PPARx-hinge+LBD insert was confirmed, midipreparations (midi-prep) were made to purify larger amounts of receptor plasmids, as well as effector- and control plasmids used in ligand activation analyses. In addition to providing a larger yield, midi-preps also generates purer preparations in contrast to mini-preps. However, the principles of the two isolation techniques are the same. Transformed *E. coli* was inoculated in LB-media under selective conditions (amp) ON. ON cultures were centrifuged the next day, and the resulting pellets were resuspended in resuspension

buffer containing RNase. RNaseA will, after lysis, prevent co-purification of bacterial RNA. The cells in the resuspension buffer were lysed by sodium dodecyl sulfate (SDS) / sodium hydroxide (NaOH) lysis. SDS, which is an ionic detergent, will disrupt cell membranes and destabilize hydrophobic interactions, thereby preventing bacterial cells to keep their integrity and promote lysis. The high alkaline pH caused by NaOH will make some ionizable groups of protein and DNA to ionize and other to deionize, thus causing the DNA to denature into single strands. Hence, denatured chromosomal DNA, RNA and proteins together with plasmid DNA will be released from the cells into the supernatant (Vennison, 2010). A neutralization buffer, containing potassium acetate (KOAc), was added to the cell lysate. KOAc lowers the pH of the solution sufficiently for allowing plasmid DNA to renature. Because plasmid DNA is small, circular, tightly supercoiled, and topologically intertwined, it will not fully separate during high pH; hydrogen bonding between base pairs will be disrupted, though the plasmid DNA will manage to renature correctly when pH is lowered again, if intensity and duration of the high pH condition is not too high. Proteins and the larger bacterial chromosomes on the other hand, will not be able to renature properly. Instead, denatured bacterial chromosomal DNA, proteins, and cell wall debris will form hydrophobic, ionic, and hydrogen bonds with each other creating large aggregates that will precipitate from the solution together with potassium dodecyl sulfate (KDS) (Vennison, 2010), thus allowing it to be pelleted and removed by centrifugation. The supernatant from the cell lysate was then bound to a silica-based column under high ionic conditions through either centrifugation in the mini-prep, or by gravity flow filtration in the midi-prep. The column-bound plasmid DNA was then washed with a buffer supplemented with ethanol (EtOH), removing residual lysate and impurities from the column. DNA molecules are negatively charged due to their backbone phosphates; hence they are highly soluble in water but insoluble in organic solvents, i.e., the wanted plasmid DNA was precipitated from the supernatant by adding EtOH to the supernatant solutions. After an additional EtOH wash, the pellets were dried at RT before dissolved in an elution buffer.

3.9.1 Mini-Prep

Small-scale plasmid purification was done prior to sequencing of cloned DNA fragments. *E. coli* colonies that showed promise to contain the recombinant plasmid of interest after colony screening (cloning plasmid: pSC-B-PPARx-hinge+LBD, effector

plasmid: pCMX-Gal4-DBD-PPAR α -hinge+LBD), were inoculated in 3 mL of LB media containing ampicillin (0.1 mg/mL). The bacteria cultures were incubated ON at 37 °C with shaking (250 rpm). Using a NucleoSpin® Plasmid EasyPure kit (Macherey-Nagel), plasmid DNA from ON cultures was isolated, purified, and eluted in a slightly alkaline elution buffer under low ionic condition. The yield was determined spectrophotometrically using a NanoDrop 1000 (3.3).

3.9.2 Midi-Prep

Medium-scale plasmid purification was done for preparation of effector plasmids (pCMX-Gal4-DBD-PPAR α -hinge+LBD), in addition to receptor- and control plasmids, used for ligand activation analysis (LRA). *E. coli* colonies, transfected with the LRA plasmids, were inoculated in 200 mL of LB media containing ampicillin (0.1 mg/mL). The inoculation was incubated ON at 37 °C and 250 rpm shaking. Plasmid DNA from the ON culture was isolated and purified using the NucleoBond® Xtra Midi plasmid purification kit (Macherey-Nagel), according to manufactures instruction with the exceptions: starter cultures were omitted, the OD was not measured, and purified plasmid DNA was reconstituted in an elution buffer (Omega) under high ionic condition by a shift from acidic to alkaline pH. The eluted DNA from the midi-prep was then further purified by isopropanol precipitation. The yield was determined spectrophotometrically using a NanoDrop 1000 (3.3).

3.10 DNA Sequencing

Sequencing of cloned DNA fragments was performed by the sequencing facility at the Department of Molecular Biology, University of Bergen, which uses automated Sanger DNA Sequencing with a 3730XL Analyzer (Applied Biosystems™). In Sanger DNA sequencing, a DNA polymerase carries out amplification of the DNA as normal using regular deoxynucleotides (dNTPs). However, in addition to the dNTPs, four fluorescently labeled dideoxynucleotides (ddNTP) (conjugated with different chromophores for each of the four ddNTPs) are added to the amplification-reaction. The ddNTPs are lacking a 3'-hydroxyl group, which thus prevents the formation of phosphodiester bonds to other nucleotides. Thus, if the DNA polymerase incorporates a ddNTP it will cause the elongation of the DNA strand to terminate, leaving the corresponding fluorescently conjugated ddNTP at the 3'-end of the extension product. The incorporation of a ddNTPs instead of a dNTPs will be random (due to a specific ratio between ddNTPs and dNTPs in the reaction mixture), resulting in DNA

fragments of all possible fragment lengths. These extension products are then separated by capillary electrophoresis that resolves them according to molecular weight by the precision of one nucleotide in difference. When eluted from the capillary, the separated and fluorescently labeled extension products are subjected to a laser beam that makes them fluorescent. Each of the four ddNTPs emits light at its specific wavelength (due to the different conjugated chromophores), producing a chromatogram that allows specific identification of the four bases and deduction of the DNA sequence. The sequencing reactions were prepared according to the BigDye terminator v 3.1 protocol (Table 34) and run in thermal cycles (Table 35) using a Thermo Cycler (DOPPIO Thermal Cycler with dual 48 well blocks, VWR).

Table 34. BigDye terminator v 3.1 protocol for DNA sequencing

Component	Concentration/ amount
Plasmid DNA as template	200 ng
BigDye sequencing buffer	1X
Plasmid specific primer	3.2 pmol
Big-Dye version 3.1	1 μ L
MilliQ water	(Up to 10 μ L total volume)

Table 35. Thermal cycle program for DNA sequencing

Cycle		Temperature	Duration
1	Initial denaturation	96 °C	5 minutes
	Denaturation	96 °C	10 seconds
25	Annealing	50 °C	5 seconds
	Extension	60 °C	4 minutes

Each reaction was diluted with an additional 10 μ L MilliQ (total volume 20 μ L) after terminated thermal cycle program.

3.11 Effector Plasmids Construction

Effector plasmids to be used in the ligand activation analysis were constructed by fusing the Atlantic cod PPAR α -hinge+LBD into a pCMX-Gal4-DBD vector. This was done by restriction digestion, dephosphorylation, and ligation. The effector plasmids (pCMX-Gal4-DBD-PPAR α -hinge+LBD) will thereby encode a fusion protein of the Gal4-DBD and the PPAR α -hinge+LBD that becomes functional in the LRA.

3.11.1 Restriction Digestion

First, the PPAR_x-hinge+LBD had to be digested out from the cloning vector (pSC-B-PPAR_x-hinge+LBD), before they could be subcloned into the effector plasmid backbone (pCMX-Gal4-DBD). Restriction endonucleases are enzymes that are able to recognize restriction sites (or recognition sequences) in DNA, and they catalyze the hydrolysis of phosphodiester bonds, hence cleaving the DNA into smaller fragments. Here, the restriction sites, BamHI and EcoRI, added to the PPAR-LBDs are also present in the MCS of the pCMX-Gal4-DBD vector. Thus, digestions with the same restriction enzymes allow the PPAR_x-hinge+LBD and the pCMX-Gal4-DBD vector to get compatible ends allowing them to be joint together. Five different restriction digestion reactions were prepared according to Table 36:

Table 36. Protocol for restriction digestion reactions

	pCMX	PPAR _α	PPAR _β	PPAR _δ	PPAR _γ
DNA	10 µg	1 µg	1 µg	1 µg	1 µg
EcoRI	0.5 U/µL	0.5 U/µL	0.5 U/µL	0.5 U/µL	0.5 U/µL
BamHI	0.5 U/µL	0.5 U/µL	0.5 U/µL	0.5 U/µL	0.5 U/µL
BSA	0.01%	0.01%	0.01%	0.01%	0.01%
K-buffer	1X	1X	1X	1X	1X
MilliQ	up to 60 µL	up to 60 µL	up to 60 µL	up to 60 µL	up to 60 µL

The reactions were incubated at 37 °C for 1.5 hours, and the resulting DNA fragments were separated using AGE (method AGE). The linearized DNA fragments corresponding to the expected lengths of the pCMX vector and the four PPAR-hinge+LBDs, were purified through gel extraction using NucleoSpin® Gel and PCR Clean-up (Macherey-Nagel) (3.6.2), and eluted in 20 µL elution buffer. The concentration of the purified pCMX-Gal4-DBD vector and PPAR_x-hinge+LBD were measured spectrophotometrically using a NanoDrop 1000 (3.3).

3.11.2 Dephosphorylation

Dephosphorylation by Shrimp Alkaline Phosphatase (SAP) was used to prevent re-ligation of the linearized pCMX vector. SAP removes the 5'-end phosphate group on the pCMX-Gal4-DBD vector, which are exposed after the restriction digestion. The dephosphorylation reaction was prepared as described in Table 37, where the volume needed for 1 pmol DNA ends was calculated using (Formula 2). The reaction mixture

was incubated at 37 °C for 45 minutes, before SAP was inactivated at 65 °C for 15 minutes.

Table 37. Dephosphorylation protocol using SAP

Component	Concentration/ amount
Gel extracted pCMX-Gal4-DBD vector	1 pmol DNA ends
SAP Buffer	1X
SAP	1 U
MilliQ water	(Up to 20 µL total volume)

$$\mu\text{g DNA} \times \frac{\text{pmol}}{660\text{pg}} \times \frac{10^6\text{pg}}{1\mu\text{g}} \times \frac{1}{N} \times 2 \times \frac{\text{kb}}{1000\text{bp}} = \text{pmol DNA ends} \quad (2)$$

N is the number of nucleotides (in kb), 660 pg/pmol is the average molecular weight of a single nucleotide pair, 2 is the number of ends in a linear DNA molecule, kb/1000bp is a conversion factor for kilobases to base pairs.

3.11.3 Ligation

The effector plasmids, pCMX-Gal4-DBD-PPARx-hinge+LBD, were finalized by ligating the purified PPARx-hinge+LBD fragment into the linearized and purified pCMX-Gal4-DBD vector using a T4 DNA ligase (TaKaRa). The ligation occurs in three main steps. First, adenylation of the T4 DNA ligase will occur when it reacts with free ATP, forming a ligase-AMP intermediate. Second, the AMP, which still is attached to the T4 DNA ligase, will then be transferred onto the DNA strand with a free 5'-phosphate group forming a DNA-adenylate bridge structure. Finally, the T4 DNA ligase will then catalyse the phosphodiester bond formation between the 5'-phosphate group of the DNA-adenylate bridge structure and the 3'-hydroxyl group of the nearby DNA strand, and thus the AMP is released from the T4 DNA ligase. Four different ligation reactions were prepared, one for each PPARx-hinge+LBD, as described in Table 38. The reactions were incubated at 12 °C for 16 hours, before the T4 DNA ligase was inactivated at 65 °C for 15 min.

Table 38. Ligation protocol using T4 DNA ligase

	PPAR α	PPAR β	PPAR β/δ	PPAR γ
pCMX-Gal4-DBD	25 ng	25 ng	25 ng	25 ng
PPARx insert	i	i	i	i
T4 buffer	1X	1X	1X	1X
T4 DNA ligase	17.5 U/ μ L	17.5 U/ μ L	17.5 U/ μ L	17.5 U/ μ L
MilliQ	up to 10 μ L	up to 10 μ L	up to 10 μ L	up to 10 μ L

*i*required mass insert (ng) = desired insert/vector molar ratio (i.e., 3:1) x mass of vector (ng) x ratio of insert to vector length.

The ligation products were transfected into StrataClone Solo Pack competent cells (Agilent). This was followed by mini-prep (3.9.1), colony screening (3.8), and sequencing (3.10) to verify the presence of the PPARx-hinge+LBD in the pCMX-Gal4-DBD vector, and that the PPARx-LBD was in correct reading frame allowing the Gal4-DBD-PPARx-hinge+LBD fusion protein to be expressed. When this was confirmed, the effector plasmids were purified with midi-prep (3.9.2), and stored at -25 °C until further downstream applications.

3.12 Ligand Activation Analysis

3.12.1 Luciferase Reporter Gene Assay (LRA)

The ability of the Atlantic cod PPARx-hinge+LBD construct to bind and become activated by environmental pollutants was tested *in vitro* with a UAS/Gal4-DBD based luciferase reporter gene assay in a COS-7 simian kidney cell line. COS-7 cells were co-transfected with: 1) the constructed effector plasmids encoding the Gal4-DBD-PPARx-hinge+LBD fusion protein, 2) luciferase reporter gene plasmids (mh(100)x4tk luc), and 3) β -galactosidase-encoding control plasmids (pCMV- β -Gal). Ligand activation of the Atlantic cod PPAR constructs was measured as luciferase activity, quantifiable by the amount of light (550-570 nm) emitted during the oxidation of luciferin into oxyluciferin. The activity of β -galactosidase, measured at 420 nm, was used to normalize transfection efficiency between experiments.

3.12.2 Reporter and Control Plasmids

Reporter plasmids (mh(100)x4tk luc) and control plasmids (pCMV- β -Gal) were prepared from glycerol stock solutions (kept at -80 °C) of previously transformed *E.*

coli cells. Overnight cultures were made, and plasmids purified the next day through midi-prep (3.9.2).

3.12.3 Control of LRA Plasmids Integrity

The conformation of the three LRA plasmids (effector-, receptor-, and control plasmids) was controlled with AGE (3.4), assuring that most of the plasmids exhibited a supercoiled conformation. The migration of a plasmid through a gel will differ depending on its current conformation, e.g. if supercoiled (fully intact) the plasmid DNA will exhibit rather high mobility due to its compact packing, whilst if linearized i.e., both DNA strands cut at one site, the plasmid DNA will migrate slower than if supercoiled. Even slower migration will be observed if the plasmid DNA is nicked i.e., only one strand is cut, resulting in an open circular conformation of the DNA molecule with relatively low mobility.

3.12.4 COS-7 Cell Culturing

COS-7 cells are adherent cells and grow as a monolayer in petri dishes. The COS-7 cells were stored in freezing media (Table 11) in a liquid nitrogen tank. Aliquots were thawed and added 10 mL fresh cell growth media (Table 12). The suspended cells were collected by centrifugation at 500 x g for 5 minutes, and the supernatant containing DMSO from the freezing media was removed. The cell pellet was re-suspended in fresh growth media and seeded in a 10 cm diameter petri dish. COS-7 cells were kept at 37 °C in an atmosphere containing 5 % CO₂. 100 U/mL of penicillin and streptomycin was added to the growth media to avoid microbial contamination. The growth media was changed 2-3 times per week, and when the cells reached a confluency of 80-95% they were subcultured. The passaging of the cells was done by removing the old growth media and washing the cells with 1X PBS (pH 7.4) two times before enzymatically dissociating the cells from the petri dish through trypsinization (*1.5 mL trypsin-EDTA (trypsin (0.05 %), EDTA 0.02 %)*) for 30 seconds at RT. The excess of trypsin-EDTA was removed and cells incubated an additional 5 minutes at 37 °C and 5 % CO₂. The cells were then aspirated in 10 mL fresh growth media, and aliquoted into a new petri dish at desired ratio and incubated further. All handling of the COS-7 cell cultures were done implementing sterile techniques.

3.12.5 Seeding of COS-7 for LRA

COS-7 cells were harvested at 80-90 % confluency through trypsinization (as described above), and aspirated in 10 mL fresh growth media. A mix of cell suspension (50 μ L) and trypan blue (50 μ L) was loaded onto a Bürker haemocytometer (Marienfeld) and the cell density was determined with a microscope (Leica DM IL inverted microscope). COS-7 cells were seeded in 96 well plates in 100 μ L growth media with a density of 5000 cells per well, and subsequently incubated at 37 °C and 5 % CO₂ for 24 hours.

3.12.6 Transient Transfection of COS-7 Cells

Transient transfection is the introduction of exogenous DNA into a eukaryotic cell. However, the introduced DNA is not incorporated into the cells genome, and will thus be expelled from the cells after a few days. The LRA was therefore terminated on the 2nd day post-transfection. 24 hours after seeding of the COS-7 cells, old growth medium was removed and the cells were transfected using TransIT[®]LT-1 transfection kit (Mirus Bio) according to the manufactures instruction. Transfection mixtures were prepared for each of the four Atlantic cod PPAR subtypes according to Table 39. The transfection mixtures were then added to the COS-7 cells (tot 101.3 μ L/ well), and incubated at 37 °C and 5 % CO₂ for 24 hours.

Table 39. Transfection mixture protocol using TransIT-LT1

Component	Amount per well (96 well plate)
Opti-MEM I	9 μ L
Plasmid mix [1000 ng/ μ L]	0.1 μ L
TransIT-LT1	0.2 μ L
Cell growth media (Table 12)	92 μ L

ⁱCell growth media was added after 30 minutes incubation at room temperature

3.12.7 Exposure to Ligands

The transfection was terminated after 24 hours by replacing the transfection mixture with 200 μ L exposure mixture. The exposure mixture consisted of ligands that had been dissolved in DMSO and serial diluted to desired concentrations in cell growth media adapted for exposure (Table 12) (Table 40). The DMSO concentration was always < 1 %, and kept at the same concentration through the serial dilution. Cell growth media (Table 12) only containing DMSO was used as negative control in

exposure experiments (solvent control). The COS-7 cells were incubated with the ligand exposure mixtures at 37 °C and 5 % CO₂ for 24 hours.

Table 40. Ligands tested *in vivo* for agonistic effects on Atlantic cod PPAR constructs

Ligand	Highest conc [μM]	Lowest conc [μM]	Dilution factor
PFOA	200	41	1.3
PFNA	200	41	1.3
PFUnDA	200	41	1.3
PFOS	200	41	1.3
PFHxS	200	41	1.3
DEHP	200	3	2
DiDP	200	3	2
MBzP	200	3	2
MBP	200	3	2
Chlorpyrifos	100	1	10
Enosulfan	100	1	10
DPTE	100 // 25	1 // 0.4	10 // 2
D4	100	1	10
D5	100	1	10
PCB 153	100	1	10

3.12.8 Cell Lysis and Measurement of Luciferase- and β-galactosidase Activity

The ligand exposure was terminated after 24 hours by removing the media, and the COS-7 cells were incubated in 125 μL of a non-denaturing lysis reagent (Table 41) for 30 minutes at RT with continuously shaking using a platform shaker (HS 501 Digital, IKA-Werke).

Table 41. Lysis reagent

Component	Concentration
Cell lysis buffer (Table 13)	1X
EGTA	4 mM
MgCl ₂	8 mM
PMFS	0.4 mM
DTT	1 mM

The lysis treatment releases the expressed luciferase and β -galactosidase enzymes from the cells. Measurements of β -galactosidase activity were prepared by transferring half of the cell lysate (50 μ L) from each well to a transparent 96 well plate (Nunc™). The cell lysate was then added 100 μ L of β -galactosidase reagent (Table 42) and allowed to incubate for approximately 20 minutes; until the yellow color of the produced ONP became visible. Absorbance was measured at 420 nm using an EnSpire 2300 Multilabel Reader (PerkinElmer).

Table 42. β -galactosidase reagent

Component	Concentration
β -galactosidase base buffer (Table 14)	1X
β -mercaptoethanol	52.9 mM
ONPG (substrate)	8.6 mM

Measurements of luciferase activity were prepared by transferring the remaining 50 μ L of cell lysate from each well to a white 96 well plate (Nunc™) designated for luminescence measurements. The luciferase reagent (Table 43) was added to one plate at the time (100 μ L/ well), and measurements at 560 nm were carried out immediately using an EnSpire 2300 Multilabel Reader (PerkinElmer).

Table 43. Luciferase reagent

Component	Concentration
Luciferase base buffer (pH 7.8) (Table 15)	1X
ATP	0.5 mM
DTT	5 mM
MilliQ	-
³ Coenzyme A	0.2 mM
³ D-luciferine	0.5 mM

³Added right before use.

3.13 Cell Viability Assays

A combination of two fluorometric assays, i.e. alamarBlue® (resazurin) (Page et al., 1993) and 5-carboxyfluorescein diacetate acetoxymethyl ester (CFDA-AM) (O'connor et al., 1991), were used to assess if the ligands used in the LRA trials were cytotoxic to the COS-7 and thus affected their viability. The nontoxic resazurin and CFDA-AM

are cell permeable, non-fluorescent, indicator dyes that when entering viable and metabolically active cells becomes enzymatically converted to fluorescent metabolites. Resazurin becomes reduced to fluorescent resorufin by oxidoreductases and the mitochondrial electron transport chain, while CFDA-AM becomes hydrolyzed by intracellular esterases to fluorescent 5-carboxyfluorescein. Thus, the conversion of resazurin and CFDA-AM is quantifiable by their metabolite's fluorescence, where the production of resorufin conventionally reflects metabolic activity, while the production and retention of 5-carboxyfluorescein indirectly confirms the plasma membrane integrity (O'connor et al., 1991; Page et al., 1993; Schirmer et al., 1997; Schreer et al., 2005). COS-7 cells were seeded in 96 well plates (3.12.5) and incubated at 37 °C and 5 % CO₂ for 48 hours. Subsequent exposures (3.12.7) were carried out for 24 hours at 37 °C and 5 % CO₂, using the three highest concentrations used of control agonists and ligands, in addition to the highest concentrations used of solvent (1 % DMSO) as control. 0.1 % and 1 % Triton X-100, diluted in exposure media, were also included as positive controls for impaired viability and cell death. When terminating the exposure, the COS-7 cells were washed with 1X PBS (pH 7.4). The cells were then added a reaction solution (100 µL/ well) (Table 44) and allowed to incubate in dark at 37 °C and 5 % CO₂ for 1 hour.

Table 44. Reaction solution used for measuring cell viability.

Component	Concentration
Resazurine	10 %
CFDA-AM	1 %
DMEM	Up to 100 %

Eight empty wells per plate were similarly added the reaction solution, allowing the determination of the background signal. Thereafter, the fluorescence signals were measured for resazurine (excitation: 530 nm/ emission: 590 nm) and for CFDA-AM (excitation: 485 nm/ emission: 530 nm) using an EnSpire 2300 Multilabel Reader (PerkinElmer). The background signal was subtracted from the fluorescence values.

3.14 Testing for Presence of Expressed Fusion Proteins in COS-7 Cells

3.14.1 Protein Sample Preparation

3.14.1.1 Seeding

COS-7 cells were harvested at 80-90 % confluency through trypsinization (3.12.4) and aspirated in 10 mL fresh growth media. A mix of cell suspension (50 μ L) and trypan blue (50 μ L) was loaded onto a Bürker haemocytometer (Marienfeld), and the cell density was calculated. COS-7 cells were seeded on 6 well plates in 2.5 mL growth media with a density of 600000 cells per well, and incubated at 37 °C and 5 % CO₂ for 24 hours.

3.14.1.2 Transfection

On the second day, the cells were transfected with the effector plasmids encoding the Gal4-DBD-PPARx-hinge+LBD fusion proteins, using the TransIT[®]LT-1 transfection kit (Mirus Bio) according the manufactures instruction. Transfection mixtures, done in experimental duplicates (Table 10) were prepared according to Table 45. The mixtures were then added to the COS-7 cells (2.8 mL/ well), and allowed to incubate at 37 °C and 5 % CO₂ for 24 hours. Two wells of COS-7 cells were kept untransfected as a negative control for downstream applications.

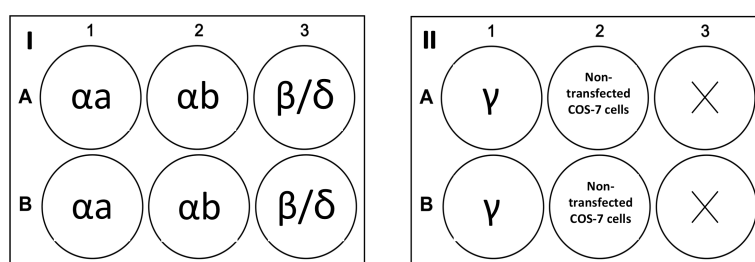


Figure 10. Overview of transfection setup. COS-7 cells were transfected in experimental duplicates with effector plasmids encoding the Gal4-DBD-PPARx-hinge+LBD fusion proteins using the TransIT[®]LT-1 transfection kit (Mirus Bio).

Table 45. Transfection mixture protocol using TransIT-LT1

Component	Amount per well (6 well plate)
Opti-MEM I	250 μ L
Plasmid mix [1000 ng/ μ L]	2.5 μ L
TransIT-LT1	5 μ L
Cell growth media (Table 12)	2.5 mL

ⁱCell growth media was added after 30 minutes incubation at room temperature

3.14.1.3 Cell Harvesting

On the third day, the transfected COS-7 cells were harvested through trypsinization (3.12.4) using 500 μ L of RT trypsin-EDTA per well. The cells were then resuspended in 1 mL growth media and centrifuged at 100 x g for 10 minutes at 4 °C using a Z 216 MK microliter centrifuge (HERMLE). The supernatant (media) was removed and the pellets were washed in 1X PBS (pH 7.4) before centrifuged again at 100 x g for 10 minutes at 4 °C. The supernatant (PBS and media residue) was removed and the cell pellets were stored at -80 °C until further downstream applications.

3.14.1.4 Lysis

The pellets were lysed in 50 μ L Triton lysis buffer (Table 16), and vortexed at maximum speed for 15 seconds. Cells were kept on ice for 10 minutes before centrifuged at 22000 x g for 5 minutes at 4 °C using a Z 216 MK microliter centrifuge (HERMLE). Aliquots of the cell lysate were stored at -80 °C until further downstream applications.

3.14.1.5 Protein Concentration Measurement - Pierce 660 nm Protein Assay

The protein concentrations of the prepared cell lysates were determined by creating a standard curve of bovine serum albumin (BSA). Six serial dilutions of BSA in triplicates with final concentrations of 1000, 500, 250, 125, and 62.5 μ g/mL were prepared. Each BSA standard, cell lysates, and blanks (Triton lysis buffer) were pipetted onto a 96 well plate in triplicates (10 μ L/ well), and then added the protein assay reagent Pierce 660 (Thermo scientific) (150 μ L/ well). The plates were covered in tin foil and mixed on a platform shaker (HS 501 Digital, IKA-Werke) at medium speed for 1 minute, and then allowed to incubate at RT for 5 minutes before the absorbance was measured at 660 nm using an EnSpire 2300 Multilabel Reader

(PerkinElmer). The average A_{660} -values of the blanks (Triton lysis buffer) were subtracted from the average A_{660} -value of each BSA standard and cell lysate samples. The corrected BSA A_{660} -values were then plotted against their corresponding concentration in Excel (Appendix VII), from where a linear equation could be derived (Formula 3, $R^2 = 0.9997$). By incorporating the average A_{660} of the cell lysates as y -value in the equation, then x (representing the protein concentration) could be solved.

$$y = -1E - 07x^2 + 0.0005x - 0.015 \quad (3)$$

3.14.2 Sodium Dodecyl Sulphate Polyacrylamide Gel Electrophoresis (SDS-PAGE) and Sample Preparation

Denaturing sodium dodecyl sulfate polyacrylamide gel electrophoresis (SDS-PAGE), allows proteins to be separated according their molecular weight (Mw). Prior to the SDS-PAGE, the protein samples were boiled together with a denaturing 5X SDS-PAGE sample buffer (5XSB) containing both the detergent sodium dodecyl sulfate (SDS) and the reducing agent β -mercaptoethanol (BME). SDS is an anionic detergent that will denature proteins and its hydrophobic backbone will bind to proteins with a ratio of 1.4 g SDS per g of protein, thereby masking the proteins native charge and giving it an overall negative charge (Farrell and Taylor, 2005). The reducing agent BME will break both inter- and intradisulphide bonds between and within proteins, respectively (Lee, 1990). Thus, the denaturing sample buffer will brake down polymeric proteins into their individual subunits and hence cause all proteins to obtain the same random coil configuration with equal charge-to-mass ratios. Proteins can then be separated solely according to their molecular weight. The denaturing sample buffer contains: 1) glycerol; that will increase the density of the sample and thereby aiding the gel loading, and 2) a loading dye, often being bromophenol blue; a small and negatively charged molecule that will migrate faster than the proteins being separated, and functions as a marker that visualize the electrophoresis while running the SDS-PAGE. Discontinuous gels were used to acquire high-resolution separation when performing the SDS-PAGE, consisting of one 12 % resolving gel with pH 8.5, and one 4 % stacking gel on top with pH 6.5. The purpose of using discontinuous gels is that proteins will migrate faster in the stacking gel due to its lower polyacrylamide concentration, but when they meet the border of the resolving gel with higher

polyacrylamide concentration they will slow down, causing the proteins to become concentrated in one band when entering the separation gel, making them more distinguishable. The resolving gel will then separate the proteins according to their size where small proteins will migrate faster. The change in pH will also affect the charge of the compounds causing differences in voltage to occur within zones pushing proteins together even further (Farrell and Taylor, 2005). Here, SDS-PAGE was used to separate the four expected Gal4-DBD-PPAR α -hinge+LBD fusion proteins.

The SDS-PA gels were casted 0.75 mm thick and ran using a Mini-PROTEAN® Tetra Cell casting and electrophoresis system (Bio-Rad). A 12 % resolving gel was prepared with a final volume of 10 mL, enough to create two separate gels (Table 17). A 4 % stacking gel mix was prepared with a final volume of 5 mL, enough to cover the two resolving gels (Table 18). The two resolving gels were poured into the spacer plates of the casting unit up to a point located about 1 cm below the gel combs. Subsequently, 70 % ethanol was added on top of the resolving gels to remove the surface tension and thus acquiring a sharp horizontal upper edge. When the resolving gels were completely polymerized the ethanol was removed, and the stacking gels were poured on top, filling up the remaining space between the spacer plates. 0.75 mm thick gel combs were immediately inserted. When the two SDS-PA gels were completely polymerized, they were transferred from the casting unit into the electrophoresis chamber and lowered into the electrophoresis tank. Gel combs were thereafter removed. 1X SDS-PAGE-running buffer (Table 19) was used to completely fill up electrophoresis tank. One of the gels was designated for Western Blotting and the other one for Coomassie Brilliant Blue staining. Both gels were loaded with 10 μ g of each protein sample. A Precision Plus Protein™ Kaleidoscope™ Prestained Protein Standards (Bio-Rad) (5 μ L) was also loaded onto the gels as an Mw reference. The SDS-PAGE was run at 200 V until (approximately 45 min) the dye front had reached the bottom of the gel.

3.14.3 Coomassie Brilliant Blue Staining

The SDS-PA gel designated for detection of the total protein content was stained with Coomassie Brilliant Blue R250 staining solution (Table 20) and allowed to incubate several hours on a platform shaker (HS 501 Digital, IKA-Werke). Then, after removing the staining solution, a destaining solution (Table 20) was added to the

SDS-PA gel and allowed to further incubate for a few hours until the protein bands were clearly visual. The gel was scanned using a ChemiDoc™ XRS+ System with a charged-coupled (CCD) camera (Bio-Rad).

3.14.4 Western Blotting

After the proteins from the COS-7 cell lysate had been separated according to their M_w with SDS-PAGE, Western blotting was used to analyze the proteins further by first transferring (or blotting) the separated and fixated proteins from the SDS-PA gel onto a polyvinylidene difluoride (PVDF) membrane by wet electrotransfer, creating a replica of the protein pattern that is more ridged and easier to handle. A 0.45 μm PVDF membrane (6x9 cm) was initially equilibrated by first being submerged in methanol for 20 seconds, then rinsed with MilliQ, before submerged into blotting buffer (Table 21) for 30 minutes, together with two fiber pads and two filter papers (8x10 cm). The SDS-PA gel was also allowed to equilibrate in blotting buffer for 10 minutes. The blotting sandwich was assembled in the gel holder cassette by placing the first fiber pad bottommost in the open cassette, followed by the first filter paper and then the membrane. The gel was then placed on top of the membrane followed by the second filter paper, and lastly the second fiber pad. After assuring that no air bubbles had been trapped between the layers, the cassette was closed and placed in a Mini Trans-Blot Cell electrode unit (Bio-Rad). The electrode unit was thereafter lowered into the buffer tank, and the tank was filled up with blotting buffer and run at 100 V for 1 hour. The membrane was blocked with 5 % dry milk (Table 24) and incubated ON on a platform shaker (HS 501 Digital, IKA-Werke) at 4 °C; By blocking areas on the membrane that have not been bound by proteins prevents non-specific binding of the antibodies in downstream steps.

Next day, the membrane was rinsed with 0.05 % TBS-tween (Table 23) two times for 5 minutes each (all washing steps done are to minimize background interference later on), before adding the primary mouse-anti Gal4 antibody diluted 1:500 in TBS-tween, and subsequently allowed to incubate for 1 hour on a platform shaker at RT. Excess mouse-anti Gal4 antibody that were not bound to epitopes, was then washed away with TBS-tween two times for 5 minutes, before the membrane was incubated with the sheep-anti-mouse IgG (immunoglobulin G) secondary antibody conjugated to horseradish peroxidase (HRP), diluted 1:2000 in TBS-tween, and allowed to

incubate for 1 hour on a platform shaker at RT. Excess secondary antibodies were washed away with TBS-tween two times for 5 minutes, and then washed with MilliQ for 5 minutes. The protein-primary-antibody-secondary antibody complex was visualized using a chemiluminisence detection system suitable for HRP-tagged secondary antibodies, in this case SuperSignal West Pico Chemiluminescent Substrate (Thermo Scientific). The membrane was drained of excess MilliQ and added a substrate solution for HRP containing equal volumes (300 μ L + 300 μ L) of luminol enhancer and stable peroxide buffer. The membrane was then allowed to incubate for about 3 minutes at RT. The antigen-antibodies complexes could then be visualized and documented using a ChemiDoc™ XRS+ System with a charged-coupled (CCD) camera (Bio-Rad).

After the detection of Gal4, the membrane was rinsed with TBS-tween two times for 5 minutes, before the membrane was incubated with a 2nd primary antibody, i.e. mouse-anti beta actin antibody diluted 1:1000 in TBS-tween. The membrane was subsequently allowed to incubate for 1 hour on a platform shaker at RT. Excess mouse-anti beta actin antibody was then washed away with TBS-tween two times for 5 minutes, before the membrane was incubated with the secondary antibody HRP sheep-anti-mouse IgG diluted 1:2000 in TBS-tween, and allowed to incubate for 1 hour on a platform shaker at RT. Excess secondary antibodies were washed away with TBS-tween X2 for 5 minutes, and then washed with MilliQ for 5 minutes before the signal was measured as described above.

3.15 Data Treatment and Statistics

Microsoft Excel 2011 was used to initially process the LRA readings retrieved by the EnSpire 2300 Multilabel Reader (PerkinElmer). First, the ligand induced luciferase activity in each well was normalized against any differences in transfection efficiency by dividing each luciferase reading by the corresponding β -galactosidase reading. The normalized luciferase values from each well were then divided by the control averages (containing only vehicle solution) within each experiment, and the resulting values could then be denoted as fold induction in ligand-induced luciferase activity compared to the solvent control. GraphPad Prism v.6 was used to produce graphs displaying the average fold induction in luciferase activity caused by each ligand tested at different concentrations, including standard error of mean (SEM). A One-way ANOVA and

Dunnet's test was used to calculate significant fold induction in the means of the different test concentrations over the control means.

3.16 *In Silico* Sequence Analyses

After the Atlantic cod PPAR α hinge+LBDs had been cloned and sequenced, the nucleotide (nt) sequences were translated *in silico* into protein sequences using the online ExPASy translating tool (SIB Bioinformatics Resource Portal). Even though the Atlantic cod genome was sequenced already in 2011 (Star et al., 2011), the PPAR-encoding genes are only gene predictions and have still have to be manually curated. Thus, comparisons between *in silico* translated protein sequences of the sequenced Atlantic cod PPAR α hinge+LBDs and the predicted PPAR α hinge+LBDs retrieved from the Ensembl Cod genome database, was done by pairwise alignments using the online tool Clustal Omega (EMBL-EBI). The alignments were then visualized and examined using Jalview v.2.9.0b2, where the alignments were colored according to percentage identity and the domains were denoted on the sequences.

Phylogenetic relationships between the amino acid sequences of the Atlantic cod PPAR α hinge+LBD and PPAR α hinge+LBDs from other relevant species were made *in silico*. Protein sequences from other species were retrieved from the UniProtKB database. A multiple protein sequence alignment was made in Clustal Omega (EMBL-EBI), and the alignment was imported into MEGA6 (v 6.06) where phylogenetic relationships were inferred using the Neighbor-Joining method (Saitou and Nei, 1987). The percentage of replicate trees in which the associated species specific PPAR-subtypes clustered together were calculated using a bootstrap test set to 1000 replicates. Evolutionary distances, denoted as units of number amino acid substitutions per site, were computed using the JTT matrix-based model (Jones et al., 1992). The rate variation among sites was modeled with a gamma distribution where the shape parameter was set to 5. The analysis involved 47 amino acid sequences. All positions containing gaps and missing data were eliminated.

4 RESULTS

Before being able to study ligand activation of the four Atlantic cod PPAR α hinge+LBD constructs with LRA, several preparatory steps had to be carried out (Fig 11). Quality control of the products from each preparatory step was performed before continuing with downstream applications.

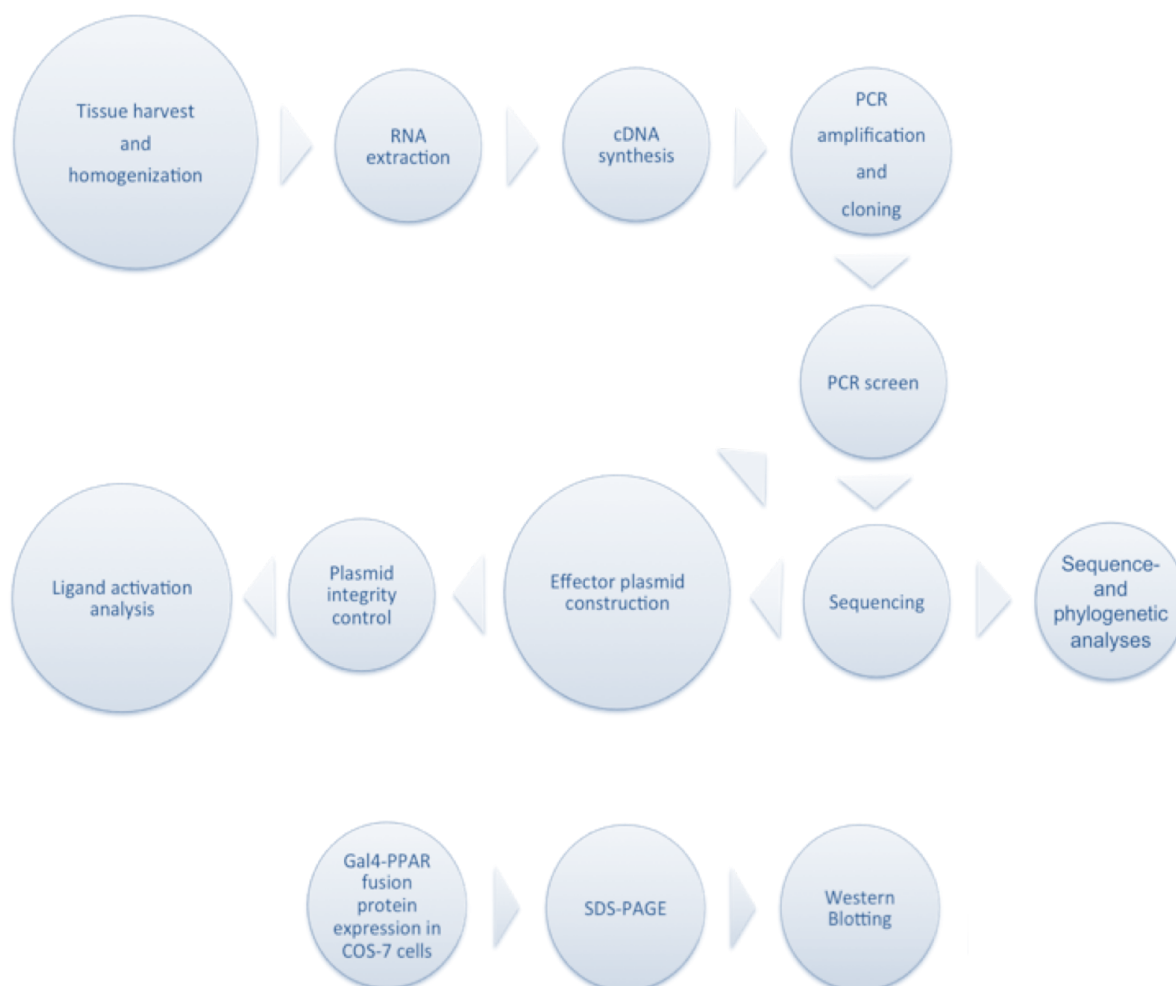


Figure 11. Workflow overview. Atlantic cod tissues were collected and homogenized. RNA was extracted and reversely transcribed into cDNA. The PPAR α hinge+LBD encoding genes were amplified through PCR using cDNA as template. The amplified gene fragments were ligated into a cloning vector and cloned by transforming *E. coli* cells. After confirming that the correct gene fragments had been cloned through sequencing, the fragments were ligated into an expression vector (effector plasmid) that were transfected into COS-7 cells. The PPAR α hinge+LBD constructs could then be analyzed *in vitro*, to test for PPAR ligand activation of different environmental contaminants. A cell viability assay was used to assess if any of the ligands tested were cytotoxic at the concentrations used in the ligand activation assay. The presence of expressed PPAR α hinge+LBD construct in COS-7 cells was examined by Western blotting.

4.1 Molecular Cloning of the Ligand Binding Domains of the Atlantic Cod PPAR Subtypes

4.1.1 RNA Extraction from Atlantic Cod Tissue

Total RNA was extracted from homogenized heart and brain tissues from Atlantic cod. The RNA integrity was assessed by agarose gel electrophoresis, which showed the presence of the 28S and 18S ribosomal RNA subunits at ~1800 bp and ~1000 bp, respectively (Fig 12). The distinct bands representing the two rRNA subunits indicate that the integrity of the total RNA was maintained and that RNA-degradation was not an issue.

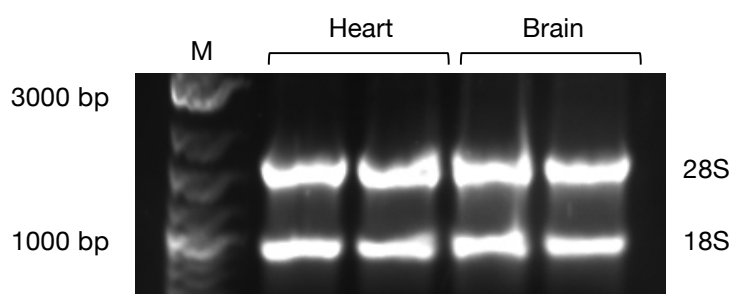


Figure 12. Assessment of RNA integrity by agarose gel electrophoresis. RNA preparations from Atlantic cod heart and brain tissue were separated on a 0.5X TBE 0.7 % agarose gel and stained with GelRed. The 28S and 18S ribosomal RNA (rRNA) subunits are indicated. M = 2 μ L DNA standard (2log DNA Ladder). Heart = 600 ng totRNA derived from heart. Brain = 600 ng totRNA derived from brain.

$A_{260\text{ nm}/280\text{ nm}}$ spectrophotometric measurements of the extracted totRNA from brain and heart tissue showed ratios close to 2 (± 0.03) (Table 46), indicating pure RNA samples free from contaminating proteins. The $A_{260\text{ nm}/230\text{ nm}}$ ratios were larger than 2.19 (Table 46), indicating that the RNA samples were not contaminated by salts and solvents. Thus, the RNA samples were of sufficient quality for downstream cDNA synthesis.

Table 46. Spectrophotometric measurements of extracted total RNA.

Sample	Concentration (ng/ μ L)	$A_{260/280}$	$A_{260/230}$
Heart 1	2109.6	2.03	2.19
Heart 2	823.8	2.01	2.37
Brain 1	685.8	2.01	2.38
Brain 2	521.7	1.98	2.40

4.1.2 cDNA Synthesis, PCR Amplification and Cloning

Single stranded cDNA was synthesized using total RNA extracted from Atlantic cod heart and brain tissue (3.2, 3.5) as template. The cDNA then served as template for PCR amplification of the PPARx hinge+LBD-encoding genes. Gene specific primers had been designed to amplify the desired gene fragments of each of the four PPAR subtypes present in Atlantic cod. The amplicons were analyzed with AGE (3.4) and their lengths corresponded well with the expected lengths of the Atlantic cod hinge+LBD fragments (Fig 4), which were derived from predicted PPAR encoding gene sequences present in the Ensembl cod genome database. PPAR α hinge+LBD (Fig 13 A) and PPAR γ hinge+LBD (Fig 13 B) were amplified from heart tissue, while PPAR α b hinge+LBD and PPAR β/δ hinge+LBD were amplified from brain tissue (Fig 13 C). Two splice variants of the PPAR β/δ hinge+LBD were amplified. Even though the smaller amplicon was more concordant with the expected length of the predicted PPAR β/δ hinge+LBD both fragments were gel extracted, cloned, and sequenced.

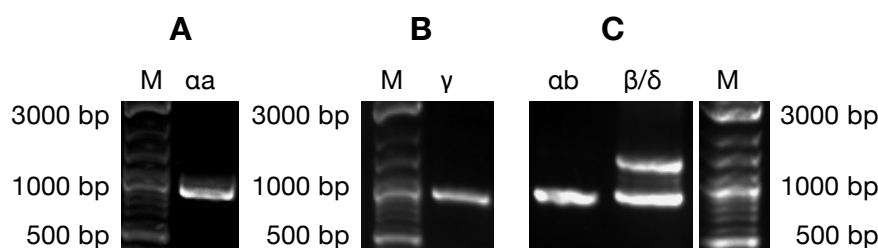


Figure 13. Agarose gel electrophoresis of amplicons of Atlantic cod PPAR subtypes. The 0.5X TBE 0.7 % agarose gel was stained with GelRed for visualization of DNA fragments (expected lengths: PPAR α hinge+LBD = 867 bp; PPAR α b hinge+LBD = 876 bp; PPAR β/δ hinge+LBD = 894 bp; PPAR γ hinge+LBD = 792 bp). A) M = 2 μ L DNA standard (2log DNA Ladder), aa = 2 μ L PPAR α hinge+LBD amplified from heart-derived cDNA. B) M = 2 μ L DNA standard (2log DNA Ladder), and γ = 2 μ L PPAR γ hinge+LBD amplified from heart-derived cDNA. C) ab = 2 μ L PPAR α b hinge+LBD amplified from brain-derived cDNA, and β/δ = 2 μ L PPAR β/δ hinge+LBD amplified from brain-derived cDNA, M = 2 μ L DNA standard (2log DNA Ladder).

The PPARx hinge+LBD amplicons were ligated into a cloning vector and transformed into competent *E. coli* cells. Positive transformants possessing antibiotic resistance were then selected for by seeding the cells on agar plates supplemented with ampicillin and incubated over night.

4.1.3 Colony Screening for Transformants

PCR with vector specific primers (Table 6) were used to screen single colonies for positive transformants harboring the cloning vector with a DNA insert of expected length. The colony PCR screening products were separated with AGE, which for certain colonies showed the presence of amplified DNA fragments of promising sizes in regard to the predicted lengths of the Atlantic cod PPAR α hinge+LBD subtypes (Fig 14).

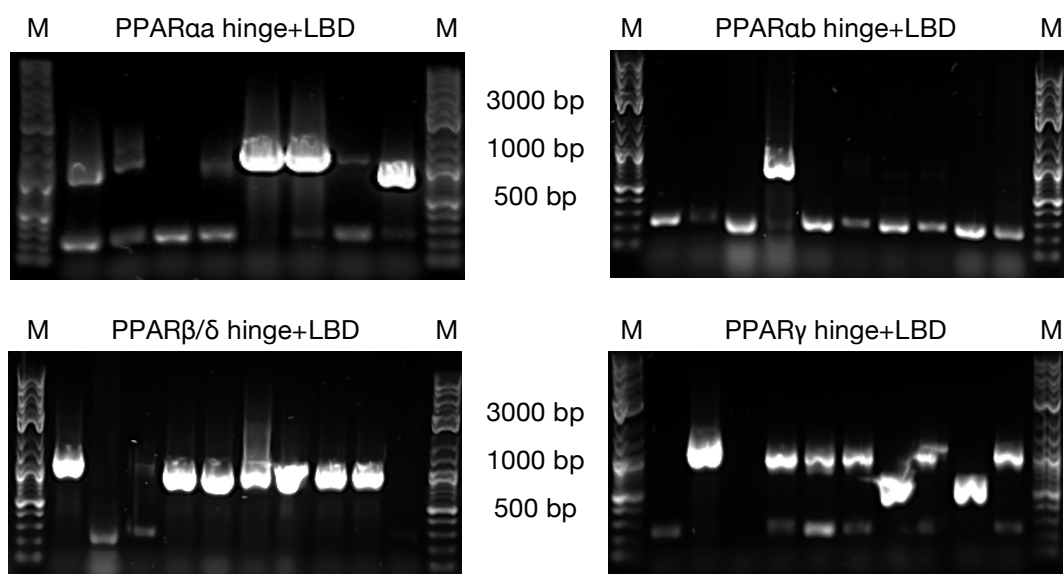


Figure 14. Screening of positive transformants containing the PPAR α hinge+LBDs. Colony PCR amplicons were separated on a 0.5X TBE 0.7 % agarose gel and stained with GelRed. Expected amplicon lengths: PPAR α hinge+LBD = 867 bp; PPAR α b hinge+LBD = 876 bp; PPAR β/δ hinge+LBD = 894 bp; PPAR γ hinge+LBD = 792 bp. M = 2 μ L DNA standard (2log DNA Ladder). 2 μ L of the amplification reaction was loaded per well.

4.1.4 Sequencing and Examination

The cloning vector was purified from the positive transformants by mini-preps (3.9.1), and then sequenced using cloning vector-specific primers to confirm the presence of correct insert (3.10). The sequencing showed that PCR products corresponded with the predicted Atlantic cod PPAR hinge+LBD's, derived from the Atlantic cod genome database in Ensembl. A pairwise alignment, between the predicted PPAR sequences and the cloned sequences, confirmed that the sequenced genes were in fact encoding the four different PPAR subtypes. However, the cloned nucleotide sequences of the four different Atlantic cod PPAR_x hinge+LBD differed to some extent when compared to the corresponding predicted genes present in the cod genome database in Ensembl (Appendix I-IV). These differences were examined further by translating all nucleotide sequences *in silico* to amino acid sequences and constructing pairwise alignments for each PPAR subtype. The cloned Atlantic cod PPAR_α hinge+LBD amino acid sequence differed by having 19 unexpected amino acid residues within the hinge region, in addition to 6 differing amino acids (Fig 15). The PPAR_β hinge+LBD amino acid sequence differed by having 1 additional amino acid residue and 1 differing amino acid within the hinge region, as well as 1 differing amino acid in the LBD (Fig 15). The PPAR_{β/δ} hinge+LBD amino acid sequence differed by 1 amino acid located in the LBD (Fig 15). The PPAR_γ hinge+LBD amino acid sequence differed by having 37 unexpected amino acid residues in the hinge region, in addition to 7 differing amino acids (Fig 15). *In silico* investigation of the sequenced Atlantic cod PPAR_α hinge+LBD, PPAR_β hinge+LBD, PPAR_{β/δ} hinge+LBD, and PPAR_γ hinge+LBD showed that the above-mentioned differences in gene sequence, in relation to the predicted gene sequence from the cod genome database (Ensembl), did not disturb their reading frames. The PPAR_α hinge+LBD, PPAR_β hinge+LBD, PPAR_{β/δ} hinge+LBD, and PPAR_γ hinge+LBD encoding sequence translated into polypeptides of 307, 292, 296, and 300 amino acids in length, respectively (Fig 15) (Appendix V-VI).

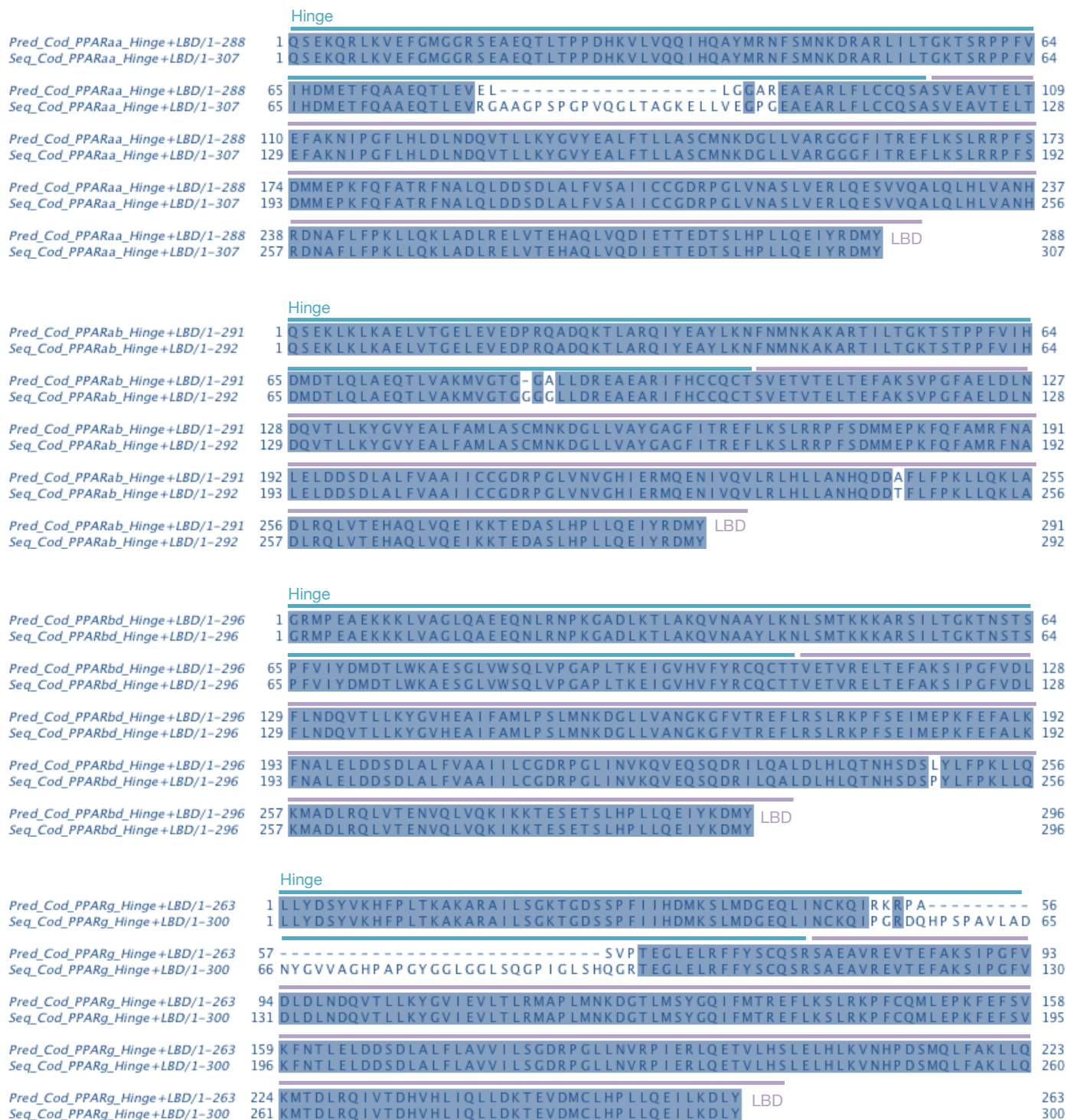


Figure 15. Pairwise sequence alignment of Ensembl-derived sequences and cloned Atlantic cod PPARx hinge+LBD. Predicted Atlantic cod PPARx hinge+LBD encoding genes were retrieved from the Ensembl cod genome database. The cloned Atlantic cod PPARx hinge+LBD encoding genes were sequenced by the sequencing facility at the Department of Molecular Biology, University of Bergen. The nucleotide sequences were translated into protein sequences *in silico*, using ExPASy Translate tool, and the protein sequences were then aligned using Clustal Omega (EMBL-EBI). The pairwise alignment was depicted in Jalview v 2.9.0b2. The alignments have been colored by percentage identity and conservation.

The unexpected nucleotids found in the hinge-encoding region of PPAR α and PPAR γ (Appendix IV), can be found in the genome sequence of the Atlantic cod by genome mining. Thus, the automatically performed gene prediction has apparently failed to include these nucleotids as exons. Furthermore, a blastp (protein BLAST) search, using only the additional amino acid residues found in the cod PPAR γ hinge region (HPSPAVLADNYGVVAGHPA PGYGGLGGLSQQPIGLSH) as query, showed a 97 % identity with PPAR γ in Polar cod (*Boreogadus saida*), and 67 % identity with PPAR γ in European hake (*Merluccius merluccius*) further strengthening that the unexpected nucleotides found in the PPAR γ hinge region has not been recognized by the automatic gene annotation made by Ensembl.

4.1.5 Phylogenetic Analysis

The identities of the cloned gene segments encoding the Atlantic cod PPARx hinge+LBDs were confirmed by constructing a Neighbor-Joining tree. A multiple protein sequence alignment between the *in silico* translated Atlantic cod PPARx hinge+LBDs, together with PPARx hinge+LBDs of other teleosts and terrestrial vertebrates was made with Clustal Omega (EMBL-EBI). Based on the alignment, an additive tree was constructed using PPAR from *Ciona intestinalis* as an outgroup to root the tree. The tree demonstrates that the protein sequences derived from the cloned Atlantic cod PPAR subtypes, clusters nicely together with corresponding PPAR subtypes from other teleost species (Fig 16).

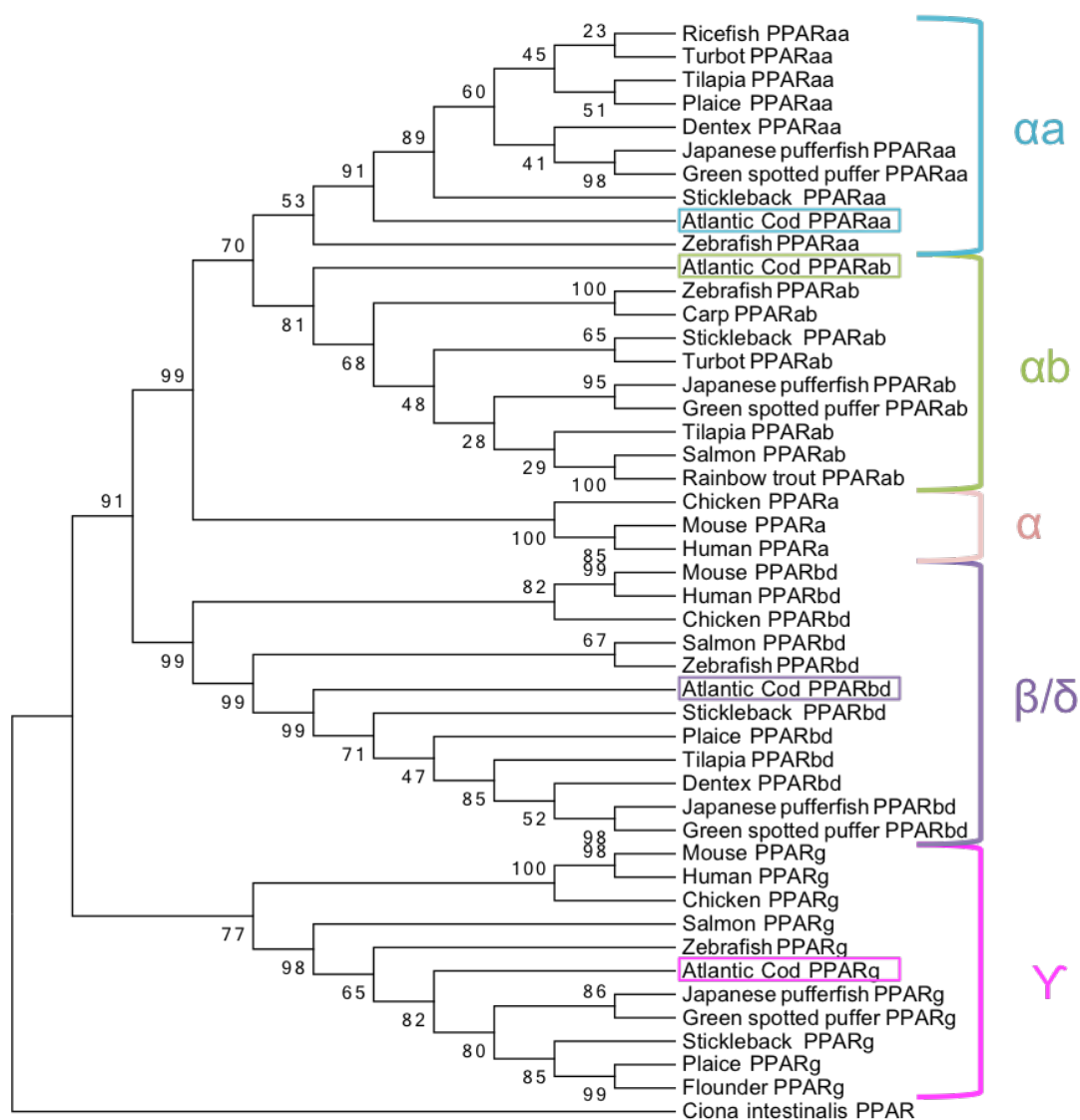


Figure 16. Neighbor-Joining tree of PPARx hinge+LBD-encoding sequences. The analysis involved 47 amino acid sequences, and the robustness of the tree is given as percentage of replicate trees in which the associated PPAR-subtypes clustered together. Bootstrap values are indicated next to the branches (bootstrap test = 1 000 replicates).

4.1.6 Amino Acids Important for Ligand Binding

Since PPARs play a crucial role in the regulation of several physiological processes, human PPARs have been extensively studied for therapeutic purposes, i.e. as targets for drug design. Certain amino acids have been established as important for binding specific ligands. In human, WY14643 is a synthetic and selective PPAR α agonist where the amino acids S280, Y314, H440, and Y464 have shown to be important for agonist recognition and binding (Bernardes et al., 2013; Narala et al., 2010). For the human PPAR β/δ , GW501516 is a potent and selective agonist where amino acids W228, H287, V298, V312, I328, H413, and Y437 are important for binding and ligand docking (Wu et al., 2017). Rosiglitazone (Rosi), a selective and potent PPAR γ agonist that is used as an antidiabetic agent in humans. PPAR γ has been extensively examined, and the amino acids that are recurrently identified as important for binding Rosi are C285, R288, S289, H323, Y327, L330, L333, V339, I341, H449, and Y473 (Annapurna et al., 2013; Chandra et al., 2008; Liberato et al., 2012; Nolte et al., 1998). To examine if the same functional important amino acids are also present in the Atlantic cod PPAR proteins, pairwise alignments were generated between the PPAR x hinge+LBD protein sequences from both cod and human *in silico*. All four amino acids important for binding WY14643 in human PPAR α were conserved in both PPAR αa and PPAR αb in cod (Fig 17 A). Five out of seven amino acids important for binding GW501516 in human PPAR β/δ were conserved in cod PPAR β/δ , differing by hV298 \rightarrow M and hH413 \rightarrow N (Fig 17 B). In cod PPAR γ , only five out of eleven amino acids important for binding Rosi in human PPAR γ were conserved, differing by hH323 \rightarrow I, hY327 \rightarrow T, hL330 \rightarrow M, hV339 \rightarrow T, hI341 \rightarrow M, and hY473 \rightarrow L (Fig 17 C).

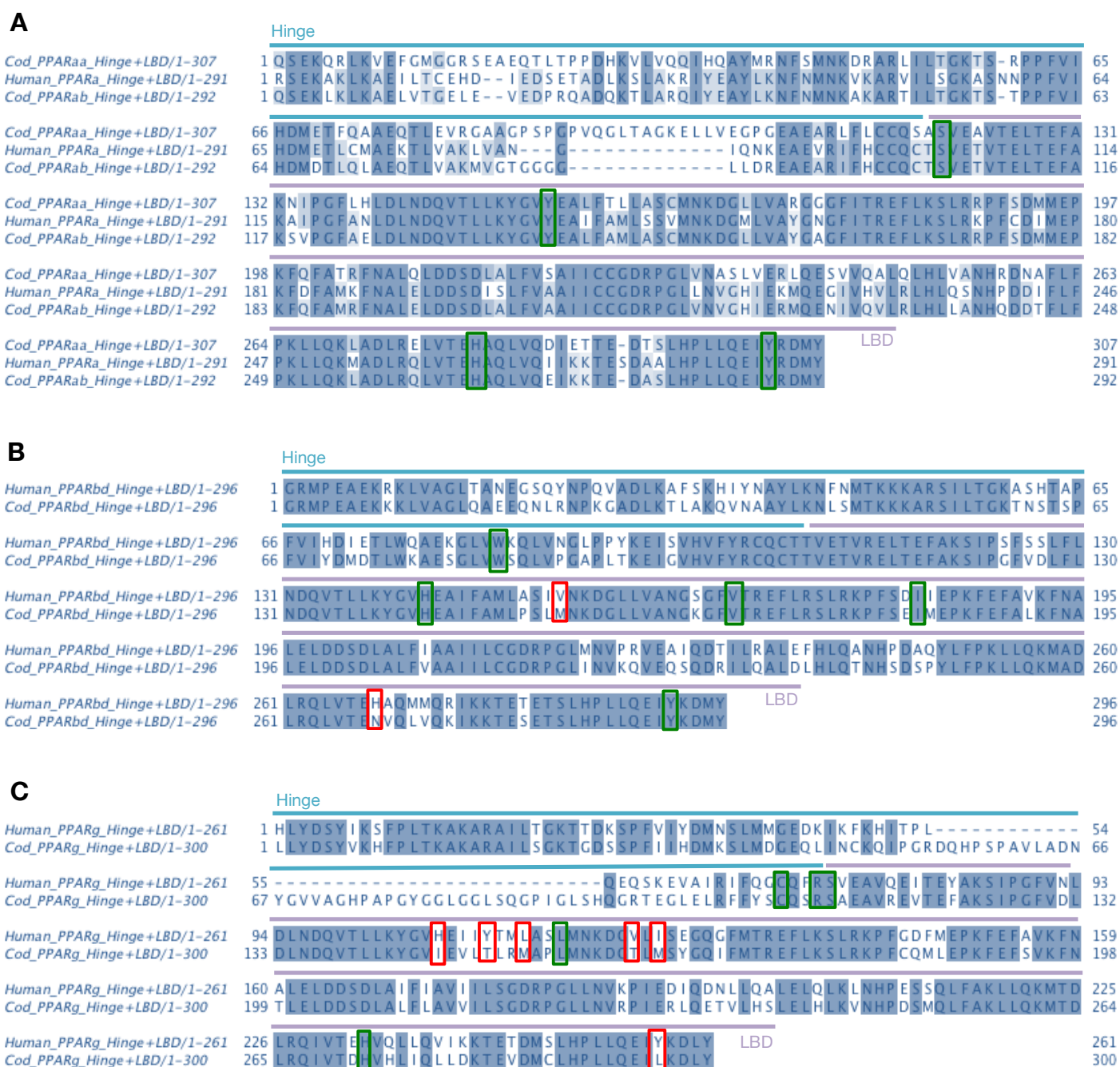


Figure 17. Pairwise sequence alignment of Atlantic cod and human PPARx hinge+LBDs. Human PPARx hinge+LBD encoding genes were retrieved from the Ensembl human genome database. The cloned Atlantic cod PPARx hinge+LBD encoding genes were sequenced by the sequencing facility at the Department of Molecular Biology, University of Bergen. The nucleotide sequences were translated into protein sequences *in silico* using ExPASy Translate tool, and the protein sequences were then aligned using Clustal Omega (EMBL-EBI). The pairwise alignments were depicted in Jalview v 2.9.0b2. The alignments has been colored by percentage identity and conservation. Conserved amino acids important for ligand binding is marked with green boxes, while non-conserved is marked with red boxes.

4.2 Effector Plasmid Construction

After confirming that the correct PPAR α hinge+LBD encoding gene fragments had been cloned, the gene fragments could be ligated into effector plasmids required for ligand activation analysis with the LRA. Effector plasmids are eukaryotic expression plasmids that allow the Atlantic cod PPAR α hinge+LBD constructs to be constitutively expressed in COS-7 cells. The abilities of the PPAR α hinge+LBD constructs to bind and become activated by environmental contaminants could then be tested *in vitro*.

4.2.1 Restriction Digestion and Ligation

The cloning vectors harboring the Atlantic cod PPAR α hinge+LBD-encoding fragments (pSC-B-PPAR α -LBD) (confirmed by sequencing), as well as the effector plasmid (pCMX-Gal4-DBD), were all digested using the BamHI and EcoRI restriction endonucleases and subsequently separated with AGE (3.11.1, 3.4). Thus, allowing the PPAR α hinge+LBD fragments to be purified from the cloning vector backbones through gel extraction. Similarly, could the effector plasmid backbones be linearized and purified through gel extraction. Small aliquots of each sample were loaded and separated on an agarose gel to monitor the process (Fig 18).

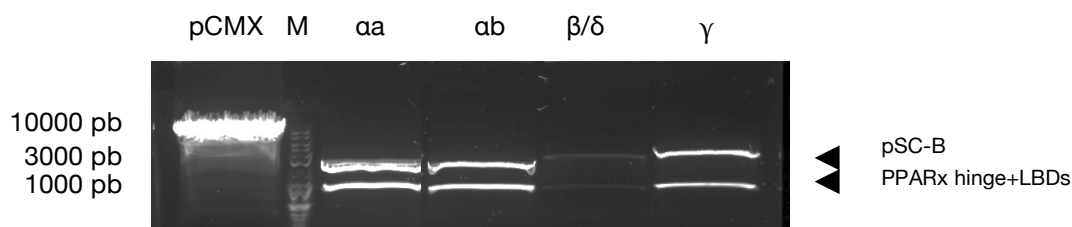


Figure 18. Restriction enzyme digestion of expression vectors and cloning vectors. The pCMX-Gal4-DBD expression vector and the cloning vectors containing the PPAR α hinge-LBDs were linearized through digestion using the BamHI and EcoRI restriction endonucleases. The resulting fragments were separated on 0.5X TBE 0.7 % agarose gel electrophoresis and stained with GelRed. pCMX = 2 μ L of the effector plasmid backbones pCMX-Gal4-DBD. M = 2 μ L DNA standard (2log DNA Ladder). $\alpha\alpha$ = 2 μ L of pSC-B-PPAR $\alpha\alpha$ -LBD. $\alpha\beta$ = 2 μ L of pSC-B-PPAR $\alpha\beta$ -LBD. β/δ = 2 μ L of pSC-B-PPAR β/δ -LBD. γ = 2 μ L of pSC-B-PPAR γ -LBD.

The gel-extracted Atlantic cod PPAR hinge+LBDs and pCMX-Gal4-DBD vector backbones could then be ligated together creating the pCMX-Gal4-DBD-PPAR α -LBD effector plasmids.

4.2.2 Colony Screening for Positive Transformants

The effector plasmids were transformed into competent *E. coli* cells and selected for by amp-resistance on agar plates. Positive transformants were then screened for inserts by colony PCR, using expression vector specific primers. The colony PCR screening products were separated with AGE, which showed the presence and amplification of fragments of expected lengths in regard to each of the Gal4-DBD-PPAR α -LBD fusion protein encoding genes (Fig 19).

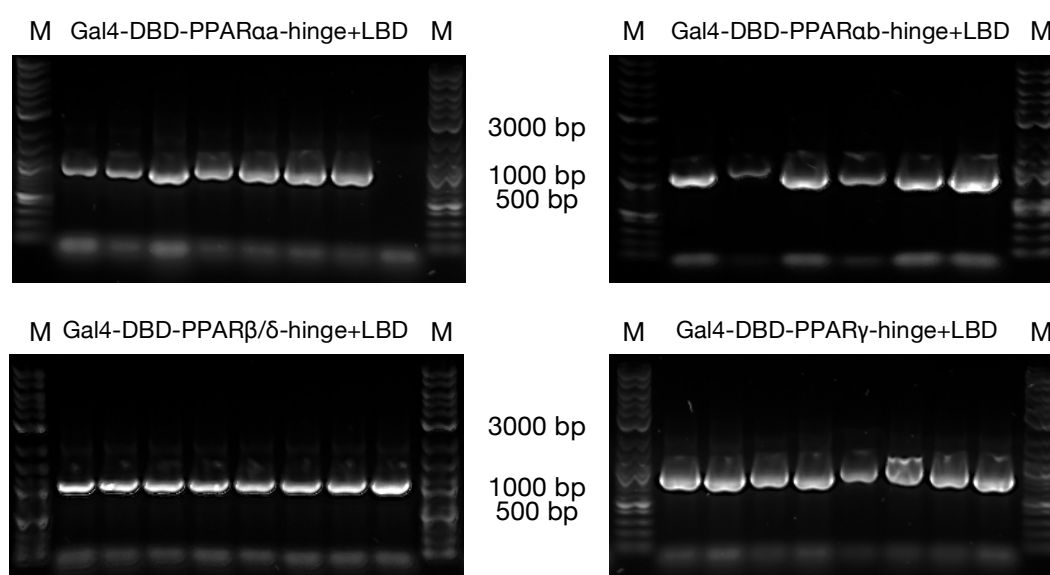


Figure 19. PCR screening for positive transformants containing the Gal4-DBD-PPAR α -LBD encoding fragment. Colony PCR screening products were separated with 0.5X TBE 0.7 % agarose gel electrophoresis. The gel was stained with GelRed to visualize the fragments. Expected lengths: Gal4-DBD-PPAR α -hinge+LBD = 1374 bp; Gal4-DBD-PPAR β -hinge+LBD = 1329 bp; Gal4-DBD-PPAR β/δ -hinge+LBD = 1344 bp; Gal4-DBD-PPAR γ -hinge+LBD = 1353 bp). M = 2 μ L DNA standard (2log DNA Ladder). 2 μ L of amplification reaction was loaded per well.

The effector plasmids were subsequently purified from the positive transformants through mini-preps. Sequencing, using expression vector specific primers, verified that the nucleotide (nt) sequences of the PCR screening products corresponded with the fragments encoding the Gal4-DBD-PPAR α -hinge+LBD fusion protein, and that the fusion proteins were in the correct reading frame (Appendix V-VI).

4.2.3 LRA Plasmids and Integrity Control

Purity and configuration of the plasmids used in the LRA were assessed prior to ligand activation analysis. Hence, after the constructed effector plasmids had been confirmed through sequencing they were, in addition to reporter and control plasmids, replicated in *E. coli* cell cultures and purified through midi-preps. The purity and concentrations of the LRA plasmids were assessed spectrophotometrically, and $A_{260/280}$ and $A_{260/230}$ ratios were measured (Table 47). The obtained values indicated little or no protein contamination and thereby sufficient quality for use with LRA.

Table 47. Spectrophotometric measurements of midi-prepped LRA plasmids.

Sample	Concentration (ng/ μ L)	$A_{260/280}$	$A_{260/230}$
PPAR α	1616.1	1.86	2.35
PPAR α β	1748.5	1.87	2.36
PPAR β/δ	1783.9	1.86	2.22
PPAR γ	1675.8	1.87	2.35
Luciferase	1372.0	1.91	2.20
β -gal	2219.6	1.86	2.26

The integrity of the three types of LRA plasmids (effector-, receptor-, and control plasmids) was verified with AGE, showing that the majority of the plasmids exhibited the supercoiled conformation needed for efficient transfection into the COS-7 cells (Fig 20).

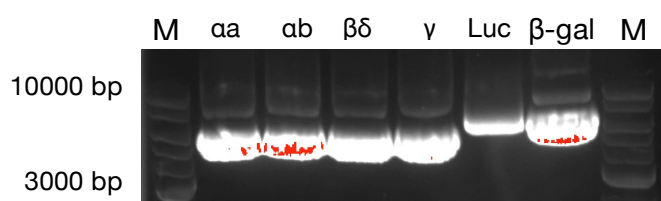


Figure 20. Analyses of integrity and conformation of effector-, reporter-, and control plasmids used in the LRA. PPAR α , PPAR α β , PPAR β/δ , and PPAR γ effector plasmids, as well as the luciferase reporter and β -gal control plasmids were separated on a 0.5X TBE 0.7 % agarose gel and stained with GelRed. M = 2 μ L DNA standard (2log DNA Ladder). $\alpha\alpha$ = 2 μ L of pCMX-Gal4-DBD-PPAR α -hinge+LBD. $\alpha\beta$ = 2 μ L of pCMX-Gal4-DBD-PPAR α β -hinge+LBD. β/δ = 2 μ L of pCMX-Gal4-DBD-PPAR β/δ -hinge+LBD. γ = 2 μ L of pCMX-Gal4-DBD-PPAR γ -hinge+LBD. Luc = 2 μ L of the reporter plasmid ((mh100) x4tk luc). β -gal = 2 μ L of the control plasmid (pCMV- β -gal).

4.3 Luciferase Reporter Gene Assay

After completing the cloning and subcloning of the PPAR α -hinge+LBD fragments, the Atlantic cod PPAR constructs were ready to be tested in the LRA assay *in vitro* by exposing them to different environmental contaminants. Before conducting full-scale LRA trials, agonists that could be used as positive controls for ligand activation had to be established. The LRA system also needed to be optimized in regard to receptor-reporter plasmid ratios. From here on, ligand activation of the PPAR receptors is denoted as fold induction in luciferase activity in cells exposed to the test compound compared to cells exposed to solvent, in this case DMSO.

4.3.1 Establishing Positive Controls for Ligand Activation of Atlantic Cod PPAR Constructs

To establish positive controls for ligand activation for each of the four Gal4-DBD-PPAR α -hinge+LBD constructs, the abilities of mammalian model PPAR agonists in activating the Atlantic cod orthologs were initially assessed. WY14643, a known mammalian PPAR α agonist, was tested on the PPAR α hinge+LBD and PPAR β hinge+LBD constructs. On the PPAR α hinge+LBD construct, WY14643 was able to elicit a maximum activation of 126-fold at 125 μ M (Fig 21 A, 0-125 μ M). While on the PPAR β hinge+LBD construct, WY14643 was able to elicit a maximum activation of 128-fold at 41 μ M (Fig 21 B, 0-80 μ M). The lowest and highest concentration of WY14643 that elicited significant minimum and maximum fold induction and EC₅₀ are summarized in table Table 48.

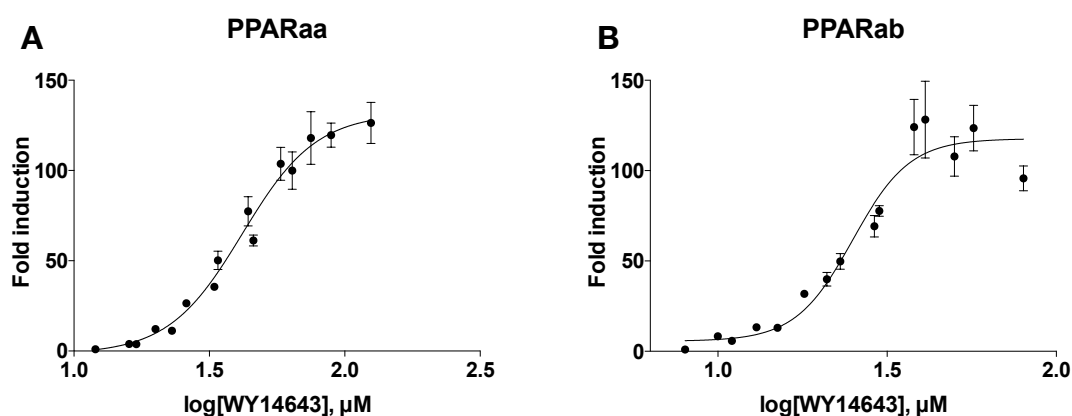


Figure 21. Establishing a positive control for ligand activation of Atlantic cod PPAR α - and PPAR β hinge+LBD constructs. Each measured point shows WY14643-induced activation of the PPAR α constructs as mean fold induction derived from 12 experimental replicates. Standard error for mean (SEM) is indicated A) COS-7 cells transfected with the PPAR α construct were exposed to WY14643 with concentrations ranging between 0-125 μ M. B) COS-7 cells transfected with the PPAR α construct were exposed to WY14643 with concentrations ranging between 0-80 μ M. Non-linear regression was implemented in the software PRISM (GraphPad) to fit a dose-response curve.

GW501516, a known mammalian PPAR β/δ agonist, was tested with LRA on the PPAR β/δ hinge+LBD construct. This compound was able to elicit a maximum activation of 126-fold at 11.3 μM of GW501516 (Fig 22 C, 0-18 μM). The lowest and highest concentration of GW501516 that produced significant minimum and maximum fold induction and EC₅₀ is summarized in table Table 48.

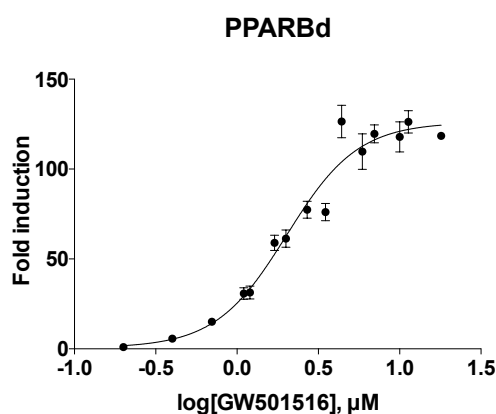


Figure 22. Establishing a positive control for ligand activation of Atlantic cod PPAR β/δ hinge+LBD construct. Each measured point shows GW501516-induced activation of the PPAR β/δ construct as mean fold induction derived from 12 experimental replicates. Standard error for mean (SEM) is indicated. The transfected COS-7 cells were exposed to GW501516 with a concentration ranging between 0-18 μM . Non-linear regression was implemented in the software PRISM (GraphPad) to fit a dose-response curve.

Table 48. Lowest and highest concentrations of control agonists used to achieve significant minimum and maximum fold induction of PPAR x hinge+LBD constructs. Ligand activation in cells exposed to the test compound over cells exposed to solvent after 24 hours. n = 9. The effect concentration (EC₅₀) was calculated in PRISM (GraphPad).

Receptor-subtype	Agonist	Lowest fold induction			Highest fold induction			EC ₅₀ (μM)
		Conc. (μM)	fold \pm SEM	p-value	Conc. (μM)	fold \pm SEM	p-value	
PPAR α	WY14643	16	4 \pm 0.4	<0.0001	125	126 \pm 16.2	<0.0001	41
PPAR β	WY14643	10	8 \pm 1.3	<0.0001	41	128 \pm 30.0	<0.0001	26
PPAR β/δ	GW501516	0.4	6 \pm 1.0	<0.0001	11.3	126 \pm 8.8	<0.0001	2
PPAR γ	Rosi	-	-	-	-	-	-	-
PPAR γ	TBBPA	-	-	-	-	-	-	-
PPAR γ	TTA	-	-	-	-	-	-	-
PPAR γ	1-triple-TTA	-	-	-	-	-	-	-
PPAR γ	2-triple-TTA	-	-	-	-	-	-	-

Five compounds that in mammalian models have shown to activate the PPAR γ receptor (i.e. rosiglitazone (Rosi), tetrabromobisphenol A (TBBPA) tetradecyl thioacetic acid (TTA), 1-triple-TTA, 2-triple-TTA) were tested in the LRA assay with the Atlantic cod PPAR γ . However, none of the typical PPAR γ agonists were able to activate the PPAR γ hinge+LBD construct (Fig 23).

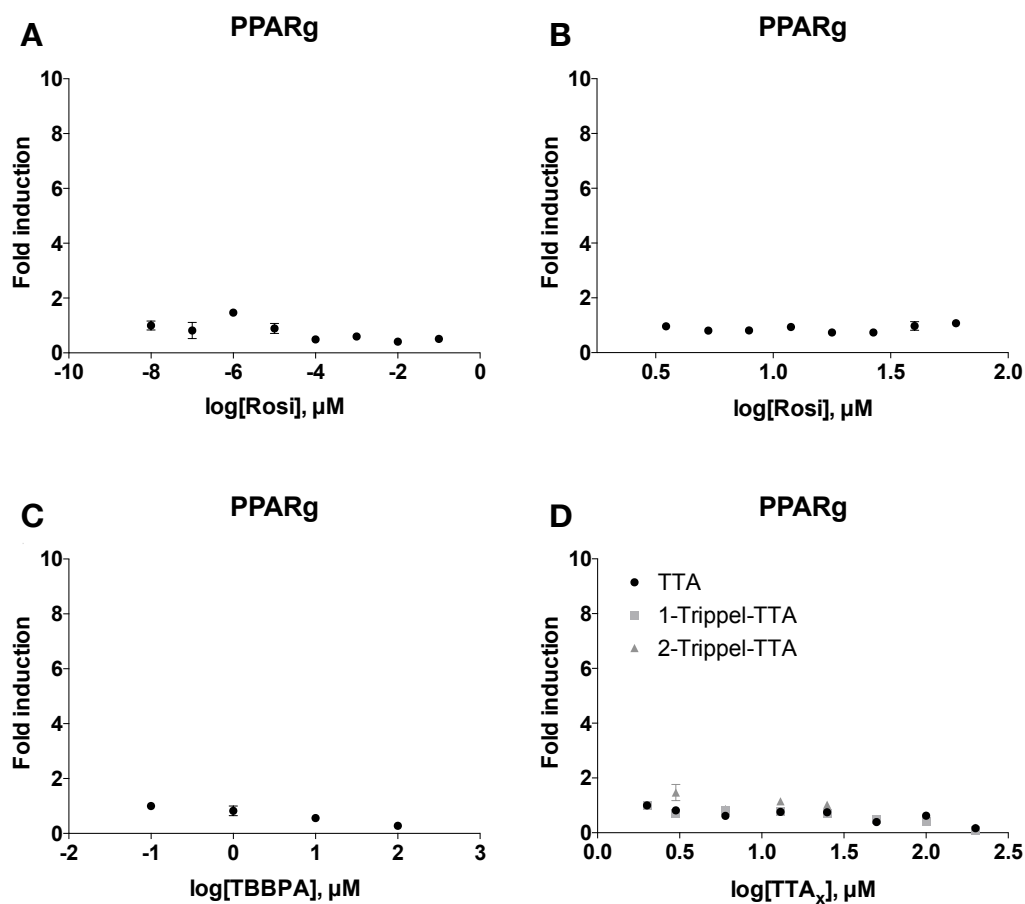


Figure 23. Assessment of five mammalian PPAR γ agonists as positive controls for ligand activation of the Atlantic cod PPAR γ hinge+LBD construct. Each measured point is based on 3 experimental replicates that include three technical replicates each (n=9), and shows standard error for mean (SEM). COS-7 cells transfected with the PPAR γ hinge+LBD construct were exposed to A) Rosiglitazone (Rosi) with concentrations ranging between 0-0.1 μM , B) Rosi with concentrations ranging between 0-60 μM , C) Tetrabromobisphenol A (TBBPA) with concentrations of 1,10, and 100 μM , D) Tetradecyl Thioacetic Acid (TTA), 1-Triple-TTA, and 2-Triple-TTA with concentrations ranging between 0-200 μM .

4.3.2 Optimization of Receptor- Reporter Plasmid Ratio in LRA

To optimize the LRA system, COS-7 cells were transfected with four different ratios between receptor- and reporter plasmids to assess which ratio that produced the best LRA sensitivity. Since we were not able to activate the Atlantic cod PPAR γ receptor *in vitro*, the following experiments were limited to the PPAR α , PPAR β , and PPAR β/δ receptors. In these experiments, the total amount of transfected plasmids were kept constant at 100 ng/well, while varying only the ratio between receptor- and reporter plasmids from 1:2, 1:5, 1:10, and 1:20 (the β -gal control plasmid was always added in the same amount as the reporter plasmid). COS-7 cells transfected with effector plasmids harboring a PPAR x hinge+LBD construct were then exposed to the above-established control agonists. The measurements are based on three experimental replicates for each PPAR subtype, and the trials were repeated two times. By assessing the data from the two trials (Fig 24 A-C) and specifically looking at the significant minimum and maximum fold induction between the different ratios, the two higher ratios, i.e. 1:10 and 1:20, more frequently resulted in higher maximum fold induction in luciferase activity at lower agonist concentrations compared to the two lower ratios of 1:2 and 1:5. For PPAR α , no clear difference between 1:10 and 1:20 could be established. Thus, the 1:10 ratio between receptor- and reporter plasmid was chosen for downstream LRA experiments for PPAR α , PPAR β , and PPAR β/δ , respectively

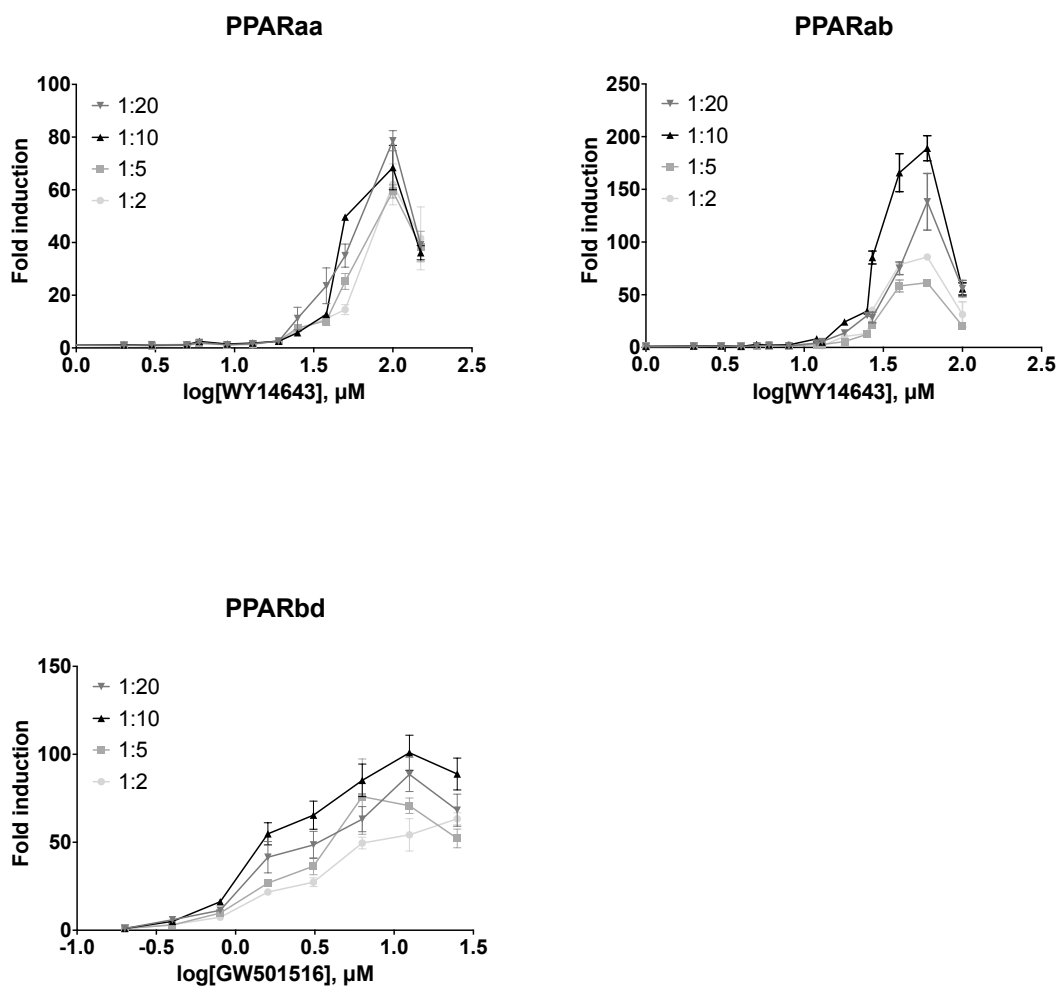


Figure 24. Optimization of receptor-reporter plasmid ratios for LRA trials. COS-7 cells were transfected with four different ratios (1:2, 1:5, 1:10, and 1:20) between receptor- (PPAR α , - β , and - δ respectively) and reporter- (luciferase) plasmids. A) PPAR α - and B) PPAR β -transfected cells were exposed to WY14643, while C) PPAR β / δ -transfected cells were exposed to GW501516, for 24 hours. Each measured point is derived from three experimental replicates of two separate trials that include three technical replicates (n=6), and shows ligand activation of the three different PPAR α hinge+LBD constructs at the four different plasmid ratios. Activation is denoted as fold induction in luciferase activity in transfected COS-7 cells exposed to the control agonists over cells exposed to the solvent DMSO (measured point with lowest x-value) with standard error for mean (SEM).

Concentrations of the agonists WY146643 and GW501516 eliciting a significant lowest and highest fold induction of their PPAR α hinge+LBD construct are summarized in Table 49.

Table 49. Lowest and highest fold induction of PPARx hinge+LBD constructs using four different receptor- reporter plasmid ratios.

Receptor-subtype	Plasmid ratio	Lowest fold induction			Highest fold induction		
		Conc. (μ M)	fold \pm SEM	p-value	Conc. (μ M)	fold \pm SEM	p-value
PPAR α	1:2	19	2.8 \pm 0.6	<0.0001	100	62.1 \pm 7.8	<0.0001
	1:5	19	2.8 \pm 0.5	<0.0001	100	59.4 \pm 2.5	<0.0001
	1:10	19	2.5 \pm 0.7	<0.0001	100	68.4 \pm 8.5	<0.0001
	1:20	19	2.5 \pm 0.2	0.0007	100	78.6 \pm 3.9	<0.0001
PPAR α b	1:2	8	2.6 \pm 0.4	0.0001	60	85.8 \pm 2.9	<0.0001
	1:5	12	2.7 \pm 0.4	<0.0001	60	61.5 \pm 0.9	<0.0001
	1:10	5	2.9 \pm 0.4	<0.0001	60	189.0 \pm 11.9	<0.0001
	1:20	12	4.2 \pm 0.7	<0.0001	60	138.3 \pm 27.0	<0.0001
PPAR β/δ	1:2	0.4	3.2 \pm 0.6	<0.0001	25	63.3 \pm 4.8	<0.0001
	1:5	0.4	3.0 \pm 0.6	<0.0001	6.3	76.0 \pm 30.4	<0.0001
	1:10	0.4	5.1 \pm 0.4	<0.0001	12.5	100.9 \pm 14.1	<0.0001
	1:20	0.4	6.0 \pm 1.4	<0.0001	12.5	88.6 \pm 13.8	<0.0001

PPAR α and PPAR α b are exposed to control agonist WY14643. PPAR β/δ is exposed to control agonist GW501516. SEM = Standard error of mean.

Since none of the tested control agonists for the Atlantic cod PPAR γ hinge+LBD construct was able to induce activation, this construct was excluded from most of the following downstream LRA's. However, based on the results of the other three PPARx hinge+LBD receptor-constructs, a 1:10 ratio was selected for the PPAR γ hinge+LBD construct in order to make LRA trials of a few selected pollutants to explore if any of them could activate of the PPAR γ hinge+LBD construct.

4.3.3 Ligand Activation Assay

The ability of the Atlantic cod PPARx hinge+LBD constructs to bind and become activated by various environmental pollutants was explored *in vitro*. COS-7 cells were co-transfected with the constructed effector plasmids encoding the Gal4-DBD-PPARx-hinge+LBD fusion proteins, together with the luciferase reporter gene plasmid and the β -galactosidase encoding control plasmid, with a 1:10 receptor-reporter plasmid ratio. The transfected COS-7 cells were then exposed to fifteen different pollutants, comprising both legacy- and emerging environmental contaminants (Table 50)

Table 50. Overview of environmental contaminants tested for agonistic effects on Atlantic cod PPARs.

Class	Compounds
Fluorosurfactants	PFOA, PFNA, PFOA, PFUnDA, PFOS, PFHxS
Phthalates	DEHP, DiDP, MBzP, MBP
Pesticides	Chlorpyrifos, Endosulfan
Brominated flame retardant	DPTE
Pharmaceuticals and personal care products	D4, D5 (Siloxanes)
Organochlorine	PCB 153

A consistent 2-fold induction in luciferase activity was set as a minimum requirement before considering the Atlantic cod PPAR_x hinge+LBD constructs to be significantly activated by the ligands. Out of the fifteen ligands tested, PFOA and PFNA were able to activate the PPAR_{ab} hinge+LBD construct (Fig 26). PFOA elicited a significant fold induction at a lower concentration, as well as a higher maximal fold induction compared to PFNA (Fig 26). Concentrations of PFOA and PFNA eliciting a significant lowest and highest fold induction of the PPAR_{ab} hinge+LBD construct are summarized in Table 51.

Table 51. Concentrations resulting in a significant lowest and highest fold induction of the PPAR_{ab} hinge+LBD construct.

Receptor-subtype	Ligand	Lowest fold induction			Highest fold induction		
		Conc. (μM)	fold ± SEM	p-value	Conc. (μM)	fold ± SEM	p-value
PPAR _{ab}	PFOA	70	2.2 ± 0.3	0.0003	150	8.2 ± 0.5	<0.0001
PPAR _{ab}	PFNA	118	2.1 ± 0.5	<0.0001	154	3.2 ± 0.6	<0.0001

Exposure to the remaining fluorosurfactants did not result in any measurable induction of the PPAR_{ab} hinge+LBD construct, nor did the phthalates or the other environmental pollutants tested (Fig 26). None of the pollutants tested were able to activate the PPAR_α-, PPAR_{β/δ}-, and PPAR_γ hinge+LBD constructs under the experimental conditions used during these LRA trials (Fig 25, Fig 27, Fig 28). The highest concentration used (100 μM) of endosulfan, D5, and PCB 153 caused a decrease (close to zero) in background luciferase activity for all four PPAR_x hinge+LBD constructs (Fig 25, Fig 26, Fig 27, Fig 28).

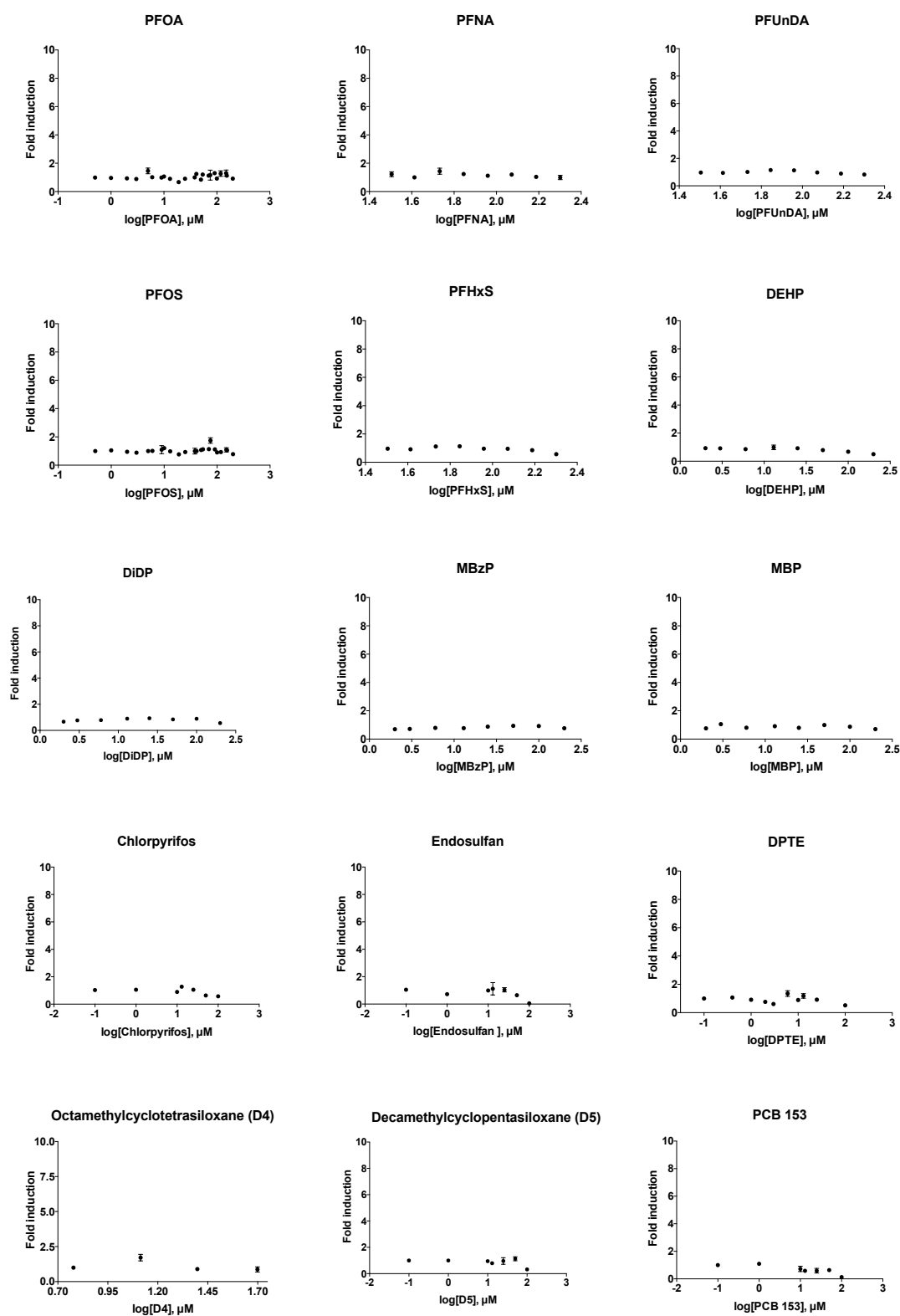


Figure 25. Ligand activation of Atlantic cod PPAR α a hinge+LBD construct exposed to fifteen different pollutants. Dose-response-curves were fitted by non-linear regression (GraphPad, Prism) on average fold induction \pm standard error of the mean (SEM). The data is based on three experimental replicates, and the trials were repeated three times (except for D4 which was only repeated once).

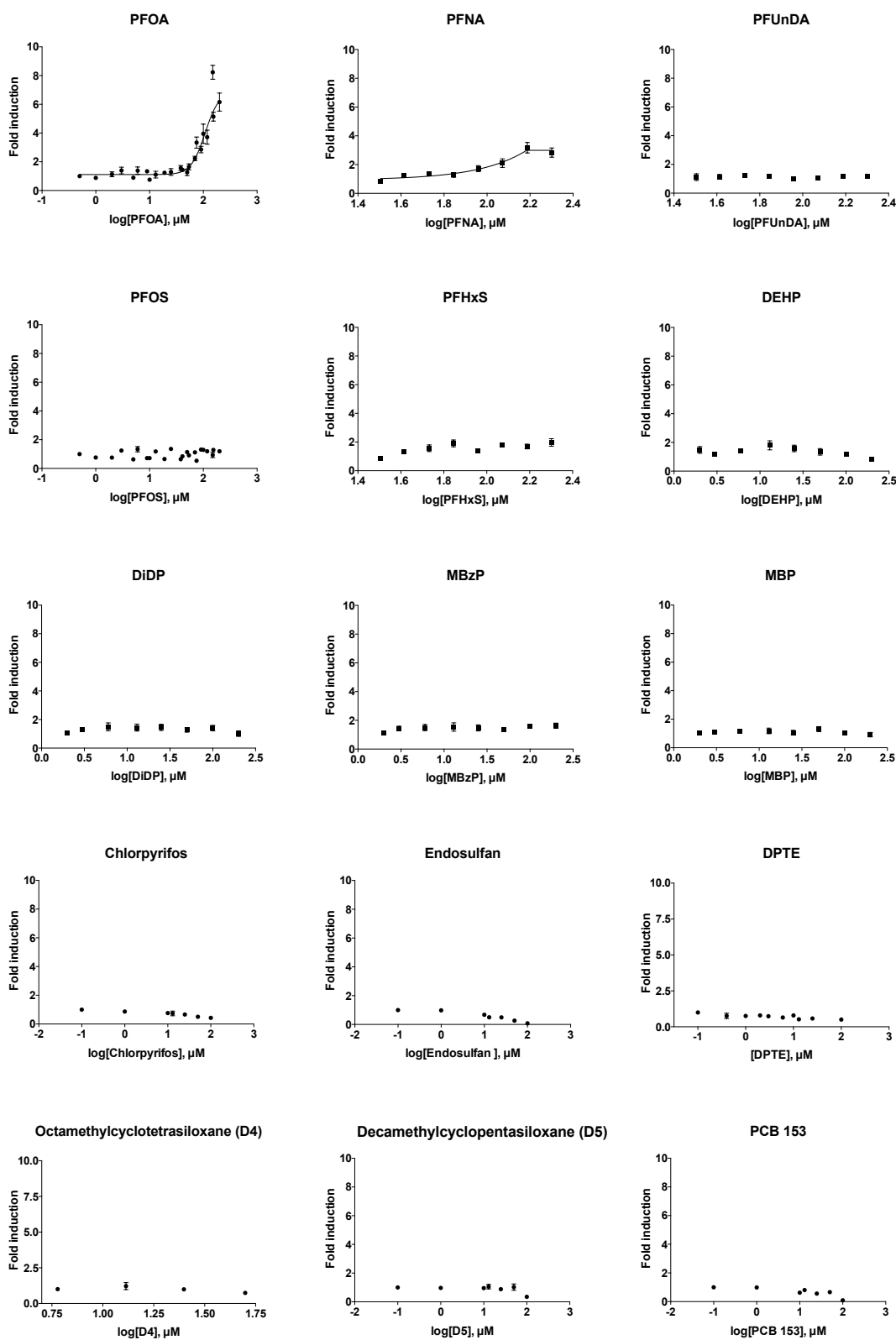


Figure 26. Ligand activation of Atlantic cod PPAR α hinge+LBD construct exposed to fifteen different pollutants. Dose-response-curves were fitted by non-linear regression (GraphPad, Prism) on average fold induction \pm standard error of mean (SEM). The data is based on three experimental replicates, and the trials were repeated three times (except for D4 which was only repeated once).

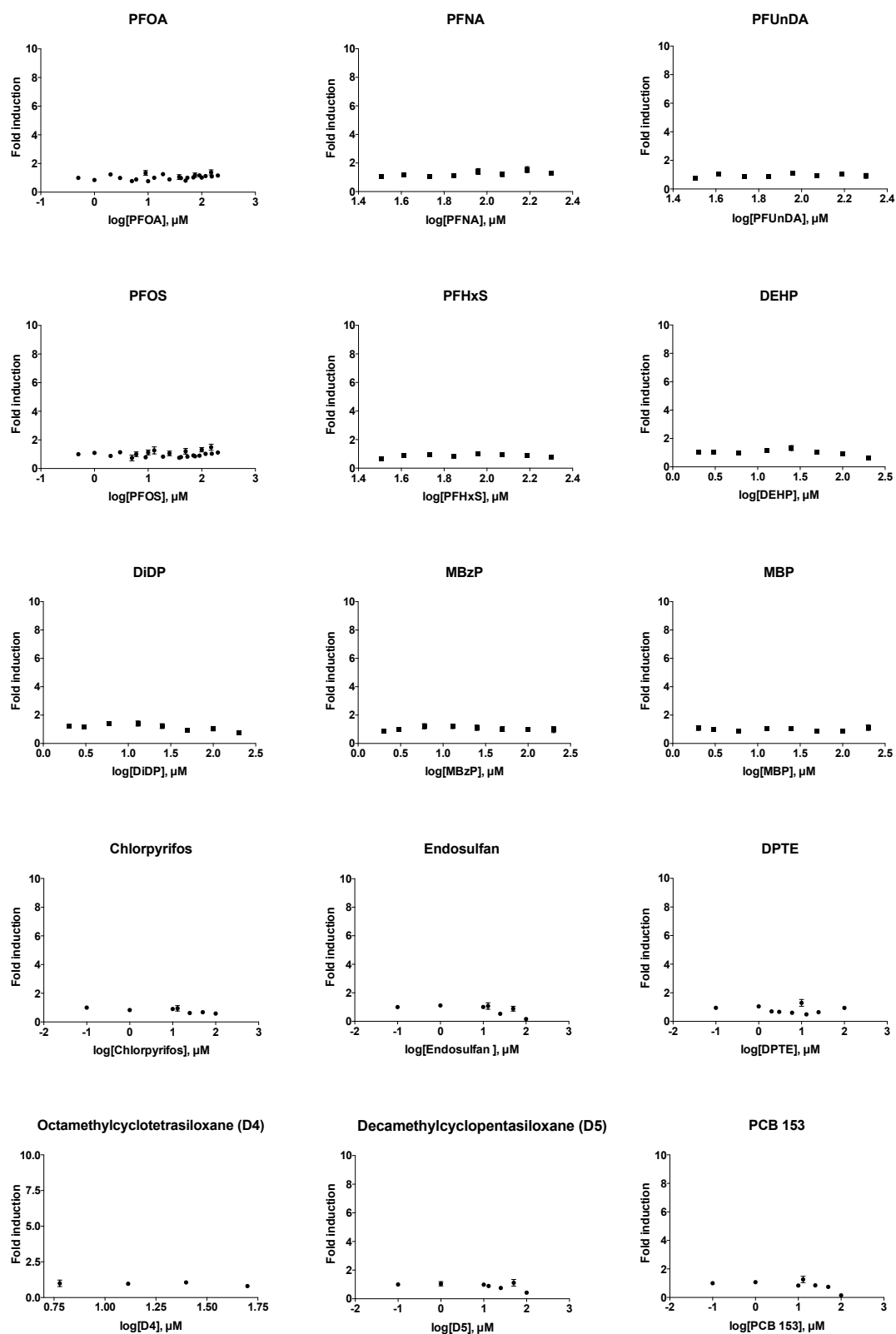


Figure 27. Ligand activation of Atlantic cod PPAR β/δ hinge+LBD construct exposed to fifteen different pollutants. Dose-response-curves were fitted by non-linear regression (GraphPad, Prism) on average fold induction \pm standard error of mean (SEM). The data is based on three experimental replicates, and the trials were repeated three times (except for D4 which was only repeated once).

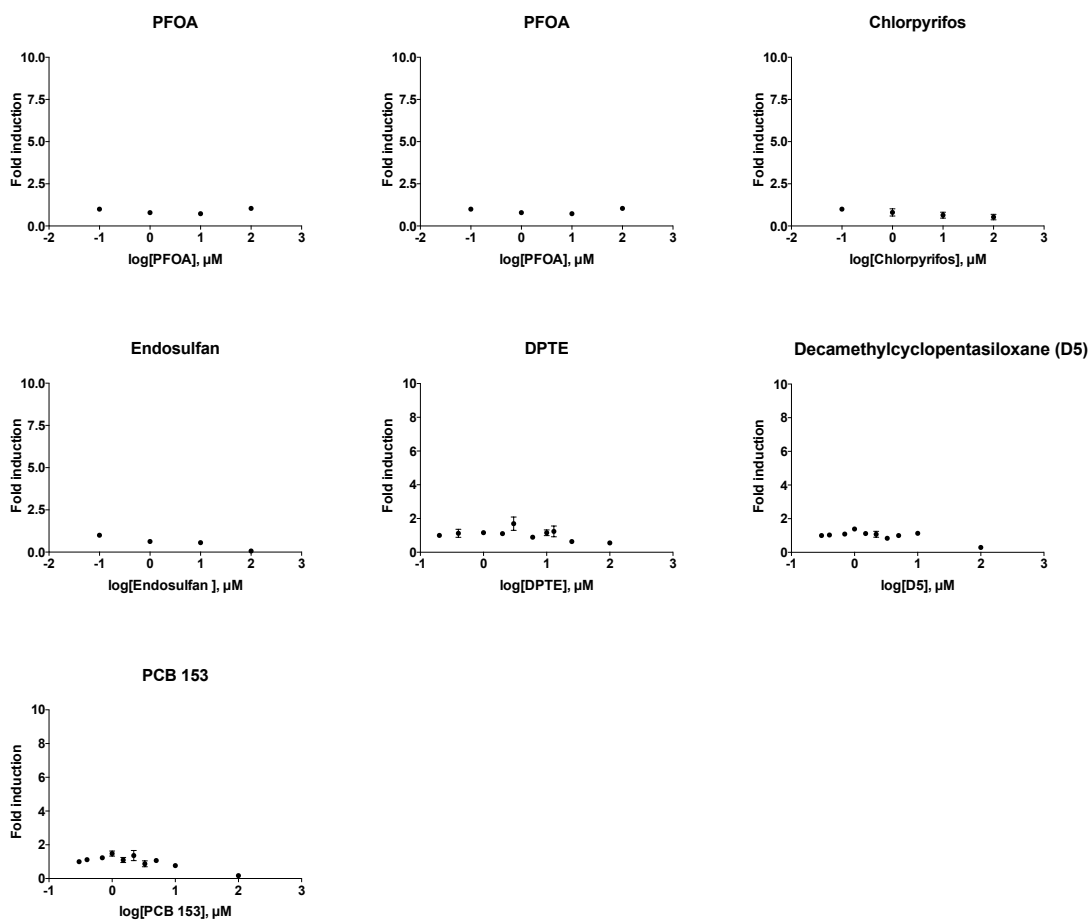


Figure 28. Ligand activation of Atlantic cod PPAR γ hinge+LBD construct exposed to seven different pollutants. Dose-response-curves were fitted by non-linear regression (GraphPad, Prism) on average fold induction \pm standard error of mean (SEM). The data is based on three experimental replicates, and the trials were repeated three times (except for D4 which was only repeated once).

4.4 Cell Viability Assays

The control agonists and all ligands used in the LRA trials were tested for cytotoxic effects on the COS-7 cells using a cell viability assay with two indicator dyes, resazurin and CFDA-AM. Resazurin was used to measure metabolic activity, while CFDA-AM was used to assess plasma membrane integrity. In viable and metabolically active COS-7 cells, resazurin and CFDA-AM become enzymatically converted to their fluorescent metabolites that can be recorded and quantified using an EnSpire 2300 Multilabel Reader (PerkinElmer). Cytotoxicity was defined as a reduction in the fluorescent signal, here denoted as % relative fluorescence, in relation to the solvent control (1 % DMSO) set as 100 %. The cell viability assay showed a significantly reduced fluorescence signal of the resazurin metabolite (reduction from 100% to 60 %) in COS-7 cells exposed to the highest concentration of TTA (200 μ M) (Fig 29, control agonists). On the contrary, the remaining compounds tested showed a significantly increased resazurin signal, except for the highest concentration of 2-triple-TTA (Fig 29, control agonists). An increased resazurin signal was also observed for the fluorosurfactants PFOA at 154 and 118 μ M, PFNA at 154 and 118 μ M, PUnDA at 118 μ M, PFOS at all concentrations, and PFHxS at 154 and 118 μ M (Fig 29, fluorosurfactant). Increased resazurin signal was also observed for the phthalates DEHP, DiDP, and MBP at all concentrations, respectively, as well as for at the two lowest concentrations of MBzP (100 and 50 μ M) (Fig 29, phthalates). This was seen also for the POPs chlorpyrifos at 100 μ M, DPTE at all concentrations, and for PCB 153 at all concentrations (Fig 29, POPs). None of the ligands tested showed any significant decreasing effect on fluorescence signal of the CFDA-AM metabolite, however a significant increase in the signal was observed for the control agonists TTA at 50 μ M, and TBBPA at 1 μ M (Fig 30, control agonists). This was also observed for the fluorosurfactant PFNA at 118 μ M (Fig 30, fluorosurfactant), as well as for one POP, DPTE, at 1 μ M (Fig 30, POPs). Although not significant, 2-triple-TTA, chlorpyrifos, endosulfan, D4, D5, and PCB 153 showed a trend of reduced fluorescence signal of the CFDA-AM metabolite, at the least in the highest concentration (Fig 30).

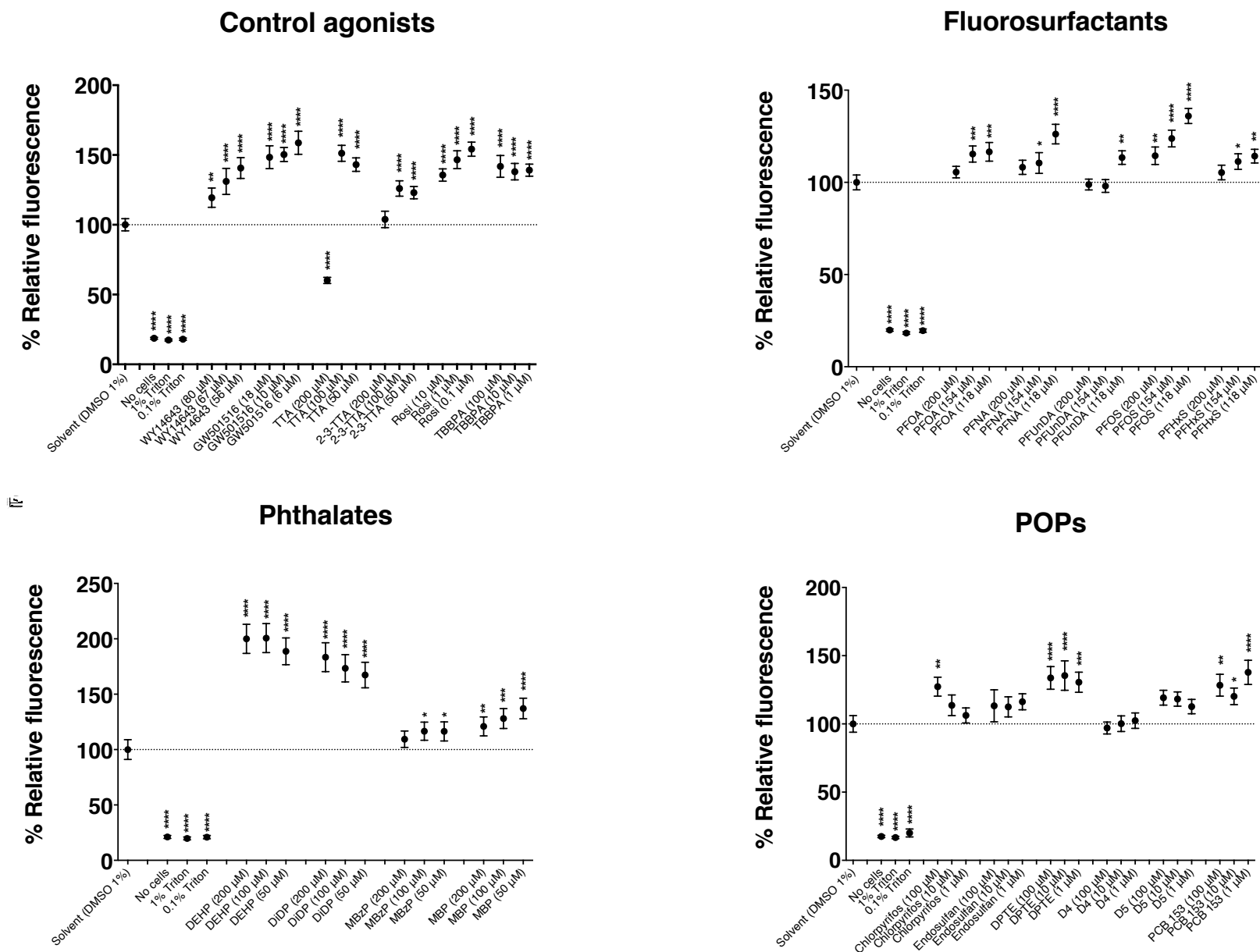


Figure 29. Assessing metabolic activity in COS-7 cells after exposure. COS-7 cells were exposed to the three highest concentrations of each compound used in the LRA experiments while incubated at 37 °C and 5 % CO₂ for 24 hours. “No cells” shows background signal. 0.1 % and 1 % Triton X-100 acts as positive controls for impaired cell viability and cell death. Cytotoxicity is indicated by a reduction in the fluorescent signal (denoted as % relative fluorescence) in relation to the solvent control (1 % DMSO, dotted line) set to 100 %. Significance is denoted as * = $p \leq 0.05$, ** = $p \leq 0.01$, *** = $p \leq 0.001$, **** = $p \leq 0.0001$, n = 4 (n = 3 for D4, D5, and PCB 153).

4.5 Examining the Presence of Expressed Fusion Proteins in COS-7 Cells

4.5.1 Protein Concentration Measurements

COS-7 cells, transfected with the effector plasmids encoding the Gal4-DBD-PPAR_x-hinge+LBD fusion proteins, were harvested and pelleted before lysed in a Triton X-100 lysis buffer. The protein concentrations of the prepared cell lysates were determined with the protein assay reagent Pierce 660 (Thermo scientific), using a standard curve of bovine serum albumin (BSA) (Appendix VII) (Table 52).

Table 52. Protein concentrations in COS-7 cell lysates.

PPAR-subtype	Concentration (µg/mL)
αa A	8386
αa B	5457
αb A	4315
αb B	5023
β/δ A	4640
β/δ B	4782
γ A	4407
γ B	4715
COS-7 A	4715
COS-7 B	2482

4.5.2 Sodium Dodecyl Sulphate Polyacrylamide Gel Electrophoresis (SDS-PAGE)

The protein samples were separated according to their M_w with SDS-PAGE. Two SDS-PA gels were made, one designated for detection of total protein content through Coomassie Brilliant Blue staining, and one for detecting the Gal-4-DBD-PPAR_x-hinge+LBD fusion proteins with Western blotting. Both gels were loaded with 10 μ g of protein per well from each of the COS-7 cell lysate samples. The Coomassie Brilliant Blue-stained PA-gel showed that the proteins in the COS-7 cell lysates had been successfully separated during the SDS-PAGE and that the total amount of protein between cell lysate samples was of similar quantity (Fig 31).

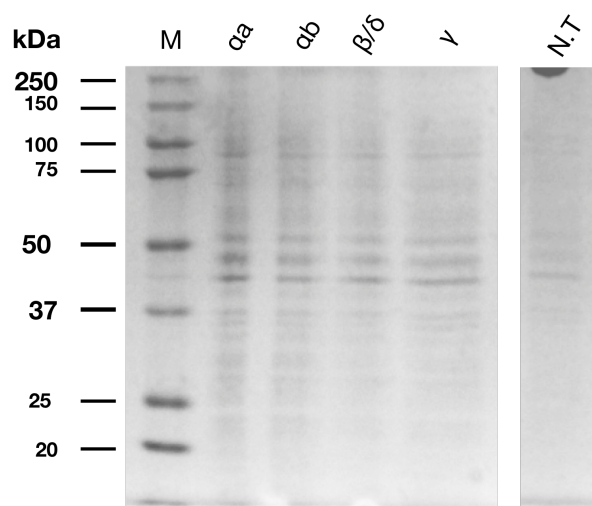


Figure 31. Protein separation of transiently transfected COS-7 cell lysates with SDS-PAGE. Protein samples of lysed COS-7 cells transiently transfected with plasmids encoding the Gal4-DBD-PPAR_x-hinge+LBD fusion proteins were separated with 12 % SDS-PAGE and stained with Coomassie Brilliant Blue. Lanes αa (PPAR αa), αb (PPAR αb), β/δ (PPAR β/δ), γ (PPAR γ), and N.T (non-transfected cells) were loaded with approx. 10 μ g of protein. Lane M was loaded with 5 μ L of Precision Plus Protein™ Kaleidoscope™ Prestained Protein Standards from Bio-Rad. A ChemiDoc™ XRS+ System with a charged-coupled (CCD) camera (Bio-Rad) was used to scan the Coomassie-stained SDS-PA gel.

4.5.3 Western Blotting

Western blotting was carried out to identify and assess the expression levels of the Gal4-DBD-PPAR α -hinge+LBD fusion proteins from the COS-7 cell lysate. The proteins on a SDS-PAGE gel were blotted onto a PVDF membrane by electrotransfer, and available binding sites on the membrane were blocked with 5% dry milk ON. The membrane was first probed with mouse-anti Gal4 antibodies (Fig 32 A), followed by mouse-anti beta actin antibodies that were used as a loading control for protein quantities between the protein samples on the membrane (Fig 32 B). The secondary antibody sheep-anti-mouse IgG was used to visualize the primary antibodies. The Gal4-PPAR fusion proteins were detected as specific bands around the size of 50 kDa in the lanes with cell lysate (CL) from transfected COS-7 cells, while absent in the non-transfected cells (Fig 32 A). The intergroup size distribution of the bands from largest to smallest was lane $\alpha\alpha > \gamma > \beta/\delta > \alpha\beta$. This corresponds well to the predicted Mw's of the Gal4-DBD-PPAR α -hinge+LBD fusion proteins, predicted to be ($\alpha\alpha$) 51.5, (γ) 50.9, (β/δ) 50.8, and ($\alpha\beta$) 50.2 kDa. The Mw of the Gal4-DBD-PPAR α -hinge+LBD fusion proteins were computed *in silico* using the online ExPASy Compute pI/Mw tool (SIB Bioinformatics Resource Portal). Beta actin was detected in all CL samples, including the CL from the non-transfected cells, at approximately 48-49 kDa (Fig 32 B).

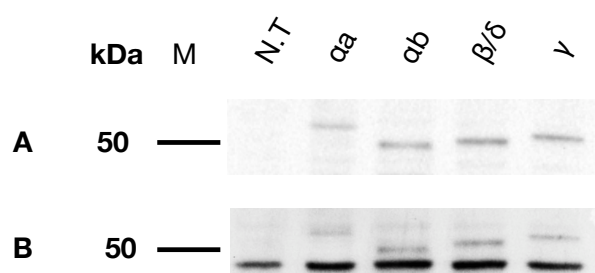


Figure 32. Detection of the Gal4-DBD-PPAR-LBD fusion proteins in transiently transfected COS-7 cells by Western Blotting. Cell lysate from COS-7 cells transiently transfected with plasmids encoding the Gal4-DBD-PPAR α -hinge+LBD fusion proteins were separated with 12 % -PAGE and blotted onto a PVDF membrane. A) Membrane probed with primary mouse-anti Gal4 antibodies diluted 1:500 in TBS-tween. B) The same membrane as shown in A) but additionally probed with mouse-anti beta actin antibodies diluted 1:1000 in TBS-tween. The secondary antibody sheep-anti-mouse IgG conjugated to HRP (diluted 1:2000 in TBS-tween) was used to visualize the primary antibodies. Lane N.T (not transfected cells), $\alpha\alpha$, $\alpha\beta$, β/δ , β/δ , and γ (PPAR subtypes) were loaded with approx. 10 μ g of protein of COS-7 cell lysate. Lane M was loaded with 5 μ L of Precision Plus Protein™ Kaleidoscope™ Prestained Protein Standards from Bio-Rad, where the 50 kDa marker band has been denoted to the left in the figure. The antigen-antibodies complexes were visualized and scanned using a ChemiDoc™ XRS+ System with a charged-coupled (CCD) camera (Bio-Rad).

5 Discussion

The overall aim of this thesis was to provide new information on how the regulation of the lipid metabolism in Atlantic cod can be affected by environmental contaminants through interactions with the PPAR receptors. To my knowledge, this is the first time the hinge+LBDs from the Atlantic cod PPAR α , PPAR α b, PPAR β/δ , and PPAR γ encoding genes have been successfully cloned. In addition, by using an *in vitro* UAS/Gal4-DBD based luciferase reporter gene assay in a COS-7 cell line, this is also the first study that have examined the ligand binding characteristics of these types of nuclear receptors from this species. Phylogenetic analyses were carried out to validate the cloned gene sequences as Atlantic cod PPARs, and examine their similarity to PPARs from other vertebrates, including a variety of teleost species. Pairwise and multiple sequence alignments, together with the construction of a Neighbor-Joining tree, confirmed the identities of the cloned gene sequences as the hinge+LBD from PPAR α , PPAR α b, PPAR β/δ , and PPAR γ . The results also showed some sequence differences in comparison to the predicted PPAR-encoding genes present in the Atlantic cod genome database (Ensembl). Studying ligand activation of the cod PPAR x hinge+LBD constructs *in vitro*, allowed assessment of both legacy and emerging contaminants for their abilities to agonistically activate the PPAR x hinge+LBD constructs. Out of the fifteen ligands tested, it was found that PFOA and PFNA acted as PPAR α b agonists, while the other ligands did not activate any of the PPAR x hinge+LBD constructs.

5.1 Sequence Analyses

Sequencing of the cloned PPAR gene segments revealed some differences in comparison to the predicted PPAR-encoding genes present in the Atlantic cod genome database (Ensembl). Minor differences found between the cloned and predicted Atlantic cod PPARs will not be further discussed here. However, the larger stretches of amino acid residues found in the hinge region of cod PPAR α and PPAR γ will be discussed further. The conservation of amino acid residues previously shown to be important for ligand binding in mammalian PPAR counterparts will also be discussed.

PPAR sequence comparisons between Atlantic cod, other teleosts, and terrestrial vertebrates suggest that teleost PPAR α and PPAR γ in general have longer hinge regions than the terrestrial vertebrate counterparts. The *Ensembl Automatic Gene Annotation System* uses algorithms and models to make preliminary gene predictions that to a large extent are based on terrestrial vertebrate sequence data (Curwen et al., 2004). Thus, inaccurate gene predictions are to be expected due to natural gene variations between different groups of animal species. It is recognized that the Atlantic cod genome still needs to be manually curated, and recently an initiative for a more comprehensive annotation of the cod genome were initiated through the ongoing dCod 1.0 project (RCN project no. 248840).

5.1.1.1 PPAR α and PPAR β

The hinge region in Atlantic cod PPAR α was 19 amino acid residues longer than expected from the predicted PPAR α sequence in Ensembl. Teleosts such as sea bass (*Dicentrarchus labrax*), rabbitfish (*Siganus canaliculatus*), hake (*Merluccius merluccius*), plaice (*Pleuronectes platessa*), sea bream (*Sparus aurata*), and Japanese pufferfish (*Takifugu rubripes*) have also been shown to have longer PPAR γ hinge regions (15-21 amino acids longer) than its human ortholog (Boukouvala et al., 2004; Kondo et al., 2007; Leaver et al., 2005; Raingard et al., 2009; You et al., 2017). In human PPAR α , it has been shown that the key amino acids involved in binding WY14643 are S280, Y314, H440, and Y464 (Bernardes et al., 2013; Narala et al., 2010). The positions of these four amino acids are conserved in both PPAR α and PPAR β in Atlantic cod (Fig 17 A). However, there are sequence differences between the two cod PPAR α subtypes. Atlantic cod PPAR β hinge+LBD and PPAR α hinge+LBD exhibits 65 % and 56 % sequence similarity to human PPAR α hinge+LBD, respectively. The fact that PPAR α has a longer hinge region compared to PPAR β , could potentially cause differences in protein folding that may affect the ligand-binding pocket. Thus, the Atlantic cod PPAR β may have ligand-binding characteristics that more closely resembles the human PPAR α .

5.1.1.2 PPAR β/δ

The cloned Atlantic cod PPAR β/δ hinge+LBD was of equal length as the predicted amino acid sequence present in Ensembl. Similarly, the lengths of PPAR β/δ in other teleosts such as brown trout (*Salmo trutta*) and rabbitfish (*Siganus canaliculatus*) are equal to the length of PPAR β/δ in terrestrial vertebrates (Batista-Pinto et al., 2005; You et

al., 2017). In human PPAR β/δ , the key amino acids involved in binding of GW501516 are W228, H287, V298, V312, I328, H413, and Y437 (Wu et al., 2017). The position of five out of these seven amino acids are conserved in Atlantic cod PPAR β/δ (Fig 17 B). The Atlantic cod differed by having a nonpolar methionine (M) instead of the human nonpolar valine (V), and by having an asparagine (N) with a polar side chain instead of the human histidine (H) with a positively charged side chain. Still, the overall sequence similarity between the Atlantic cod PPAR β/δ hinge+LBD and the human PPAR β/δ hinge+LBD is 79 %. Despite the rather high sequence similarity, the discrepancy of the two amino acids where one possesses very different chemical properties compared to the amino acid found in the human sequence, might give rise to differences in agonist selectivity and specificity between the Atlantic cod PPAR β/δ and the human counterpart.

5.1.1.3 PPAR γ

The hinge region in Atlantic cod PPAR γ was 37 amino acid residues longer than expected from the predicted PPAR γ sequence in Ensembl. Teleosts such as brown trout, rabbitfish, sea bass, hake, Atlantic salmon (*Salmo salar*), Japanese pufferfish (*Takifugu rubripes*), Nile tilapia (*Oreochromis niloticus*), olive flounder (*Paralichthys olivaceus*), and yellow catfish (*Pelteobagrus fulvidraco*) have also been shown to have longer PPAR γ hinge regions (9-39 amino acids longer) than its human ortholog (Andersen et al., 2000; Batista-Pinto et al., 2005; Boukouvala et al., 2004; Cho et al., 2009; He et al., 2015; Kondo et al., 2007; Raingeard et al., 2009; Wafer et al., 2017; You et al., 2017; Zheng et al., 2015). In human PPAR γ , the key amino acids for binding Rosi are C285, R288, S289, H323, Y327, L330, L333, V339, I341, H449, and Y473 (Annapurna et al., 2013; Chandra et al., 2008; Liberato et al., 2012; Nolte et al., 1998). Interestingly, only five amino acid positions out of these eleven are conserved in Atlantic cod PPAR γ (Fig 17 C), and the overall sequence similarity between the cod and human PPAR γ hinge+LBD is only 62 %. The lack of conservation of amino acids in positions involved in binding of Rosi in the Atlantic cod PPAR γ hinge+LBD, as well as the low sequence similarity to human PPAR γ , strongly suggests that the Atlantic cod PPAR γ have different ligand-binding properties than the human PPAR γ .

5.2 Ligand Activation Analyses

Based on work in mammalian models, PPARs have long been considered as lipid sensors and master regulators of the energy metabolism (Desvergne and Wahli, 1999;

Kliwer et al., 1997; Varga et al., 2011). Naturally occurring fatty acids and derivatives control PPAR activation, which in turn induces downstream gene transcription and production of proteins important for lipid- and carbohydrate metabolism. PFCs with their long carbon backbones resemble fatty acids, e.g. by exhibiting the fatty acid octanoic acid structure or octanoic sulfonate structure. However, instead of hydrogen atoms, the carbon backbones are either poly- or perfluorinated. Thus, their ability to mimic fatty acids has long been suspected (Shabalina et al., 2016). Phthalates, similar to PFCs, also carries side-chains that give them a molecular structure resembling that of fatty acids. The ligands tested within this thesis have been chosen due to the characteristics mentioned above, as well as other POP-like properties and presence in the environment at concerning levels. The results from the LRA showed that some PFCs were able to elicit activation of the Atlantic cod PPAR α hinge+LBD construct, and that the level of receptor induction seemed to be correlated to the length of the carbon backbone and functional group of the ligand. On the other hand, the phthalates and POPs tested did not significantly activate any of the Atlantic cod PPAR constructs.

5.2.1.1 Why Use LRA as a Method?

A UAS/Gal4-DBD based luciferase reporter gene assay is a method that allows high throughput screening of potential ligands of nuclear receptors, as well as comparison of the potency and efficacy between different ligands (Wolf et al., 2008). When doing transgenic gene expression in cell lines with a UAS/Gal4-DBD system, it is possible to circumvent the requirement of nuclear receptor-specific response elements, in this case PPREs. This system can therefore be used to characterize different nuclear receptors without the need to clone nuclear receptor-specific response elements and construct receptor specific reporter plasmids for each experiment (Wang et al., 2017). *In vivo*, PPARs bind to DNA as obligate permissive heterodimers with the RXR (Desvergne and Wahli, 1999; Széles et al., 2010). Thus, in models including RXR, it is not possible to distinguish if the heterodimer becomes activated due to ligand-interaction with the LBD of PPAR, or by ligand-interaction with the LBD of RXR. However, PPAR γ has also been shown to function as homodimer in *in vitro* experimental systems, with an affinity constant almost equivalent to that of the PPAR:RXR heterodimer (Okuno et al., 2001). The COS-7 cell line, commonly used to express recombinant proteins, is robust and easy to work with. Importantly,

expression of endogenous PPAR and RXR is either low or undetectable in the COS-7 cells (Herdick et al., 2000; Umemoto and Fujiki, 2012), minimizing interference with the ligand activation experiment. Therefore, using a UAS/Gal4-DBD based system in COS-7 cells specifically allows assessment of ligand-binding properties of PPARs (Colliar et al., 2011; Mukherjee et al., 1998).

5.2.1.2 COS-7 Cell Viability

None of the pollutants that were tested for ligand activation exhibited significantly diminishing effects on the metabolic activity of the COS-7 cells, nor on the cell membrane integrity, at the concentrations used in this thesis. The control agonist TTA, which is a synthetic fatty acid, did exhibit a significant negative effect on the metabolic activity of the COS-7 cells at the highest concentration used (Fig 29). This compound was only tested on the Atlantic cod PPAR γ hinge+LBD construct in order to identify a potential PPAR γ activator (agonist). However, since TTA did not induce any activation it was not used in any further experiments. It has previously been shown that high concentrations of fatty acids are cytotoxic to leukaemia and melanoma cell lines (de Sousa Andrade et al., 2005; Lima et al., 2002; Otton and Curi, 2005). TTA functions as a lipid-lowering agent that cannot be beta-oxidized, but is instead incorporated into the phospholipid membranes of cells (Skrede et al., 1997). In this way, TTA was cytotoxic on glioma cells (Berge et al., 2003). In this study, all control agonists (WY14643, GW501516, TTA, 2-triple-TTA, Rosi, and TBBPA), except the highest concentration of TTA and 2-triple-TTA, caused a varying but significant, increase in the COS-7 cells metabolic activity (Fig 29). This was also observed with the lower concentrations of the fluorosurfactants, most phthalates (except MBzP 200 μ M), and for the POPs chlorpyrifos (at 100 μ M), DPTE, and PCB 153. It might therefore be possible that these control agonists and pollutants in some way stimulated the activity of the COS-7 cells, but further analyses are necessary to unveil the mechanisms behind these observations.

5.2.1.3 Control Agonists

The control agonist WY14643 activated both the Atlantic cod PPAR α - and PPAR β hinge+LBD construct, although with different potency. WY14643 caused a significant activation of the PPAR α hinge+LBD construct at 16 μ M, while 10 μ M was the lowest concentration needed to significantly activate the PPAR β hinge+LBD

construct (Table 48). Even though the highest fold induction was rather similar for both PPAR α subtypes (between 126 and 128 fold) (Fig 21 A, B), WY14643 elicited the highest fold induction in PPAR α at 125 μ M. For PPAR α b, WY14643 induced the highest fold induction already at 41 μ M. Apart from being a commonly used agonist for mammalian PPAR α (Bernardes et al., 2013; Ip et al., 2004; Narala et al., 2010; Varga et al., 2011), WY14643 has also been successfully used as a control agonist for PPAR α -activation in other teleosts (Colliar et al., 2011; Kondo et al., 2007; Leaver et al., 2005). The control agonist WY14643 was initially designed to target human PPAR α . The amino acids that are important for binding WY14643 are all conserved in both PPAR α subtypes present in Atlantic cod. However, the sequence analyses revealed that Atlantic cod PPAR α b exhibits an overall higher sequence similarity to the human PPAR α compared to the Atlantic cod PPAR α a. This could explain why WY14643 appears to be a more potent agonist for the Atlantic cod PPAR α b. That is, WY14643 exhibited an EC₅₀ at 11 μ M on PPAR α b, while for PPAR α a EC₅₀ was determined to be 41 μ M (Table 48).

GW501516 acted as a potent agonist for the Atlantic cod PPAR β/δ hinge+LBD construct, and caused a significant fold induction at 0.4 μ M, while a highest fold activation of 126 fold was elicited at 11.3 μ M (Fig 22) (Table 48). This well-known mammalian PPAR β/δ agonist, has also been successfully used as an inducer and control agonist for PPAR β/δ in Atlantic salmon and in plaice (Colliar et al., 2011; Leaver et al., 2007). GW501516 had an EC₅₀ at 2 μ M on the Atlantic cod PPAR β/δ (Table 48), while in human PPAR β/δ the EC₅₀ have been shown to be as low as 1 nM (Oliver et al., 2001). The sequence analysis revealed Atlantic cod PPAR β/δ to only possess five out of seven amino acids shown important for binding GW501516 in human PPAR β/δ . Instead of having a histidine (H) with an electrically charged side chain, the cod PPAR β/δ has an asparagine (N) with a polar side chain in this position. Thus, the different chemical properties of the amino acids might explain the observed difference in agonist potency.

None of the typical mammalian PPAR γ agonists (Rosi, TBBPA, TTA, 1-triple TTA, and 2-triple TTA) were able to elicit any response in the Atlantic cod PPAR γ hinge+LBD construct, and neither did any of the other fifteen ligands tested (Fig 23, Fig 28). PPAR γ in other teleost species such as plaice, sea bream, medaka (*Oryzias latipes*), and Japanese pufferfish have also been non-responsive to Rosi, fatty acids, and

PUFAs (Colliar et al., 2011; Kondo et al., 2007; Kondo et al., 2010; Leaver et al., 2005). Leaver et al. (2005) even repeated their experiments using a different cell line to make sure no essential factors involved in transcriptional activation were missing, but still got the same results. In this thesis, Western blotting with anti-Gal4 antibodies was used to confirm that the Gal4-DBD-PPAR γ -hinge+LBD fusion protein was produced in the transfected COS-7 cells (Fig 32), thus excluding the possibility that the lack in activation was due to inefficient synthesis of the fusion protein. The absence of PPAR γ -activation by mammalian ligands such as Rosi, might be explained by several non-conserved amino acid residues in the Atlantic cod LBD that are essential for binding Rosi in human PPAR γ (Fig 17 C) (Annapurna et al., 2013; Chandra et al., 2008; Liberato et al., 2012; Nolte et al., 1998). In addition, the overall sequence similarity between human and Atlantic cod PPAR γ hinge+LBD is only 62 %. It is therefore likely that PPAR γ in Atlantic cod folds into a different tertiary structure compared to the human counterpart, and thus promoting different ligand-binding characteristics. It has been suggested that a potential driving mechanism of the observed divergence is the energy metabolism of ectothermic teleosts, requiring PPAR γ to function differently compared to its orthologs in endothermic terrestrial vertebrates (He et al., 2015). Another potential explanation is differences in diet between teleosts and terrestrial vertebrates. Humans, for example, consume a high proportion of carbohydrates to meet their energy demands, while a teleost such as Atlantic cod mainly consume protein and fat to meet theirs (Polakof et al., 2012; Tocher, 2003). More information about tissue-specific patterns of teleost PPARs might help elucidate their functions, especially the function of PPAR γ .

Great efforts have been made to map the expression patterns of PPARs in mammals. The tissue-specific expression of the different PPAR subtypes is to a large degree reflected by their different physiological functions (Ferré, 2004; Georgiadi and Kersten, 2012; Hiji et al., 2002; Wagner and Wagner, 2010). Far less studies have examined PPAR tissue-specific expression patterns in teleosts. One study on turbot found that PPAR α was predominantly expressed in the heart, while PPAR β expression was ubiquitous among all tissues (Urbatzka et al., 2013). Two other studies reported that teleost PPAR α and PPAR β/δ tissue-specific expression patterns resemble what is found in terrestrial mammals (Batista-Pinto et al., 2005; Leaver et al., 2005). Tissue-specific expression of teleost PPAR γ on the other hand, appears to be

more indistinct. Batista-Pinto et al. (2005) only detected PPAR γ from brown trout in the trunk kidney and liver, whereas PPAR γ dominated in the intestines and adipose tissue of sea bream and plaice (Leaver et al., 2005). Contradicting results have also been reported regarding the levels of the different PPAR subtypes in different tissues in teleosts. Batista-Pinto et al. (2005) found that the expression of PPAR β/δ was slightly higher than the expression of PPAR α , and that PPAR γ was the least expressed subtype in brown trout. In sea bream and plaice, on the other hand, Leaver et al. (2005) reported equal levels of PPAR γ and PPAR β/δ in all tissues tested, contradicting also what is found in terrestrial vertebrates (Ferré, 2004; Georgiadi and Kersten, 2012; Hiji et al., 2002; Wagner and Wagner, 2010). It is evident that more research is needed before we have a clear map over the expression patterns of PPARs in teleosts, and potential teleost species-specific differences in PPAR expression.

5.2.1.4 Fluorosurfactants

Perfluorinated carboxylic acids (PFCAs) elicited activation of the Atlantic cod PPAR α hinge+LBD construct while perfluorinated sulfonic acids (PFSAs) did not. The level of activation by the PFCAs decreased with increasing length of the carbon backbone from eight to eleven carbon atoms (C8 to C11). The shortest of the carboxylates tested, PFOA (C8), exhibited the highest activation potency and elicited a significant fold induction of the PPAR α hinge+LBD construct at the lowest concentration (70 μ M) of all PFCAs (Table 51). PFOA (C8) also prompted the highest fold induction (8-fold) at 150 μ M (Table 51). The one-carbon longer PFNA (C9) was able to elicit a significant fold induction of the PPAR α hinge+LBD construct at 118 μ M, indicating that PFNA is a weaker agonist than PFOA. The highest fold induction prompted by PFNA (3-fold) was also lower than that of PFOA (Fig 26). PFUnDA (C11) was the longest PFCA tested and were not able to activate the PPAR α hinge+LBD construct at any of the concentrations tested Fig 26). Mammalian models have also reported correlation between length of the carbon backbone and activation of PPARs using UAS/Gal4-DBD based luciferase reporter gene assays. Wolf et al. (2008) showed PFCAs to activate human PPAR α in a similar matter as in Atlantic cod. The receptor activation increased when exposed to carboxylates with C4 up to C9, but at C10 the carboxylate became unable to activate the human PPAR α . Buhrke et al. (2013) also showed in their study on human PPARs that PFCAs (C<8) activated PPAR α , and that activation potency decreased with decreasing alkyl chain length,

with PFOA being most potent. In addition, PFCAs also weakly activated human PPAR γ and PPAR β/δ . Similarly, although using other systems than UAS/Gal4-DBD based luciferase reporter gene assays, Zhang et al. (2014) showed human PPAR γ activation of PFCAs to increase with increasing alkyl chain length from C4 up to C11, before decreasing with C>11. Leaver et al. (2005) found that PFOA activated both plaice and sea bream PPAR α :RXR heterodimers. It is very interesting that PFOA and PFNA only activated PPAR β and not PPAR α in Atlantic cod. However, even though both PPAR α and PPAR β contained all amino acid residues shown to be important for binding the control agonist, the longer hinge region of PPAR α , as well as other differences in amino acid residues within the ligand-binding domain, might affect the ligand specificity and selectivity. The question still remains if PFOA and PFNA are able to bind to the PPAR α ligand-binding pocket and not activate the receptor, but instead act as antagonists.

The sulfonates tested in this thesis, i.e. PFHxS (C6) and PFOS (C8), did not elicit a measurable fold induction of any of the Atlantic cod PPARx hinge+LBD constructs. In plaice, PFOS was also unable to activate any of the PPAR subtypes (Colliar et al., 2011). However, several studies have shown sulfonates, such as PFOS, to target mammalian PPAR α in transactivation assays, although being less potent compared to the carboxylates (Heuvel et al., 2006; Shipley et al., 2004; Takacs and Abbott, 2007; Wolf et al., 2008). Although PFOS contains the same number of carbon atoms as PFOA, PFOS could not significantly activate any of the PPAR subtypes. However, the functional group differs with PFOS having a sulfonic group instead of a carboxyl group. This difference is most likely what makes PFCAs potent PPAR β activators but not PFSAs.

A recent monitoring survey mapped PFCs levels in livers from Atlantic cod that had been sampled in fjords and harbors along the Norwegian coast (Valdersnes et al., 2017). Out of the 16 PFCs analyzed, PFOS dominated in most locations, with the highest level measured to 21.8 $\mu\text{g kg}^{-1}$ wet weight. In general, they found the eastern part of the Norwegian coast to be more polluted than the western and northern parts. Still, they concluded that the levels of PFCs in livers of Atlantic cod in Norwegian waters are low. In this thesis, it was found that PFOA and PFNA could activate the PPAR β construct. However, the concentrations of PFCAs and PFSAs used in this

thesis are of course not directly comparable to the levels found in wild-caught Atlantic cod. When exposure experiments are carried out *in vitro*, it is assumed that most of the dose will become available inside the cells, which is not necessarily true. The permeability of the cell membrane might affect the pollutants' ability to enter the cells to some degree. Furthermore, in living organisms there are several factors affecting how much of the exposure dose that reaches its target site, i.e., the absorption rate; if pre-systemic elimination occurs, if a pollutant is distributed towards or away from the target tissue or organ, whether the pollutant is detoxified or activated, and the efficiency of the biotransformation, elimination and excretion. The elimination half-life of PFCs in rats have been reported to be approx. 60 days for females and 43 days for males for PFOS, 2-4 hours females and 4-6 days males for PFOA, and 41 days females and 31 days males for PFNA (Benskin et al., 2009; Chang et al., 2008; Chengelis et al., 2009; Heuvel et al., 1991; Hundley et al., 2006; Lau, 2012; Ohmori et al., 2003; Olsen et al., 2009; Tatum-Gibbs et al., 2011). This is in contrast to humans, where the elimination half-life of PFCs have been reported to be 8.5 years for PFHxS, 5.4 years for PFOS, and 2.3 - 3.8 years for PFOA (Bartell et al., 2010; Harada et al., 2005; Lau, 2012; Olsen et al., 2007). The elimination half-life of PFCs in Atlantic cod is still unknown, since we don't know how well Atlantic cod metabolize and eliminate PFCs. It is known that PFCs bioaccumulate over time and biomagnifies up in higher trophic levels (Martin et al., 2004). Importantly, this study shows that PFCAs can activate at least one Atlantic cod PPAR subtype.

5.2.1.5 Phthalates

The phthalates tested in this study (i.e., DEHP, DiDP, MBzP, and MBP) did not activate any of the Atlantic cod PPAR constructs. Colliar et al. (2011) examined activation potency of four phthalates on plaice PPARs; two parent compounds (dimethylphthalate (DMP) and benzylbutylphthalate (BzBP)) and two metabolites (mono-1-methylhexyl phthalate (MMHP) and mono-benzyl phthalate (MBzP)). None of the parent phthalates activated any of the plaice PPAR subtypes. However, at 100 μ M the metabolite MMHP activated PPAR α (16-fold), and PPAR β/δ weakly (2-fold). Interestingly, they found that the other metabolite, MBzP, also activated both plaice PPAR α and PPAR β/δ at 100 μ M, although only weakly (2-fold). As already stated, MBzP did not activate any of the Atlantic cod PPAR subtype constructs in this study. It should be noted that, apart from using a fish cell line, Colliar et al. (2011) also used

ethanol as their vehicle control and not DMSO as used in this study. Bility et al. (2004) reported that phthalate monoesters activated both mouse and human PPAR α and PPAR γ , but mouse PPARs were activated at lower concentrations. In addition, they concluded that the longer the side-chains of the phthalates, the more potent and efficient activators they became (Bility et al., 2004). It appears as that PPARs sensitivity towards activation of phthalates varies greatly between different species.

In a monitoring survey, the phthalates DEHP and DiDP were undetectable in livers from Atlantic cod sampled around coastal waters of Norway (Green et al., 2015). However, in the Norwegian arctic DEHP was detected in liver samples of Atlantic cod in Kongsfjorden, where the highest concentration measured was 203 ng/g wet weight. (Warner et al., 2010). As mentioned in the introduction, phthalates are not persistent in the environment and organisms can usually metabolize them relatively fast. The problem is that they are extensively used worldwide in everyday-products, allowing them to be continuously released into the environment (Frederiksen et al., 2007).

5.2.1.6 POPs

The remaining POPs tested for ligand activation abilities (i.e., chlorpyrifos, endosulfan, DPTE, siloxane D4 and D5, and PCB 153) were unable to activate any of the Atlantic cod PPAR constructs. However, at the highest concentration (100 μ M), endosulfan, siloxane D5, and PCB 153 caused the luciferase activity to decrease below the solvent control in all four Atlantic cod PPAR constructs (Fig 25, Fig 26, Fig 27, Fig 28). This could either be a sign of antagonistic effect of these POPs on the PPARs, or that they are cytotoxic to the COS-7 cells at the highest concentrations. However, endosulfan, siloxane D5, and PCB 153 did not show any signs of negatively impacting COS-7 cell metabolic activity or membrane integrity at the concentrations used (Fig 29, Fig 30). Although, it is possible that this is a COS-7 cellular response against these POPs affecting another endpoint not accounted for in the cell viability assay. In order to answer what endpoint is causing this response in the COS-7 cells, the mechanism of cytotoxicity of each compound needs to be established (Riss and Moravec, 2004).

Kojima et al. (2010) used a transactivation assay in a CV-1 cell line to screen two hundred pesticides (including chlorpyrifos and endosulfan) and found that only three activated mouse PPAR α and PPAR γ , namely diclofop-methyl, pyrethrins and

imazalil. It seems that most pesticides are not targeting PPARs. Siloxanes have been detected in liver samples from Atlantic cod at high concentrations in fjords close to large human settlements. D5 was measured to be as high as 1978.5 ng/g wet weight in Atlantic cod sampled in Oslofjorden, while the highest concentration of D4 was measured to 134.4 ng/g wet weight. (Schlabach et al., 2007). In Kongsfjorden located on Svalbard, D4 and D5 were measured at lower concentrations of 3.9 ng/g wet weight. Thus, siloxanes appear to be a larger hazard to Atlantic cod living closer to densely populated areas. However, based on the findings in this study, siloxanes does not appear to target Atlantic cod PPARs, nor does PCB 153 and DPTE. However, PCB 153 has been reported to affect the lipid metabolism in Atlantic cod liver (Yadatie et al., 2014; Yadatie et al., 2017). PCB 153 is highly bioaccumulative and biomagnifying, and has been measured to be as high as 1940 ng/g fresh weight in livers from Atlantic cod sampled in Oslofjord in 2014 (Thomas et al., 2015). Brominated flame-retardants, such as DPTE, could not be detected in Atlantic cod liver during an environmental screening in 2009 (Møskeland, 2010). Importantly, the authors state that it was the first study on these types of pollutants and called for more studies before concluding that the overall levels in Norway are low.

5.2.1.7 Potential weaknesses and limitations with the LRA method

Luciferase reporter gene assays are easy to use, and well established for studying nuclear receptor-function (Paguio et al., 2010). Still, a downside is that they are time-consuming as it takes four days to complete one single experiment. Since the system requires a cell line in order to express the receptor- and reporter proteins, cells need to be cultured and maintained in special and costly facilities. As with most scientific experiments, there is always a degree of between-experiment variations, e.g. cell proliferation might be affected by prolonged stress, and reporter plasmid quality can vary between midi-preps. Therefore, it is important to minimize this variability by using cells that have been subjected to equal handling, and to make a large enough reporter plasmid preparation to sustain repeated experiments until completion. The UAS/Gal4-DBD based luciferase reporter gene assay is a great system for conducting high-throughput ligand screening, and it is possible to test ligand interaction of PPARs while excluding RXR from the system, as well as endogenous PPREs. However, it is also these advantages that limit how far the results can be extrapolated. This system evaluates the ability, efficacy, and potency of a ligand to activate the PPARx

hinge+LBD construct and expression of the luciferase reporter gene *in vitro*. It is a simplified model compared to an *in vivo* situation, where RXR, coactivators, corepressors, and PPREs are present and contribute to the full-scale heterodimer activation and target gene expression. Although the assay can be used to provide knowledge of potential activation of nuclear receptors by numerous ligands, but the system does not convey which pathway(s) are affected. Nor does it verify that the ligand-interaction produces a toxicological response in the organism (Wolf et al., 2008).

5.3 Conclusion

This thesis has for the first time successfully isolated and cloned the hinge+LBDs from Atlantic cod PPAR α , PPAR β , PPAR β/δ , and PPAR γ , and further subjected them to functional characterization with regard to ligand activation. Sequence analyses and phylogenetic reconstruction validated and confirmed the identities of the cloned gene sequences from Atlantic cod as the hinge+LBD from PPAR α , PPAR β , PPAR β/δ , and PPAR γ . The UAS/Gal4-DBD based luciferase reporter gene assay in a COS-7 cell line was successfully established and a useful system to test the ligand specificity of the different PPAR subtypes and make comparisons of ligand-binding properties in relation to control agonists, as well as to environmental contaminants. The control agonist WY14643 activated both PPAR α subtypes in Atlantic cod. The EC₅₀ was found to be lower for PPAR β compared to PPAR α . The control agonist GW501516 activated PPAR β/δ . Notably, none of the typical mammalian PPAR γ agonists activated Atlantic cod PPAR γ , even though its expression in COS-7 cells was confirmed through Western Blotting. Among the pollutants tested, only PFCAs between 8 to 9 carbons long activated the PPAR β subtype. The PFSAs, phthalates, and POPs that were tested were all unable to activate any of the Atlantic cod PPAR subtypes. In conclusion, if Atlantic cod are exposed to compounds with long carbon-backbones that harbor a carboxyl-group, the lipid metabolism could potentially be modulated through direct interference with at least one PPAR subtype.

5.4 Future work

This study showed that PFCAs were able to activate PPAR β . However, PFCAs did not activate PPAR α , and why did not the PFSAs activate any of the PPARs? Due to time limitation, this study did not test the pollutants for antagonistic effects on the Atlantic cod PPARs. However, that would be an interesting continuation of this study,

especially to test if PFOS and PFOA can bind PPAR α and antagonistically inhibit activation induced by a control agonist. In addition, studying ligand-receptor interactions *in silico* doing modeling based on crystallized PPARs from other species followed by ligand-docking analyses, could help elucidate which specific amino acids in the Atlantic cod PPAR-LBDs that are important for binding these ligands and agonists used in this study. Such predictions could then be followed-up by targeted *in-vitro* mutagenesis of selected amino acid residues and subsequent ligand activation analyses.

In line with the 3R principles (replacement, reduction and refinement), systems like the UAS/Gal4-DBD based luciferase reporter gene assay are great for conducting initial screening of potential ligands in order to identify hazardous compounds before exposing large numbers of living fish, which in addition to an animal welfare issue is both costly and time consuming. A way to make the initial screening even more time- and cost efficient, allowing an even higher throughput of producing ligand activation data, would be to establish a cell line-independent system. An AlphaLISA bead based system (PerkinElmer) would be an interesting alternative for studying ligand activation of nuclear receptors. Traditionally, AlphaLisa is used to detect and characterize interactions between antibodies and antigens (Bielefeld-Sevigny, 2009). A modification to the AlphaLISA system, by incorporating the UAS/Gal4-DBD principles, could allow interaction between ligands and nuclear receptor-LBDs to be studied. An adaptation of the AlphaLisa system for this purpose is currently being explored in the environmental toxicology laboratory (UiB).

The natural next step of the research presented here would be to test the findings in a more realistic setting, by conducting exposure studies *ex vivo* or *in vivo*. Studying chemical exposure *ex vivo*, using the established precision-cut liver slices (PCLS) method (Eide et al., 2014; Lerche-Langrand and Toutain, 2000), makes it possible to examine the response to pollutants in a system where cell-interactions are intact. Still, avoiding a full-scale exposure experiment on living fish. From the exposure study using PCLS, it would be possible to extract RNA and e.g. perform quantitative real-time polymerase chain reactions (qPCR) for measuring changes in gene expression. PPAR target genes could thus be analyzed to map which signaling pathways that are affected by the exposure. Lastly, conducting *in vivo* exposure studies on live fish, testing

those chemicals that are most likely to have an affect on the organism. Here, it would also be interesting to examine tissue-specific expression patterns before and after exposure, to help elucidate the still unknown functions of the PPAR subtypes in teleost species.

6 Referenses

- Andersen, Ø., et al., 2000. Multiple variants of the peroxisome proliferator-activated receptor (PPAR) γ are expressed in the liver of Atlantic salmon (*Salmo salar*). *Gene*. 255, 411-418.
- Annapurna, H. V., et al., 2013. Isolation and in silico evaluation of antidiabetic molecules of *Cynodon dactylon* (L.). *Journal of Molecular Graphics and Modelling*. 39, 87-97.
- Aviv, H., Leder, P., 1972. Purification of biologically active globin messenger RNA by chromatography on oligothymidylic acid-cellulose. *Proceedings of the National Academy of Sciences*. 69, 1408-1412.
- Bainy, A. C., et al., 2013. Functional characterization of a full length pregnane X receptor, expression in vivo, and identification of PXR alleles, in zebrafish (*Danio rerio*). *Aquatic toxicology*. 142, 447-457.
- Bakke, T., et al., 2013. Environmental impacts of produced water and drilling waste discharges from the Norwegian offshore petroleum industry. *Marine Environmental Research*. 92, 154-169.
- Bao, L.-J., et al., 2015. Global trends of research on emerging contaminants in the environment and humans: a literature assimilation. *Environmental Science and Pollution Research*. 22, 1635-1643.
- Barroso, E., et al., 2011. The PPAR β/δ activator GW501516 prevents the down-regulation of AMPK caused by a high-fat diet in liver and amplifies the PGC-1 α -Lipin 1-PPAR α pathway leading to increased fatty acid oxidation. *Endocrinology*. 152, 1848-1859.
- Bartell, S. M., et al., 2010. Rate of decline in serum PFOA concentrations after granular activated carbon filtration at two public water systems in Ohio and West Virginia. *Environmental health perspectives*. 118, 222.
- Batista-Pinto, C., et al., 2005. Identification and organ expression of peroxisome proliferator activated receptors in brown trout (*Salmo trutta f. fario*). *Biochimica et Biophysica Acta (BBA)-Gene Structure and Expression*. 1731, 88-94.
- Benskin, J. P., et al., 2009. Disposition of perfluorinated acid isomers in sprague - dawley rats; Part 1: Single dose. *Environmental toxicology and chemistry*. 28, 542-554.
- Berge, K., et al., 2003. Impact of mitochondrial β -oxidation in fatty acid-mediated inhibition of glioma cell proliferation. *Journal of lipid research*. 44, 118-127.
- Bernardes, A., et al., 2013. Molecular mechanism of peroxisome proliferator-activated receptor α activation by WY14643: a new mode of ligand recognition and receptor stabilization. *Journal of molecular biology*. 425, 2878-2893.
- Bertazzi, P. A., et al., 1998. The Seveso studies on early and long-term effects of dioxin exposure: a review. *Environmental Health Perspectives*. 106, 625-633.

- Bertrand, S., et al., 2007. Unexpected novel relational links uncovered by extensive developmental profiling of nuclear receptor expression. *PLoS genetics*. 3, e188.
- Bielefeld-Sevigny, M., 2009. AlphaLISA immunoassay platform—the “no-wash” high-throughput alternative to ELISA. *Assay and drug development technologies*. 7, 90-92.
- Bility, M. T., et al., 2004. Activation of mouse and human peroxisome proliferator-activated receptors (PPARs) by phthalate monoesters. *Toxicological Sciences*. 82, 170-182.
- Bizarro, C., et al., 2016. Single and mixture effects of aquatic micropollutants studied in precision-cut liver slices of Atlantic cod (*Gadus morhua*). *Aquatic Toxicology*. 177, 395-404.
- Blumberg, B., et al., 1998. SXR, a novel steroid and xenobioticsensing nuclear receptor. *Genes & development*. 12, 3195-3205.
- Boukouvala, E., et al., 2004. Molecular characterization of three peroxisome proliferator-activated receptors from the sea bass (*Dicentrarchus labrax*). *Lipids*. 39, 1085-1092.
- Bråte, I. L. N., et al., 2016. Plastic ingestion by Atlantic cod (*Gadus morhua*) from the Norwegian coast. *Marine Pollution Bulletin*. 112, 105-110.
- Bryan, G., et al., 1979. Bioaccumulation of marine pollutants [and discussion]. *Philosophical Transactions of the Royal Society of London B: Biological Sciences*. 286, 483-505.
- Buhrke, T., et al., 2013. In vitro toxicological characterization of perfluorinated carboxylic acids with different carbon chain lengths. *Toxicology letters*. 218, 97-104.
- Casals-Casas, C., Desvergne, B., 2011. Endocrine disruptors: from endocrine to metabolic disruption. *Annual review of physiology*. 73, 135-162.
- Casals-Casas, C., et al., 2008. Interference of pollutants with PPARs: endocrine disruption meets metabolism. *International Journal of Obesity*. 32, S53-S61.
- Chakravarthy, M. V., et al., 2005. “New” hepatic fat activates PPAR α to maintain glucose, lipid, and cholesterol homeostasis. *Cell metabolism*. 1, 309-322.
- Chandra, V., et al., 2008. Structure of the intact PPAR- γ -RXR- α nuclear receptor complex on DNA. *Nature*. 456, 350-356.
- Chang, S.-C., et al., 2008. Comparative pharmacokinetics of perfluorobutyrate in rats, mice, monkeys, and humans and relevance to human exposure via drinking water. *Toxicological Sciences*. 104, 40-53.
- Chengelis, C. P., et al., 2009. Comparison of the toxicokinetic behavior of perfluorohexanoic acid (PFHxA) and nonafluorobutane-1-sulfonic acid (PFBS) in cynomolgus monkeys and rats. *Reproductive Toxicology*. 27, 400-406.
- Cho, H. K., et al., 2009. Molecular cloning and characterization of olive flounder (*Paralichthys olivaceus*) peroxisome proliferator-activated receptor γ . *General and comparative endocrinology*. 163, 251-258.
- Choi, J.-M., Bothwell, A. L., 2012. The nuclear receptor PPARs as important regulators of T-cell functions and autoimmune diseases. *Molecules and cells*. 33, 217-222.

- Chomczynski, P., 1993. A reagent for the single-step simultaneous isolation of RNA, DNA and proteins from cell and tissue samples. *Biotechniques*. 15, 532-4, 536-7.
- Chomczynski, P., Mackey, K., 1995. Substitution of chloroform by bromochloropropane in the single-step method of RNA isolation. *Analytical biochemistry*. 225, 163-164.
- Clark, R. B., et al., 1989. *Marine pollution*. Clarendon Press Oxford.
- Colliar, L., et al., 2011. Tributyltin is a potent inhibitor of piscine peroxisome proliferator-activated receptor α and β . *Comparative Biochemistry and Physiology Part C: Toxicology & Pharmacology*. 153, 168-173.
- Consortium, U., 2014. UniProt: a hub for protein information. *Nucleic acids research*. gku989.
- Cunningham, F., et al., 2014. Ensembl 2015. *Nucleic acids research*. 43, D662-D669.
- Curwen, V., et al., 2004. The Ensembl automatic gene annotation system. *Genome research*. 14, 942-950.
- Darnerud, P. O., 2003. Toxic effects of brominated flame retardants in man and in wildlife. *Environment international*. 29, 841-853.
- Davis, M., ApE: a plasmid editor. 2012.
- De Laender, F., et al., 2011. Ecotoxicological mechanisms and models in an impact analysis tool for oil spills. *Journal of Toxicology and Environmental Health, Part A*. 74, 605-619.
- de Sousa Andrade, L. N., et al., 2005. Toxicity of fatty acids on murine and human melanoma cell lines. *Toxicology in vitro*. 19, 553-560.
- Delerive, P., et al., 2000. Oxidized phospholipids activate PPAR α in a phospholipase A2 - dependent manner. *FEBS letters*. 471, 34-38.
- Den Broeder, M. J., et al., 2015. Zebrafish as a model to study the role of peroxisome proliferator-activated receptors in adipogenesis and obesity. *PPAR research*. 2015.
- Desvergne, B., Wahli, W., 1999. Peroxisome proliferator-activated receptors: nuclear control of metabolism 1. *Endocrine reviews*. 20, 649-688.
- Diab, A., et al., 2002. Peroxisome Proliferator-Activated Receptor- γ Agonist 15-Deoxy- Δ 12, 1412, 14-Prostaglandin J2 Ameliorates Experimental Autoimmune Encephalomyelitis. *The Journal of Immunology*. 168, 2508-2515.
- Eide, M., et al., 2014. Precision-cut liver slices of Atlantic cod (*Gadus morhua*): an in vitro system for studying the effects of environmental contaminants. *Aquatic toxicology*. 153, 110-115.
- Enerstvedt, K. S., et al., 2017. Study of the plasma proteome of Atlantic cod (*Gadus morhua*): Effect of exposure to two PAHs and their corresponding diols. *Chemosphere*.
- Evenset, A., 2009. Screening of New Contaminants in Samples from the Norwegian Arctic. 2510/2009. Norwegian Pollution Control Authority, Oslo, Norway.
- Falandysz, J., et al., 2006. Is fish a major source of fluorinated surfactants and repellents in humans living on the Baltic Coast? *Environmental science & technology*. 40, 748-751.

- Falandysz, J., et al., 2007. Perfluorinated compounds in some terrestrial and aquatic wildlife species from Poland. *Journal of Environmental Science and Health Part A*. 42, 715-719.
- Farrell, S., Taylor, L., 2005. *Experiments in Biochemistry: A Hands-on Approach*. Cengage Learning.
- Ferré, P., 2004. The biology of peroxisome proliferator-activated receptors. *Diabetes*. 53, S43-S50.
- Fisher, B. E., 1999. Most unwanted. *Environmental health perspectives*. 107, A18.
- Foekema, E., et al., 2012. Toxic concentrations in fish early life stages peak at a critical moment. *Environmental toxicology and chemistry*. 31, 1381-1390.
- Fonnum, F., et al., 2006. Molecular mechanisms involved in the toxic effects of polychlorinated biphenyls (PCBs) and brominated flame retardants (BFRs). *Journal of Toxicology and Environmental Health, Part A*. 69, 21-35.
- Forman, B. M., et al., 1997. Hypolipidemic drugs, polyunsaturated fatty acids, and eicosanoids are ligands for peroxisome proliferator-activated receptors α and δ . *Proceedings of the National Academy of Sciences*. 94, 4312-4317.
- Forman, B. M., et al., 1995a. 15-deoxy- Δ 12, 14-prostaglandin J₂ is a ligand for the adipocyte determination factor PPAR γ . *Cell*. 83, 803-812.
- Forman, B. M., et al., 1995b. Unique response pathways are established by allosteric interactions among nuclear hormone receptors. *Cell*. 81, 541-550.
- Frederiksen, H., et al., 2007. Metabolism of phthalates in humans. *Molecular nutrition & food research*. 51, 899-911.
- Fry, D. M., 1995. Reproductive effects in birds exposed to pesticides and industrial chemicals. *Environmental Health Perspectives*. 103, 165.
- Georgiadi, A., Kersten, S., 2012. Mechanisms of gene regulation by fatty acids. *Advances in Nutrition: An International Review Journal*. 3, 127-134.
- Goksøyr, A., 1985. Purification of hepatic microsomal cytochromes P-450 from β -naphthoflavone-treated Atlantic cod (*Gadus morhua*), a marine teleost fish. *Biochimica et Biophysica Acta (BBA)-General Subjects*. 840, 409-417.
- Goksøyr, A., Use of cytochrome P450 1A (CYP1A) in fish as a biomarker of aquatic pollution. *Toxicology in Transition*. Springer, 1995, pp. 80-95.
- Goksøyr, A., et al., 1987. Species characteristics of the hepatic xenobiotic and steroid biotransformation systems of two teleost fish, Atlantic cod (*Gadus morhua*) and rainbow trout (*Salmo gairdneri*). *Toxicology and applied pharmacology*. 89, 347-360.
- Goksøyr, A., Husøy, A.-M., Immunochemical approaches to studies of CYP1A localization and induction by xenobiotics in fish. *Fish ecotoxicology*. Springer, 1998, pp. 165-202.
- Goksøyr, A., et al., 1986. Regioselective metabolism of phenanthrene in Atlantic cod (*Gadus morhua*): studies on the effects of monooxygenase inducers and role of cytochromes P-450. *Chemico-biological interactions*. 60, 247-263.
- Green, N. W., et al., 2015. Contaminants in coastal waters of Norway 2014.
- Harada, K., et al., 2005. Renal clearance of perfluorooctane sulfonate and perfluorooctanoate in humans and their species-specific excretion. *Environmental research*. 99, 253-261.

- He, A.-Y., et al., 2015. Molecular characterization, transcriptional activity and nutritional regulation of peroxisome proliferator activated receptor gamma in Nile tilapia (*Oreochromis niloticus*). *General and comparative endocrinology*. 223, 139-147.
- Herdick, M., et al., 2000. Carboxylic ester antagonists of 1 α , 25-dihydroxyvitamin D 3 show cell-specific actions. *Chemistry & biology*. 7, 885-894.
- Herzke, D., et al., Perfluorinated Alkylated Substances, Brominated Flame Retardants and Chlorinated Paraffins in the Norwegian Environment-Screening 2013. Norwegian Environment Agency. NILU–Norsk Institutt for Luftforskning. SWECO, Tromsø, Norway, 2013.
- Heuvel, J. P. V., et al., 1991. Tissue distribution, metabolism, and elimination of perfluorooctanoic acid in male and female rats. *Journal of Biochemical and Molecular Toxicology*. 6, 83-92.
- Heuvel, J. P. V., et al., 2006. Differential activation of nuclear receptors by perfluorinated fatty acid analogs and natural fatty acids: a comparison of human, mouse, and rat peroxisome proliferator-activated receptor- α , - β , and - γ , liver X receptor- β , and retinoid X receptor- α . *Toxicological Sciences*. 92, 476-489.
- Higgins, L. S., DePaoli, A. M., 2010. Selective peroxisome proliferator-activated receptor γ (PPAR γ) modulation as a strategy for safer therapeutic PPAR γ activation. *The American journal of clinical nutrition*. 91, 267S-272S.
- Hihi, A., et al., 2002. PPARs: transcriptional effectors of fatty acids and their derivatives. *Cellular and Molecular Life Sciences*. 59, 790-798.
- Holub, B. J., 2002. Clinical nutrition: 4. Omega-3 fatty acids in cardiovascular care. *Canadian Medical Association Journal*. 166, 608-615.
- Hundley, S., et al., 2006. Absorption, distribution, and excretion of ammonium perfluorooctanoate (APFO) after oral administration to various species. *Drug and chemical toxicology*. 29, 137-145.
- Hurst, C. H., Waxman, D. J., 2003. Activation of PPAR α and PPAR γ by environmental phthalate monoesters. *Toxicological Sciences*. 74, 297-308.
- Ip, E., et al., 2004. Administration of the potent PPAR α agonist, Wy - 14,643, reverses nutritional fibrosis and steatohepatitis in mice. *Hepatology*. 39, 1286-1296.
- Jones, D. T., et al., 1992. The rapid generation of mutation data matrices from protein sequences. *Bioinformatics*. 8, 275-282.
- Julshamn, K., et al., 2013a. A baseline study on levels of polychlorinated dibenzo-p-dioxins, polychlorinated dibenzofurans, non-ortho and mono-ortho PCBs, non-dioxin-like PCBs and polybrominated diphenyl ethers in Northeast Arctic cod (*Gadus morhua*) from different parts of the Barents Sea. *Marine pollution bulletin*. 75, 250-258.
- Julshamn, K., et al., 2013b. A baseline study of levels of mercury, arsenic, cadmium and lead in Northeast Arctic cod (*Gadus morhua*) from different parts of the Barents Sea. *Marine pollution bulletin*. 67, 187-195.
- Julshamn, K., et al., 2013c. A baseline study of metals in cod (*Gadus morhua*) from the North Sea and coastal Norwegian waters, with focus on mercury, arsenic, cadmium and lead. *Marine pollution bulletin*. 72, 264-273.
- Karl, H., Lahrssen-Wiederholt, M., 2009. Dioxin and dioxin-like PCB levels in cod-liver and -muscle from different fishing grounds of the North- and Baltic

- Sea and the North Atlantic. *Journal für Verbraucherschutz und Lebensmittelsicherheit*. 4, 247-255.
- Karlsen, O. A., et al., 2011. Integrative environmental genomics of cod (*Gadus morhua*): the proteomics approach. *Journal of Toxicology and Environmental Health, Part A*. 74, 494-507.
- Karlsen, O. A., et al., 2012. Mass spectrometric analyses of microsomal cytochrome P450 isozymes isolated from β -naphthoflavone-treated Atlantic cod (*Gadus morhua*) liver reveal insights into the cod CYPome. *Aquatic toxicology*. 108, 2-10.
- Kliwer, S. A., et al., 1997. Fatty acids and eicosanoids regulate gene expression through direct interactions with peroxisome proliferator-activated receptors α and γ . *Proceedings of the National Academy of Sciences*. 94, 4318-4323.
- Kliwer, S. A., et al., 2000. Peroxisome proliferator-activated receptors: from genes to physiology. *Recent progress in hormone research*. 56, 239-263.
- Kojima, H., et al., 2010. Endocrine-disrupting potential of pesticides via nuclear receptors and aryl hydrocarbon receptor. *Journal of Health Science*. 56, 374-386.
- Kondo, H., et al., 2007. Ligand-dependent transcriptional activities of four torafugu pufferfish *Takifugu rubripes* peroxisome proliferator-activated receptors. *General and comparative endocrinology*. 154, 120-127.
- Kondo, H., et al., 2010. Transcriptional activities of medaka *Oryzias latipes* peroxisome proliferator-activated receptors and their gene expression profiles at different temperatures. *Fisheries Science*. 76, 167.
- Kota, B. P., et al., 2005. An overview on biological mechanisms of PPARs. *Pharmacological Research*. 51, 85-94.
- Krey, G., et al., 1997. Fatty acids, eicosanoids, and hypolipidemic agents identified as ligands of peroxisome proliferator-activated receptors by coactivator-dependent receptor ligand assay. *Molecular Endocrinology*. 11, 779-791.
- Kumar, A., Garg, N., 2005. *Genetic Engineering*. Nova Biomedical Books.
- Lapinskas, P. J., et al., 2005. Role of PPAR α in mediating the effects of phthalates and metabolites in the liver. *Toxicology*. 207, 149-163.
- Lau, C., *Perfluoroalkyl acids: recent research highlights*. Pergamon, 2012.
- Lau, C., et al., 2007. Perfluoroalkyl acids: a review of monitoring and toxicological findings. *Toxicological sciences*. 99, 366-394.
- Leaver, M. J., et al., 2005. Three peroxisome proliferator-activated receptor isoforms from each of two species of marine fish. *Endocrinology*. 146, 3150-3162.
- Leaver, M. J., et al., 2007. Multiple peroxisome proliferator-activated receptor β subtypes from Atlantic salmon (*Salmo salar*). *Journal of Molecular Endocrinology*. 38, 391-400.
- Lee, V., 1990. *Peptide and Protein Drug Delivery*. Taylor & Francis.
- Lehmann, J. M., et al., 1995. An antidiabetic thiazolidinedione is a high affinity ligand for peroxisome proliferator-activated receptor γ (PPAR γ). *Journal of Biological Chemistry*. 270, 12953-12956.
- Lerche-Langrand, C., Toutain, H. J., 2000. Precision-cut liver slices: characteristics and use for in vitro pharmaco-toxicology. *Toxicology*. 153, 221-253.

- Liberato, M. V., et al., 2012. Medium chain fatty acids are selective peroxisome proliferator activated receptor (PPAR) γ activators and pan-PPAR partial agonists. *PLoS One*. 7, e36297.
- Lima, T., et al., 2002. Ranking the toxicity of fatty acids on Jurkat and Raji cells by flow cytometric analysis. *Toxicology in vitro*. 16, 741-747.
- Link, J. S., et al., 2009. Trophic role of Atlantic cod in the ecosystem. *Fish and Fisheries*. 10, 58-87.
- Louveau, I., et al., 1991. An improved method for isolating RNA from porcine adipose tissue. *Analytical biochemistry*. 196, 308-310.
- Macdonald, R., et al., 2000. Contaminants in the Canadian Arctic: 5 years of progress in understanding sources, occurrence and pathways. *Science of the Total Environment*. 254, 93-234.
- Maglich, J. M., et al., 2003. The first completed genome sequence from a teleost fish (*Fugu rubripes*) adds significant diversity to the nuclear receptor superfamily. *Nucleic acids research*. 31, 4051-4058.
- MANUAL, I., StrataClone Blunt PCR Cloning Kit.
- Martin, J. W., et al., 2002. Collection of airborne fluorinated organics and analysis by gas chromatography/chemical ionization mass spectrometry. *Analytical Chemistry*. 74, 584-590.
- Martin, J. W., et al., 2004. Identification of long-chain perfluorinated acids in biota from the Canadian Arctic. *Environmental Science & Technology*. 38, 373-380.
- Metpally, R. P. R., et al., 2007. Genome inventory and analysis of nuclear hormone receptors in *Tetraodon nigroviridis*. *Journal of biosciences*. 32, 43-50.
- Moore, J., et al., 2003. Environmental and Health Assessment of Perfluorooctane Sulfonic Acid and its Salts. St. Paul, MN M. 3.
- Møskeland, T., 2010. Environmental screening of selected "new" brominated flame retardants and selected polyfluorinated compounds 2009. Det Norske Veritas, Oslo. 158.
- Mukherjee, R., et al., 1998. RXR agonists activate PPAR α -inducible genes, lower triglycerides, and raise HDL levels in vivo. *Arteriosclerosis, thrombosis, and vascular biology*. 18, 272-276.
- Mullis, K. B., 1990. The unusual origin of the polymerase chain reaction. *Scientific American*. 262, 56-61.
- Narala, V. R., et al., 2010. Leukotriene B₄ is a physiologically relevant endogenous peroxisome proliferator-activated receptor- α agonist. *Journal of Biological Chemistry*. 285, 22067-22074.
- Naruhn, S., et al., 2010. 15-hydroxyeicosatetraenoic acid is a preferential peroxisome proliferator-activated receptor β/δ agonist. *Molecular pharmacology*. 77, 171-184.
- Nelson, D. L., et al., 2008. *Lehninger principles of biochemistry*. Macmillan.
- Nolte, R. T., et al., 1998. Ligand binding and co-activator assembly of the peroxisome proliferator-activated receptor-gamma. *Nature*. 395, 137.
- O'connor, S., et al., 1991. Multifluorescent assays reveal mechanisms underlying cytotoxicity-phase I. CTFA compounds. *In vitro toxicology*. 4, 197-206.
- Ohmori, K., et al., 2003. Comparison of the toxicokinetics between perfluorocarboxylic acids with different carbon chain length. *Toxicology*. 184, 135-140.

- Okuno, M., et al., 2001. Dual DNA-binding specificity of peroxisome-proliferator-activated receptor γ controlled by heterodimer formation with retinoid X receptor α . *Biochemical Journal*. 353, 193-198.
- Oliver, W. R., et al., 2001. A selective peroxisome proliferator-activated receptor δ agonist promotes reverse cholesterol transport. *Proceedings of the national academy of sciences*. 98, 5306-5311.
- Olsen, G. W., et al., 2007. Half-life of serum elimination of perfluorooctanesulfonate, perfluorohexanesulfonate, and perfluorooctanoate in retired fluorochemical production workers. *Environmental health perspectives*. 115, 1298.
- Olsen, G. W., et al., 2009. A comparison of the pharmacokinetics of perfluorobutanesulfonate (PFBS) in rats, monkeys, and humans. *Toxicology*. 256, 65-74.
- Organization, W. H., 2010. Persistent organic pollutants: impact on child health.
- Otton, R., Curi, R., 2005. Toxicity of a mixture of fatty acids on human blood lymphocytes and leukaemia cell lines. *Toxicology in vitro*. 19, 749-755.
- Page, B., et al., 1993. A new fluorometric assay for cytotoxicity measurements in vitro. *International journal of oncology*. 3, 473-473.
- Paguio, A., et al., 2010. Improved dual-luciferase reporter assays for nuclear receptors. *Current chemical genomics*. 4.
- Polakof, S., et al., 2012. Glucose metabolism in fish: a review. *Journal of Comparative Physiology B*. 182, 1015-1045.
- Poothong, S., et al., 2012. Determination of perfluorooctane sulfonate and perfluorooctanoic acid in food packaging using liquid chromatography coupled with tandem mass spectrometry. *Journal of hazardous materials*. 205, 139-143.
- Raingear, D., et al., 2009. Cloning and transcription of nuclear receptors and other toxicologically relevant genes, and exposure biomarkers in European hake (*Merluccius merluccius*) after the Prestige oil spill. *Marine genomics*. 2, 201-213.
- Renner, R., Growing concern over perfluorinated chemicals. ACS Publications, 2001.
- Rigaud, C., et al., 2013. Relative potency of PCB126 to TCDD for sublethal embryotoxicity in the mummichog (*Fundulus heteroclitus*). *Aquatic toxicology*. 128, 203-214.
- Rigét, F., et al., 2010. Temporal trends of legacy POPs in Arctic biota, an update. *Science of the Total Environment*. 408, 2874-2884.
- Riss, T. L., Moravec, R. A., 2004. Use of multiple assay endpoints to investigate the effects of incubation time, dose of toxin, and plating density in cell-based cytotoxicity assays. *Assay and drug development technologies*. 2, 51-62.
- Routti, H., et al., 2016. Environmental chemicals modulate polar bear (*Ursus maritimus*) peroxisome proliferator-activated receptor gamma (PPARG) and adipogenesis in vitro. *Environmental Science & Technology*. 50, 10708-10720.
- Rustan, A. C., Drevon, C. A., 2005. Fatty acids: structures and properties. eLS.
- Saitou, N., Nei, M., 1987. The neighbor-joining method: a new method for reconstructing phylogenetic trees. *Molecular biology and evolution*. 4, 406-425.

- Sauer, S., 2015. Ligands for the nuclear peroxisome proliferator-activated receptor gamma. *Trends in pharmacological sciences*. 36, 688-704.
- Schirmer, K., et al., 1997. Methodology for demonstrating and measuring the photocytotoxicity of fluoranthene to fish cells in culture. *Toxicology in vitro*. 11, 107115-113119.
- Schlabach, M., et al., 2007. Siloxanes in the Environment of the Inner Oslofjord. NILU OR. 27, 2007.
- Schreer, A., et al., 2005. Application of Alamar blue/5-carboxyfluorescein diacetate acetoxymethyl ester as a noninvasive cell viability assay in primary hepatocytes from rainbow trout. *Analytical biochemistry*. 344, 76-85.
- Shabalina, I. G., et al., 2016. Metabolically inert perfluorinated fatty acids directly activate uncoupling protein 1 in brown-fat mitochondria. *Archives of toxicology*. 90, 1117-1128.
- Shen, L., Wania, F., 2005. Compilation, evaluation, and selection of physical-chemical property data for organochlorine pesticides. *Journal of Chemical & Engineering Data*. 50, 742-768.
- Shipley, J. M., et al., 2004. Trans-activation of PPAR α and induction of PPAR α target genes by perfluorooctane-based chemicals. *Toxicological sciences*. 80, 151-160.
- Skrede, S., et al., 1997. Thia fatty acids, metabolism and metabolic effects. *Biochimica et Biophysica Acta (BBA)-Lipids and Lipid Metabolism*. 1344, 115-131.
- Sotoca, A., et al., 2010. Superinduction of estrogen receptor mediated gene expression in luciferase based reporter gene assays is mediated by a post-transcriptional mechanism. *The Journal of steroid biochemistry and molecular biology*. 122, 204-211.
- Star, B., et al., 2011. The genome sequence of Atlantic cod reveals a unique immune system. *Nature*. 477, 207-210.
- Suedel, B., et al., Trophic transfer and biomagnification potential of contaminants in aquatic ecosystems. *Reviews of Environmental Contamination and Toxicology*. Springer, 1994, pp. 21-89.
- Surma, M., Zieliński, H., 2015. What do We Know about the Risk Arising from Perfluorinated Compounds. *Polish Journal of Environmental Studies*. 24.
- Széles, L., et al., 2010. Research resource: transcriptome profiling of genes regulated by RXR and its permissive and nonpermissive partners in differentiating monocyte-derived dendritic cells. *Molecular endocrinology*. 24, 2218-2231.
- Takacs, M. L., Abbott, B. D., 2007. Activation of mouse and human peroxisome proliferator-activated receptors (α , β/δ , γ) by perfluorooctanoic acid and perfluorooctane sulfonate. *Toxicological Sciences*. 95, 108-117.
- Tamura, K., et al., 2013. MEGA6: molecular evolutionary genetics analysis version 6.0. *Molecular biology and evolution*. 30, 2725-2729.
- Tanabe, S., 2002. Contamination and toxic effects of persistent endocrine disruptors in marine mammals and birds. *Marine pollution bulletin*. 45, 69-77.
- Tatum-Gibbs, K., et al., 2011. Comparative pharmacokinetics of perfluorononanoic acid in rat and mouse. *Toxicology*. 281, 48-55.

- Thomas, K. V., et al., 2015. Screening programme 2014. Phosphites, selected PBT substances and non-target screening. Norwegian Environment Agency. 148.
- Tocher, D. R., 2003. Metabolism and functions of lipids and fatty acids in teleost fish. *Reviews in fisheries science*. 11, 107-184.
- Tseng, Y.-C., et al., 2011. Exploring uncoupling proteins and antioxidant mechanisms under acute cold exposure in brains of fish. *PLoS One*. 6, e18180.
- Umemoto, T., Fujiki, Y., 2012. Ligand - dependent nucleo - cytoplasmic shuttling of peroxisome proliferator - activated receptors, PPAR α and PPAR γ . *Genes to Cells*. 17, 576-596.
- UNEP, C., 2001. Stockholm Convention on Persistent Organic Pollutants (POPs). Geneva: UNEP Chemicals.
- UNEP, U., Report of the Conference of the Parties of the Stockholm Convention on Persistent Organic Pollutants on the work of its fifth meeting. United Nations Environment Programme: Stockholm Convention on Persistent Organic Pollutants. Geneva, 2011, pp. 132.
- Urbatzka, R., et al., 2013. Tissue expression of PPAR-alpha isoforms in *Scophthalmus maximus* and transcriptional response of target genes in the heart after exposure to WY-14643. *Fish physiology and biochemistry*. 39, 1043-1055.
- Valdersnes, S., et al., 2017. Geographical trends of PFAS in cod livers along the Norwegian coast. *PloS one*. 12, e0177947.
- Varga, T., et al., 2011. PPARs are a unique set of fatty acid regulated transcription factors controlling both lipid metabolism and inflammation. *Biochimica et Biophysica Acta (BBA)-Molecular Basis of Disease*. 1812, 1007-1022.
- Vennison, J. S., 2010. Laboratory Manual For Genetic Engineering. Prentice-Hall Of India Pvt. Limited.
- Vorkamp, K., Rigét, F. F., 2014. A review of new and current-use contaminants in the Arctic environment: evidence of long-range transport and indications of bioaccumulation. *Chemosphere*. 111, 379-395.
- Wafer, R., et al., 2017. The Role of Peroxisome Proliferator-Activated Receptor Gamma (PPARG) in Adipogenesis: Applying Knowledge from the Fish Aquaculture Industry to Biomedical Research. *Frontiers in endocrinology*. 8.
- Wagner, K.-D., Wagner, N., 2010. Peroxisome proliferator-activated receptor beta/delta (PPAR β/δ) acts as regulator of metabolism linked to multiple cellular functions. *Pharmacology & therapeutics*. 125, 423-435.
- Wallington, T., et al., 2006. Formation of C7F15COOH (PFOA) and other perfluorocarboxylic acids during the atmospheric oxidation of 8: 2 fluorotelomer alcohol. *Environmental science & technology*. 40, 924-930.
- Wang, H., et al., 2017. cGAL, a temperature-robust GAL4-UAS system for *Caenorhabditis elegans*. *Nature methods*. 14, 145-148.
- Warner, N. A., et al., 2010. Volatile siloxanes in the European Arctic: Assessment of sources and spatial distribution. *Environmental science & technology*. 44, 7705-7710.
- Warner, N. A., et al., 2014. Allometric relationships to liver tissue concentrations of cyclic volatile methyl siloxanes in Atlantic cod. *Environmental Pollution*. 190, 109-114.

- Waterhouse, A. M., et al., 2009. Jalview Version 2—a multiple sequence alignment editor and analysis workbench. *Bioinformatics*. 25, 1189-1191.
- Westerlund, L., et al., 2000. Early life - stage mortality in zebrafish (*Danio rerio*) following maternal exposure to polychlorinated biphenyls and estrogen. *Environmental toxicology and chemistry*. 19, 1582-1588.
- Wolf, C. J., et al., 2008. Activation of mouse and human peroxisome proliferator-activated receptor alpha by perfluoroalkyl acids of different functional groups and chain lengths. *Toxicological Sciences*. 106, 162-171.
- Wu, C.-C., et al., 2017. Structural basis for specific ligation of the peroxisome proliferator-activated receptor δ . *Proceedings of the National Academy of Sciences*. 114, E2563-E2570.
- Yadatie, F., et al., 2016. Quantitative analyses of the hepatic proteome of methylmercury-exposed Atlantic cod (*Gadus morhua*) suggest oxidative stress-mediated effects on cellular energy metabolism. *BMC genomics*. 17, 554.
- Yadatie, F., et al., 2014. Liver transcriptome analysis of Atlantic cod (*Gadus morhua*) exposed to PCB 153 indicates effects on cell cycle regulation and lipid metabolism. *BMC genomics*. 15, 481.
- Yadatie, F., et al., 2013. Global transcriptome analysis of Atlantic cod (*Gadus morhua*) liver after in vivo methylmercury exposure suggests effects on energy metabolism pathways. *Aquatic toxicology*. 126, 314-325.
- Yadatie, F., et al., 2017. Quantitative proteomics analysis reveals perturbation of lipid metabolic pathways in the liver of Atlantic cod (*Gadus morhua*) treated with PCB 153. *Aquatic Toxicology*. 185, 19-28.
- Yin, G., et al., 2016. A refined method for analysis of 4, 4'-dicofol and 4, 4'-dichlorobenzophenone.
- You, C., et al., 2017. Cloning and expression characterization of peroxisome proliferator-activated receptors (PPARs) with their agonists, dietary lipids, and ambient salinity in rabbitfish *Siganus canaliculatus*. *Comparative Biochemistry and Physiology Part B: Biochemistry and Molecular Biology*. 206, 54-64.
- Zhang, L., et al., 2014. Structure-dependent binding and activation of perfluorinated compounds on human peroxisome proliferator-activated receptor γ . *Toxicology and applied pharmacology*. 279, 275-283.
- Zheng, J.-L., et al., 2015. Peroxisome proliferator-activated receptor gamma (PPAR γ) in yellow catfish *Pelteobagrus fulvidraco*: molecular characterization, mRNA expression and transcriptional regulation by insulin in vivo and in vitro. *General and comparative endocrinology*. 212, 51-62.

7 Appendix I

PPAR α hinge+LBD nt sequence

Predicted (Ensemble)

CAGTCGGAGAAACAGAGGTTGAAGGTGGAATTTGGGATGGGGGGGAGGAGCGAGGCGGAGCAAACCCTAA
CGCCCCCGACCACAAGGTCCTGGTGCAGCAGATCCACCAGGCCTACATGAGGAACTTCAGCATGAACAAGGA
CAGGGCCAGACTGATACTGACCGGCAAGACCAGCCGACCGCATTGTTATCCACGACATGGAGACCTTCCAG
GCGGCGGAGCAAACCCTGGAGGTGGAGCTCCTGGGAGGGGCCCCGGGAGGCAGAGGCCCGGCTGTTCCCTCTG
CTGCCAGAGCGCCTCAGTGGAGGCGGTACAGAGCTGACGGAGTTCGCCAAGAACATCCCTGGCTTTCTCCAC
CTCGACCTCAACGACCAGGTGACCCTGTTGAAGTACGGTGTGTACGAGGCCCTTTCACCTCCTGCTCCTGCG
ATGAATAAAGACGGCCTCCTGGTGGCGCGGGGGGCTTCATCACCCGTGAGTTCCTGAAAAGTCTGCGGC
GGCCCTTTAGTGACATGATGGAGCCCAAGTTCAGTTTGCCACGCGCTTCAACGCTCTGCAGCTGGATGACAGC
GACCTGGCGCTGTTCTCTGCAATCATCTGCTGCGGAGATCGTCCAGGGTTAGTGAACGCTCCCTGGTGGGA
GCGACTCCAGGAGAGTGTGTGAGGCTCTGCAGCTTCATCTGGTGGCCAACCACCGTGACAATGCCTTCTCT
TCCCTAAGCTGCTGCAGAAGTTGGCCGACCTGCGAGAGCTGGTCACCGAGCATGCTCAGTTGGTGCAGGACAT
TGAGACGACGGAGGACACGTCTCTCCATCCGCTCCT**GCAAGAGATTTACAGGGACATGTA**CTGA

867 nt

Sequenced

CAGTCGGAGAAACAGAGGTTGAAGGTGGAATTTGGGATGGGGGGGAGGAGCGAGGCGGAGCAAACCCTAA
CGCCCCCGACCACAAGGTCCTGGTGCAGCAGATCCACCAGGCCTACATGAGGAACTTCAGCATGAACAAGGA
CAGGGCCAGACTGATACTGACCGGCAAGACCAGCCGACCGCATTGTTATCCACGACATGGAGACCTTCCAG
GCGGCGGAGCAAACCCTGGAGGTG**AGAGGTGCAGCAGGGCCTAGCCCCGGCCAGTCCAAGGCCTCACAGC**
TGGGAAGGAGCTCCTGGT**TG**GAGGGGGCCCCGG**C**GAGGCAGAGGCCCGGCTGTTCCCTGCTGCTGCCAGAGCGCCTC
AGTGGAGGCGGTACAGAGCTGACGGAGTTCGCCAAGAACATCCCTGGCTTTCTCCACCTCGACCTCAACGACC
AGGTGACCCTGTTGAAGTACGGTGTGTACGAGGCCCTTTCACCTCCTTGCCTCCTGCATGAATAAAGACGGC
CTCCTGGTGGCGCGCGGGGGCTTCATCACCCGTGAGTTCCTGAAAAGTCTGCGGCGGCCCTTTAGTGACA
TGATGGAGCCCAAGTTCAGTTTGCCACGCGCTTCAACGCTCTGCAGCTGGATGACAGCGACCTGGCGCTGTT
GTCTGCAATCATCTGCTGCGGAGATCGTCCAGGGTTAGTGAACGCTCCCTGGTGGAGCGACTCCAGGAGA
GTGTTGTGAGGCTCTGCAGCTTCATCTGGTGGCCAACCACCGTGACAATGCCTTCTCTCCCTAAGCTGCTGC
AGAAGTTGGCCGACCTGCGAGAGCTGGTCACCGAGCATGCTCAGTTGGTGCAGGACATTGAGACGACGGAGG
ACACGTCTCTCCATCCGCTCCT**GCAAGAGATTTACAGGGACATGTA**CTGA

924 nt

8 Appendix II

PPARab hinge+LBD nt sequence

Predicted (Ensemble)

CAGTCGGAGAAGCTGAAGCTGAAGGCGGAGCTGGTGACGGGGGAGCTGGAGGTGGAGGACCCCCGTCAGG
CGGACCAGAAGACCCTGGCCCGGCAGATCTACGAGGCCTACCTGAAGAACTTCAACATGAACAAGGCCAAGGC
TCGCACCATCCTCACCGGCAAGACCAGCACCCCCCTTCGTCATCCACGACATGGACACCCTGCAGCTGGCCG
AGCAGACCCTGGTGGCCAAGATGGTGGGCACGGGGGGGGCGCTGCTGGACCGCGAGGCGGAGGCCCGCATC
TTCCACTGCTGCCAGTGCACCTCGGTGGAGACGGTGACGGAGCTCACCGAGTTCGCCAAGTCGGTGCCGGGCT
TCGCCGAGCTGGACCTCAACGACCAGGTGACGCTGCTCAAGTACGGTGTGTACGAAGCGCTGTTCCGCATGCT
GGCGTCGTGCATGAACAAGGACGGGCTGCTGGTGGCGTACGGCGCCGGCTTCATCACGCGGAGTTCCTCAA
GAGCCTGCGGGGCCCTTCAGCGACATGATGGAGCCCAAGTTCAGTTCGCCATGAGGTTCAACGCCCTGGAG
CTGGACGACAGTGACCTGGCGCTGTTCTGGCCGCAATCATCTGCTGTGGAGACCGGCCGGGGCTGGTGAAC
GTGGGTACATCGAGCGCATGCAGGAGAACATCGTGCAGGTGCTGCGGCTCCACCTGCTGGCCAACCACCAG
ACGACGCTTCTCTTCCCAAGCTGCTGCAGAAGCTGGCCGACCTGCGGCAGCTGGTCACGGAGCACGCTCA
GCTGGTGCAGGAGATCAAGAAGACGGAGGACGCTCGCTGCACCCGCTACTGCAGGAGATCTACCGTGACAT
GTACTGA

876 nt

Sequenced

CAGTCGGAGAAGCTGAAGCTGAAGGCGGAGCTGGTGACGGGGGAGCTGGAGGTGGAGGACCCCCGTCAGG
CGGACCAGAAGACCCTGGCCCGGCAGATCTACGAGGCCTACCTGAAGAACTTCAACATGAACAAGGCCAAGGC
TCGCACCATCCTCACCGGCAAGACCAGCACCCCCCTTCGTCATCCACGACATGGACACCCTGCAGCTGGCCG
AGCAGACCCTGGTGGCCAAGATGGTGGGCACGGGGGGCGGCGGCTGCTGGACCGCGAGGCGGAGGCCCGC
ATCTTCCACTGCTGCCAGTGCACCTCGGTGGAGACGGTGACGGAGCTCACCGAGTTCGCCAAGTCGGTGCCGG
GCTTCGCCGAGCTGGACCTCAACGACCAGGTGACGCTGCTCAAGTACGGTGTGTACGAAGCGCTGTTCCGCAT
GCTGGCGTCGTGCATGAACAAGGACGGGCTGCTGGTGGCGTACGGCGCCGGCTTCATCACGCGGAGTTCCTC
AAGAGCCTGCGGGGCCCTTCAGCGACATGATGGAGCCCAAGTTCAGTTCGCCATGAGGTTCAACGCCCTGG
AGCTGGACGACAGTGACCTGGCGCTGTTCTGGCCGCAATCATCTGCTGTGGAGACCGGCCGGGGCTGGTGA
ACGTGGGTACATCGAGCGCATGCAGGAGAACATCGTGCAGGTGCTGCGGCTCCACCTGCTGGCCAACCACCA
GGACGACACCTTCTCTTCCCAAGCTGCTGCAGAAGCTGGCCGACCTGCGGCAGCTGGTCACGGAGCACGCT
CAGCTGGTGCAGGAGATCAAGAAGACGGAGGACGCTCGCTGCACCCGCTACTGCAGGAGATCTACCGTGAC
ATGTACTGA

879 nt

9 Appendix III

PPAR β/δ hinge+LBD nt sequence

Predicted (Ensemble)

TATGGACGCATGCCTGAAGCTGAGAAGAAAAAGCTGGTGGCGGGCCTACAGGCAGAGGAACAGAACCTCCG
CAATCCTAAAGGTGCAGACCTCAAGACGCTGGCCAAACAGGTCAACGCAGCCTACTTGAAAAACCTCAGTATG
ACCAAGAAAAAGGCCCGCAGTATCCTCACGGGCAAGACCAACAGCACCTCGCCCTTTGTCATCTATGACATGGA
CACCCATATGGAAGCGGAGAGCGGTTTAGTATGGAGCCAGTTGGTGCCGGGGGCACCCCTGACCAAGGAGAT
TGGGGTCCATGTGTTCTACCGCTGCAGTGCCTACAGTGGAGACTGTGAGGGAGCTCACAGAGTTTGCCAAG
TCCATTCCAGGCTTTGTGGACCTCTTCTCAATGACCAGGTGACTTTGTTGAAGTATGGTGTGCATGAGGCTATT
TTCGCCATGCTCCCCTCGCTCATGAACAAAGATGGACTTTTGGTGGCCAATGGCAAAGATTTGTGACCAGAGA
GTTCTGCGAAGTTTAAGGAAGCCCTTCAGTGAGATAATGGAGCCCAAGTTTGAGTTTGCCTTAAAGTTCAATG
CTCTGGAGTTGGACGACAGTGACCTGGCACTGTTTGTTCAGCCATCATACTCTGTGGAGATCGCCAGGGCTG
ATAAACGTGAAGCAGGTGGAACAGAGTCAGGACAGGATACTGCAGGCCCTTGATCTGCACCTCCAGACCAACC
ACTCTGACTCGCTCTACCTCTTCCCAAGCTGCTGCAAAAGATGGCCGACCTCCGACAGCTGGTTCACAGAGAAT
GTTGAGCTGGTTCAGAAGATTAAAAAAAGTACTGAGTCTGAGACCTCGCTCCACCCTCTGTT**GCAGGAGATCTACAA
AGACATGTACTAG**

894 nt

Sequenced

TATGGACGCATGCCTGAAGCTGAGAAGAAAAAGCTGGTGGCGGGCCTACAGGCAGAGGAACAGAACCTCCG
CAATCCTAAAGGTGCAGACCTCAAGACGCTGGCCAAACAGGTCAACGCAGCCTACTTGAAAAACCTCAGTATG
ACCAAGAAAAAGGCCCGCAGTATCCTCACGGGCAAGACCAACAGCACCTCGCCCTTTGTCATCTATGACATGGA
CACCCATATGGAAGCGGAGAGCGGTTTAGTATGGAGCCAGTTGGTGCCGGGGGCACCCCTGACCAAGGAGAT
TGGGGTCCATGTGTTCTACCGCTGCAGTGCCTACAGTGGAGACTGTGAGGGAGCTCACAGAGTTTGCCAAG
TCCATTCCAGGCTTTGTGGACCTCTTCTCAATGACCAGGTGACTTTGTTGAAGTATGGTGTGCATGAGGCTATT
TTCGCCATGCTCCCCTCGCTCATGAACAAAGATGGACTTTTGGTGGCCAATGGCAAAGATTTGTGACCAGAGA
GTTCTGCGAAGTTTAAGGAAGCCCTTCAGTGAGATAATGGAGCCCAAGTTTGAGTTTGCCTTAAAGTTCAATG
CTCTGGAGTTGGACGACAGTGACCTGGCACTGTTTGTTCAGCCATCATACTCTGTGGAGATCGCCAGGGCTG
ATAAACGTGAAGCAGGTGGAACAGAGTCAGGACAGGATACTGCAGGCCCTTGATCTGCACCTCCAGACCAACC
ACTCTGACTCGCTCTACCTCTTCCCAAGCTGCTGCAAAAGATGGCCGACCTCCGACAGCTGGTTCACAGAGAAT
GTTGAGCTGGTTCAGAAGATTAAAAAAAGTACTGAGTCTGAGACCTCGCTCCACCCTCTGTT**GCAGGAGATCTACAA
AGACATGTACTAG**

894 nt

10 Appendix IV

PPAR γ hinge+LBD nt sequence

Predicted (Ensemble)

CTCCTCTACGACTCCTACGTCAAGCACTTCCCCCTACCAAGGCCAAGGCCCGAGCCATCCTGTCTGGGAAGAC
CGGGGACAGCTCGCCGTTTATTATCCACGACATGAAGTCTCTGATGGATGGAGAACAGTTGATCAACTGCAAAC
AGATTCGGAAGAGACCAGCATCCGTCCCCACGGAGGGCCTGGAGTTGCGCTTCTTACTCCTGCCAGTCCCGC
TCTGCCGAGGCCGTGAGGGAGTTACGGAGTTCGCCAAGAGCATCCCCGGCTTTGTAGATCTGGATCTCAACG
ACCAGGTGACGTTGCTGAAGTACGGCGTGATAGAGGTGCTGACCCTCAGGATGGCTCCCCTGATGAACAAGGA
CGGCACGCTGATGTCTACGGCCAGATCTTCATGACGCGGGAGTTCCTCAAGAGCCTACGCAAGCCCTTCTGCC
AGATGCTGGAGCCCAAGTTTGAGTTTCCGTCAAGTTCAACACCCTGGAGCTGGACGACAGCGACCTGGCTCTG
TTCCTGGCCGTCGTATCCTCAGCGGCGACCGGCCGGCCTGCTGAACGTGCGGCCATCGAGCGGCTCCAGG
AGACGGTGCTCCACTCCCTGGAGCTCACCTGAAGGTCAACCACCCGGACTCCATGCAGCTGTTCCGCAAGCTG
CTGCAGAAGATGACGGACCTGCGGCAGATCGTGACCGACCAGTGCACCTCATCCAGCTGCTGGACAAGACCG
AGGTGGACATGTGCTTACACCCGCTGCTGCAG**GGAGATCCTGAAGGACTTGTATTAG**

792 nt

Sequenced

CTCCTCTACGACTCCTACGTCAAGCACTTCCCCCTACCAAGGCCAAGGCCCG**G**GCCATCCTGTCTGGGAAGAC
CGGGGACAGCTCGCCGTTTATTATCCACGACATGAAGTCTCTGATGGATGGAGAACAGTTGATCAACTGCAAAC
AGATTC**CC**GGAAGAGACCAGCATCCGTCCCCA**GCTGTCTGGCTGACA**ACTATGGGGT**CGTGCGGGCCACCC**
GGCGCCAGGGTACGGGGGCTGGGGGTCTGTCCAGGGGCCATCGGGCTCAGTACCAGGGGCGGACG
GAGGGCCTGGAGTTGCGCTTCTTACTCCTGCCAGTCCCGCTCTGCCGAGGCCGTGAGGGAGGTTACGGAGT
TCGCCAAGAGCATCCCCGGCTTTGTAGATCTGGATCTCAACGACCAGGTGACGTTGCTGAAGTACGGCGTGATA
GAGGTGCTGACCCTCAGGATGGCTCCCCTGATGAACAAGGACGGCACGCTGATGTCCTACGGCCAGATCTTCA
TGACGCGGGAGTTCCTCAAGAGCCTACGCAAGCCCTTCTGCCAGATGCTGGAGCCCAAGTTTGAGTTCTCCGTC
AAGTTCAACACCCTGGAGCTGGACGACAGCGACCTGGCTCTGTTCTGGCCGTCGTATCCTCAGCGGCGACCG
GCCGGCCTGCTGAACGTGCGGCCATCGAGCGGCTCCAGGAGACGGTGCTCCACTCCCTGGAGCTCCACCTG
AAGGTCAACCACCCGGACTCCATGCAGCTGTTCCGCAAGCTGCTGCAGAAGATGACGGACCTGCGGCAGATCG
TGACCGACCAGTGCACCTCATCCAGCTGCTGGACAAGACCGAGGTGGACATGTGCTTACACCCGCTGCTGCA
GGAGATCCTGAAGGACTTGTATTAG

903 nt

11 Appendix V

GAL4-DBD-PPAR α -LBD nt sequence

ATGAAGCTACTGTCTTCTATCGAACAAGCATGCGATATTTGCCGACTTAAAAAGCTCAAGTGCTCCAAA
GAAAAACCGAAGTGCGCCAAGTGTCTGAAGAACAACCTGGGAGTGTGCTACTCTCCCAAACCAAAGG
TCTCCGCTGACTAGGGCACATCTGACAGAAGTGAATCAAGGCTAGAAAGACTGGAACAGCTATTTCTA
CTGATTTTTCTCGAGAAGACCTTGACATGATTTTGAAAATGGATTCTTTACAGGATATAAAAAGCATTG
TTAACAGGATTATTTGTACAAGATAATGTGAATAAAGATGCCGTCACAGATAGATTGGCTTCAGTGGAG
ACTGATATGCCTCTAACATTGAGACAGCATAGAATAAGTGCACATCATCATCGGAAGAGAGTAGTAAC
AAAGGTCAAAGACAGTTGACTGTATCGCCG**GAATTC**CAGTCGGAGAAACAGAGGTTGAAGGTGGAATTT
GGGATGGGGGGGAGGAGCGAGGCGGAGCAAACCTAACGCCCCCGACCACAAGGTCCTGGTGCAGCAG
ATCCACAGGCCTACATGAGGAACCTCAGCATGAACAAGGACAGGGCCAGACTGATCTGACCGCAAG
ACCAGCCGACCCGATTTGTTATCCACGACATGGAGACCTTCCAGGCGGGGAGCAAACCTGGAGGTG
AGAGGTGCAGCAGGGCCAGCCCGGCCAGTCCAAGGCTCACAGCTGGGAAGGAGCTCCTGG**TGGAG**
GGGCCCGG**CGAGGCAGAGCCCGGCTGTTCTCTGCTGCCAGAGCGCCT**CAGTGGAGGCGGTCACAGAG
CTGACGGAGTTCGCCAAGAACATCCCTGGCTTTCTCCACCTCGACCTCAACGACCAGGTGACCCTGTTG
AAGTACGGTGTGTACGAGGCCCTCTTACCCTCCTTGCCCTGCATGAATAAAGACGGCCTCCTGGTG
GCGCGCGGGGGGCTTCATCACCCGTGAGTTCTGAAAAGTCTGCGGGCGGCCCTTTAGTGACATGATG
GAGCCCAAGTTCCAGTTTGCCACGCGCTTCAACGCTCTGCAGCTGGATGACAGCGACCTGGCGCTGTTT
GTCTCTGCAATCATCTGCTGCGGAGATCGTCCAGGGTTAGTGAACGCCTCCCTGGTGGAGCGACTCCAG
GAGAGTGTGTGCAGGCTCTGCAGCTTCATCTGGTGGCCAACCACCGTGACAATGCCTTCTCTCCCT
AAGCTGCTGCAGAAGTTGGCCGACCTGCGAGAGCTGGTACCAGCATGCTCAGTTGGTGCAGGACATT
GAGACGACGGAGACACGTCTCTCCATCCGCTCCT**GCAAGAGATTTACAGGGACATGTACTGA**

1374 nt

GAL4-DBD-PPAR β -LBD nt sequence

ATGAAGCTACTGTCTTCTATCGAACAAGCATGCGATATTTGCCGACTTAAAAAGCTCAAGTGCTCCAAA
GAAAAACCGAAGTGCGCCAAGTGTCTGAAGAACAACCTGGGAGTGTGCTACTCTCCCAAACCAAAGG
TCTCCGCTGACTAGGGCACATCTGACAGAAGTGAATCAAGGCTAGAAAGACTGGAACAGCTATTTCTA
CTGATTTTTCTCGAGAAGACCTTGACATGATTTTGAAAATGGATTCTTTACAGGATATAAAAAGCATTG
TTAACAGGATTATTTGTACAAGATAATGTGAATAAAGATGCCGTCACAGATAGATTGGCTTCAGTGGAG
ACTGATATGCCTCTAACATTGAGACAGCATAGAATAAGTGCACATCATCATCGGAAGAGAGTAGTAAC
AAAGGTCAAAGACAGTTGACTGTATCGCCG**GAATTC**CAGTCGGAGAAGCTGAAGCTGAAGCGGAGCTG
GTGACGGGGGAGCTGGAGGTGGAGGACCCCGTCAGGCGGACCAGAAGACCTGGCCCGGCAGATCTAC
GAGGCTACCTGAAGAACTTCAACATGAACAAGGCCAAGGCTCGCACCATCCTACCGGCAAGACCAGC
ACCCCCCCTTCGTATCCACGACATGGACACCCTGCAGCTGGCCGAGCAGACCCTGGTGGCCAAGATG
GTGGGCACGGGGGG**CGGCGGCCT**GCTGGACCGCGAGGCGGAGGCCCGCATCTTCCACTGCTGCCAGTGC
ACCTCGGTGGAGACGGTGCAGGAGCTCACCGAGTTCGCCAAGTCCGTGCCGGGCTTCGCCGAGCTGGAC
CTCAACGACCAGGTGACGCTGCTCAAGTACGGTGTGTACGAAGCGCTGTTCCGATGCTGGCGTCTGTC
ATGAACAAGGACGGGCTGCTGGTGGCGTACGGCGCCGGCTTCATCACGCGGAGTTCTCAAGAGCCTG
CGGCGGCCCTTCAGCGACATGATGGAGCCCAAGTTCAGTTCGCCATGAGGTTCAACGCCCTGGAGCTG
GACGACAGTGACCTGGCGCTGTTCTGGCCGAATCATCTGCTGTGGAGACCGGCCGGGGCTGGTGAAC
GTGGGTACATCGAGCGCATGCAGGAGAACATCGTGCAGGTGCTGCGGCTCCACCTGCTGGCCAACCAC
CAGGACGACACCTTCTCTTCCCAAGCTGCTGCAGAAGCTGGCCGACCTGCGGCAGCTGGTACGGAG
CAGCTCAGCTGGTGCAGGAGATCAAGAAGACGGAGGACGCCTCGCTGCACCCGCTACTGCAG**GGAGATC**
TACCGTGACATGTACTGA

1329 nt

12 Appendix VI

GAL4-DBD-PPAR β/δ -LBD nt sequence

ATGAAGCTACTGTCTTCTATCGAACAAGCATGCGATATTTGCCGACTTAAAAAGCTCAAGTGCTCCAAA
GAAAAACCGAAGTGCGCCAAGTGTCTGAAGAACAACCTGGGAGTGTGCTACTCTCCCAAACCAAAGG
TCTCCGCTGACTAGGGCACATCTGACAGAAGTGAATCAAGGCTAGAAAGACTGGAACAGCTATTTCTA
CTGATTTTTCTCGAGAAGACCTTGACATGATTTTGAAAATGGATTCCTTACAGGATATAAAAAGCATTG
TTAACAGGATTATTTGTACAAGATAATGTGAATAAAGATGCCGTCACAGATAGATTGGCTTCAGTGGAG
ACTGATATGCCTCTAACATTGAGACAGCATAGAATAAGTGCAGCATCATCATCGGAAGAGAGTAGTAAC
AAAGGTCAAAGACAGTTGACTGTATCGCCG**GAATTC**TAT**GGACGCATGCCTGAAG**CTGAGAAGAAAAAG
CTGGTGGCGGGCTACAGGCAGAGGAACAGAACCTCCGCAATCCTAAAGGTGCAGACCTCAAGACGCTG
GCCAAACAGGTCAACGCAGCCTACTTGAAAAACCTCAGTATGACCAAGAAAAAGGCCCGCAGTATCCTC
ACGGGCAAGACCAACAGCACCTCGCCCTTTGTTCATATGACATGGACACCCATGGAAAGCGGAGAGC
GGTTTAGTATGGACAGCTTGGTGGCGGGGACCCCTGACCAAGGAGATTGGGTCCATGTGTTCTAC
CGCTG**TCAGTGC**ACTACAGTGGAGACTGTGAGGGAGCTCACAGAGTTTGCCAAGTCCATTCCAGGCTTT
GTGGACCTCTTCTCAATGACCAGGTGACTTTGTTGAAGTATGGTGTGCATGAGGCTATTTTCGCCATG
CTCCCCTCGCTCATGAACAAAGATGGACTTTTGGTGGCCAAATGGCAAAGGATTTGTGACCAGAGAGTTC
CTGCGAAGTTTAAAGGAAGCCCTTCAGTGAGATAATGGAGCCCAAGTTTGAGTTTGCCTTAAAGTTCAAT
GCTCTGGAGTTGGACGACAGTGACCTGGCACTGTTTGTGTCAGCCATCATACTCTGTGGAGATCGCCCA
GGGCTGATAAACGTGAAGCAGGTGGAACAGAGTCAGGACAGGATACTGCAGGCCCTTGATCTGCACCTC
CAGACCAACCACTCTGACTCGC**CTACCT**CTTCCCAAGCTGCTGCAAAAGATGGCCGACCTCCGACAG
CTGGTTCACAGAGAATGTTTCAGCTGGTTCAGAAGATTAAAAAAAGTCTGAGTCTGAGACCTCGCTCCACCCT
CTGTT**GCAGGAGATCTACAAAGACATGTACTAG**

1344 nt

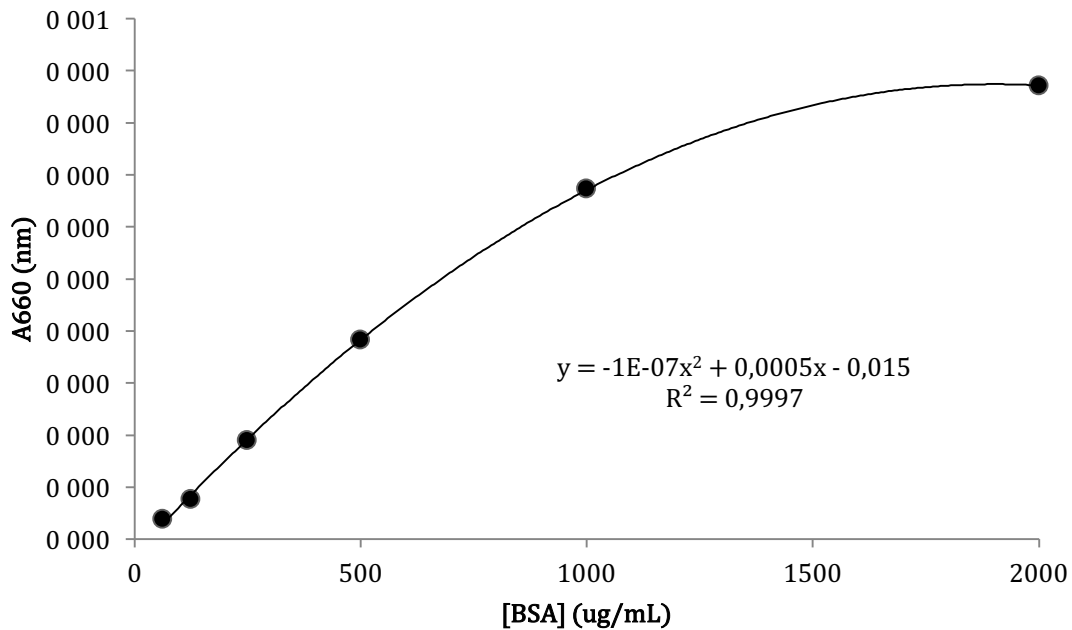
GAL4-DBD-PPAR γ -LBD nt sequence

ATGAAGCTACTGTCTTCTATCGAACAAGCATGCGATATTTGCCGACTTAAAAAGCTCAAGTGCTCCAAA
GAAAAACCGAAGTGCGCCAAGTGTCTGAAGAACAACCTGGGAGTGTGCTACTCTCCCAAACCAAAGG
TCTCCGCTGACTAGGGCACATCTGACAGAAGTGAATCAAGGCTAGAAAGACTGGAACAGCTATTTCTA
CTGATTTTTCTCGAGAAGACCTTGACATGATTTTGAAAATGGATTCCTTACAGGATATAAAAAGCATTG
TTAACAGGATTATTTGTACAAGATAATGTGAATAAAGATGCCGTCACAGATAGATTGGCTTCAGTGGAG
ACTGATATGCCTCTAACATTGAGACAGCATAGAATAAGTGCAGCATCATCATCGGAAGAGAGTAGTAAC
AAAGGTCAAAGACAGTTGACTGTATCGCCG**GAATTC****CTCCTCTACGACTCCTAC**GTCAAGCACTTCCCC
CTCACCAAGGCCAAGGCCCGGGCCATCCTGTCTGGGAAGACCGGGGACAGCTCGCCGTTTATTATCCAC
GACATGAAGTCTCTGATGGATGGAGAACAGTTGATCAACTGCAAAACAGATT**CCGGAAGAGACCAGCAT**
CCGTCCCCAGCTGTCTGGCTGACAACTATGGGGTCTG**GGCGGGCCACCCGGCGCCAGGGTACGGGGGG**
CTGGGGGGTCTGTCCAGGGGCCCATCGGGCTCAGTACCAGGGGCGGACGGAGGGCTGGAGTTGCGC
TTCTTCTACTCCTGCCAGTCCCGCTCTGCCGAGGCCGTGAGGGAGGTTACGGAGTTCGCCAAGAGCATC
CCCGGCTTTGTAGATCTGGATCTCAACGACCAGGTGACGTTGCTGAAGTACGGCGTGATAGAGGTGCTG
ACCCTCAGGATGGCTCCCCTGATGAACAAGGACGGCACGCTGATGTCTTACGGCCAGATCTTCATGACG
CGGGAGTTCTCAAGAGCCTACGCAAGCCCTTCTGCCAGATGCTGGAGCCCAAGTTTGGAGTTCTCCGTC
AAGTTCAACACCCTGGAGCTGGACGACAGCGACCTGGCTCTGTTCCTGGCCGTGTCATCCTCAGCGGC
GACCGGCCGGGCTGCTGAACGTGCGGCCCATCGAGCGGCTCCAGGAGACGGTGTCCACTCCCTGGAG
CTCCACCTGAAGGTCAACCACCCGACTCCATGCAGCTGTTCCCAAGCTGCTGCAGAAGATGACGGAC
CTGCGGCAGATCGTGACCGACACGTGCACCTCATCCAGCTGCTGGACAAGACCGAGGTGGACATGTGC
TTACACCCGCTGCTGCAG**GAGATCCTGAAGGACTTGTATTAG**

1353 nt

13 Appendix VII

Table 53. Standard curve of bovine serum albumin (BSA) for determination of protein concentration in COS-7 cell lysate.



BSA, with a concentration of 10 mg/mL, was prepared and diluted with Triton lysis buffer to obtain the concentrations of 62.5, 125, 250, 500, 1000, and 2000 $\mu\text{g/mL}$. BSA samples, blank samples (Triton lysis buffer), and COS-7 cell lysates were made in triplicates in 96 wells plates. The plates were added the protein assay reagent Pierce 660 (Thermo scientific), and Absorbance was measured at 660 nm using an EnSpire 2300 Multilabel Reader (PerkinElmer). Average absorbance (Abs_{660}) of the blank triplicates was calculated and subtracted from the average of the BSA triplicates, before plotting the corrected BSA Abs_{660} against corresponding BSA standard concentration. Average Abs_{660} of the ten different COS-7 cell lysate were incorporated into the equation to calculate the unknown protein concentration.